ISTANBUL TECHNICAL UNIVERSITY ★ ENERGY INSTITUTE

SYNTHESIS OF POLY(IMIDE) SILOXANE BLOCK COPOLYMER, STRUCTURAL CHARACTERIZATION AND COMPARISON OF IRRADIATION EFFECT IN RADIATION SHIELDING PROPERTIES FOR FLEXIBLE SHEET AND PELLETIZED FORM

Ph.D. THESIS

Türkan DOĞAN

Energy Science and Technology Department

Energy Science and Technology Programme

APRIL 2020

ISTANBUL TECHNICAL UNIVERSITY ★ ENERGY INSTITUTE

SYNTHESIS OF POLY(IMIDE) SILOXANE BLOCK COPOLYMER, STRUCTURAL CHARACTERIZATION AND COMPARISON OF IRRADIATION EFFECT IN RADIATION SHIELDING PROPERTIES FOR FLEXIBLE SHEET AND PELLETIZED FORM

Ph.D. THESIS

Türkan DOĞAN
(301072008)

Energy Science and Technology Department

Energy Science and Technology Programme

Thesis Advisor: Prof. Dr. Nilgün BAYDOĞAN

APRIL 2020

ISTANBUL TEKNİK ÜNİVERSİTESİ ★ ENERJİ ENSTİTÜSÜ

POLİ(İMİD) SİLOKSAN BLOK KOPOLİMERİN SENTEZİ, YAPISAL KARAKTERİZASYONU VE IŞINLAMA ETKİSİNİN ESNEK LEVHA VE PELETLEŞTİRİLMİŞ FORMLARINDA RADYASYON ZIRHLAMA ÖZELLİKLERİNİN KARŞILAŞTIRILMASI

DOKTORA TEZİ

Türkan DOĞAN
(301072008)

Enerji Bilimi ve Teknolojisi Bölümü

Enerji Bilimi ve Teknolojisi Programı

Tez Danışmanı: Prof. Dr. Nilgün BAYDOĞAN

NİSAN 2020

Türkan DOĞAN, a Ph.D. student of ITU Energy Institute of Energy Science and Technology student ID 301072008, successfully defended the thesis/dissertation entitled "SYNTHESIS OF POLY(IMIDE) SILOXANE BLOCK COPOLYMER, STRUCTURAL CHARACTERIZATION AND COMPARISON OF IRRADIATION EFFECT IN RADIATION SHIELDING PROPERTIES FOR FLEXIBLE SHEET AND PELLETIZED FORM", which she prepared after fulfilling the requirements specified in the associated legislations, before the jury whose signatures are below.

Thesis Advisor : **Prof. Dr. Nilgün BAYDOĞAN**   ....
Istanbul Technical University

Jury Members : **Assoc. Prof. Dr. Sevilay HACIYAKUPOĞLU** ....
Istanbul Technical University

Assoc. Prof. Dr. Serço Serkis YEŞİLKAYA ....
Yildiz Technical University

Prof. Dr. Sema ERENTÜRK   ....
Istanbul Technical University

Prof.Dr. Tülay BAL DEMİRCİ   ....
Istanbul University-Cerrahpasa

Date of Submission : 6 February 2020
Date of Defense   : 18 April 2020

In memory of my dearest aunt and uncle,

FOREWORD

First and foremost, I would like to thank to my supervisor, Prof.Dr.Nilgun BAYDOĞAN for her guidance through each stage of the process and for inspiring my interest in the development of innovative technologies. I would like to present my gratitude and sincerely thank to her for all her encouragement and inspiration throughout my Ph.D. research.

I would like to thank to, Prof.Dr.Nilgun KIZILCAN and Assoc.Prof.Dr.Nesrin KOKEN for their support and assistance. I am really grateful for all their support.

I would like to thank Assoc.Prof.Dr.Aliye ARABACI for guidance to turn pelletized form from powder form of the block copolymer samples.

I would like to thank to Prof.Dr.Nilgun YAVUZ for her assistance in TGA analysis.

I would like to thank to Dr.Esin Ates GUVEL and Chemist Elif ERKMAN for their meaningful discussions on my research and their selfless help for my experimental work.

I would like to thank former members of the resin-polymer research group - Gorkem ULKU, Nilay TANRİVER, Emre KILIC- for their friendships in the lab during my experiments. It was great sharing laboratory with all of them along my experiments.

I would like to thank to Dr. Sahip KIZILTAS and Chemist Zeynep CAMTAKAN for their technical support during my radiation measurements.

I would also like to extend thanks to Dr.Barbaros AKKURT, Dr. Hasan GOKCE, Dr.Bihter ZEYTUNCU, Dr. Tansu ERSOY for their technical support.

Finally, I would like to acknowledge my family for their love, encouragement and inspiration. Thanks for believing and supporting me along this tiring journey...

February 2020   Türkan DOĞAN
                                                                                                              (Physicist M.Sc.)

TABLE OF CONTENTS

ABBREVIATIONS

AFM	**:** Atomic Microscopy
APPS	**:** Poly(dimethyl siloxane) bis (3-aminopropyl)-terminated
BI	**:** Poly(imide siloxane) Block Copolymers in Flexible Sheet
BII	**:** Poly(imide siloxane) Block Copolymers in Pelletized Form
BTDA	**:** 3 3' 4 4'-Benzophenone tetracarboxylic acid dianhydride
Co-60	**:** Cobalt-60 Radioisotope
CIGS	**:** Copper Indium Gallium Selenide Solar Cells
Cs-137	**:** Cesium-137 Radioisotope
DMA	**:** Dynamic Mechanics Analysis
DSC	**:** Differential Scanning Calorimetry
E	**:** Effective Dose
FTIR	**:** Fouirer Transform Infrared Spektrofotometre
HT	**:** Equivalent Dose
HVL	**:** Half Value Layer
I_B	**:** Bonding Energy
keV	**:** Kilo Electron Volt
Ke	**:** Kinetic Energy
MeV	**:** Mega Electron Volt
MPa	**:** Mega Pascal
NH-3	**:** Neutron Howitzer
NMP	**:** Methyl-2-pyrrolidinone
ODA	**:** 4 4'-Oxydianiline
ODCB	**:** 1-2 Dichlorobenzene
PET	**:** Polyethylene Terephthalate
PIS	**:** Poly(imide siloxane)
PV	**:** Photovoltaic
^{239}Pu-Be	**:** Plutonium-Beryllium 238
^{241}Pu-Be	**:** Plutonium-Beryllium 241
Q	**:** Quality Factor
RI	**:** Randomly Segmented Poly(imide siloxane) Copolymers
SEM	**:** Scanning Electron Microscopy
Sr-90	**:** Strontium Radioisotope
T_d	**:** Thermal Degradation
TGA	**:** Thermogravimetric Analysis
TPE	**:** Thermoplastic Elastomer
XRD	**:** X-Ray Powder Diffraction
Y-90	**:** Yittrium-90 Radioisotope

SYMBOLS

Bq   : Becquerel
c   **:** Speed of the light
Ci   : Curie
μCi   : Micro Curie
mCi   **:** Mili Curie
μ   **:** Linear attenuation coefficient
μ$_m$ **:** Mass attenuation coefficient
mSv   **:** Mili Sievert
μSv   **:** Micro Sievert
Gy   **:** Gray
kGy   **:** Kilo Gray
h   **:** Planck constant
I   **:** Counts transmitted to the polymer and detected in the detector
I$_0$ **:** Counts detected in the detector
Ra   **:** Roughness Factor
ρ   **:** Density
v   **:** Frequency of the light

LIST OF TABLES

LIST OF FIGURES

SYNTHESIS OF POLY(IMIDE) SILOXANE BLOCK COPOLYMER, STRUCTURAL CHARACTERIZATION AND COMPARISION OF IRRADIATION EFFECT IN RADIATION SHIELDING PROPERTIES FOR FLEXIBLE SHEET AND PELLETIZED FORM

SUMMARY

Flexible polymers play an important role in enabling radioisotopes to be used effectively in polymeric materials in a wide variety of radiation-dependent applications where flexible materials are required. Since poly(imide siloxane) (PIS) block copolymers can be used flexibly, they can be applied to a wide variety of industrial materials as compatible polymers.

These materials are proper to be used in various application areas like biomedical products, biocompatible materials, and several industrial applications such as solar cell technologies, aerospace applications, and flexible organic electronic devices. Flexible polymers play an important role in many applications because they provide effective use in polymeric materials. Improvement and development of high-performance polymers enable the use of radioisotope-containing radiopharmaceuticals in medicines, diagnostics, and medical products.

In this study, we aimed to produce flexible substrates to be able to be used in electronics, medical applications, aerospace technologies as well as substrates in solar energy technology. The produced poly(imide siloxane) (PIS) copolymers have the properties of flexible substrates, which are required for use in solar cells. On the other hand, elastomeric rubber poly(imide siloxane) block copolymer materials have wide applications in electronics. Poly(imide siloxane), which can be produced with the desired form and conformed at different configurations, is important in such areas.

The copolymer structures and many of these copolymers are obtained by adjusting and increasing soft block segments, and copolymers are synthesized by adjusting soft and hard segment lengths. This synthetic approach supports the synthesis of copolymers with siloxane blocks randomly linked with imide units. In this study, poly(imide siloxane) block copolymers were synthesized using amine terminated APPS to examine changes in structural properties. Flexible poly(imide siloxane) block copolymers (BI) were produced in the form of a flexible rubber (elastomeric rubber).

The flexible form of the structure was changed and adjusted by increasing the ODA and reducing the APPS. Flexible poly(imide siloxane) block copolymers were produced by this technique. Thus, the new poly(imide siloxane) was produced from aminopropyl terminated siloxane as diamines and aromatic dianhydrides.

ODA (4,4'-oxydianiline) and BTDA (benzophenone -3 3′-4 4′-tetracarboxylic dianhydride) are hard segments, APPS and BTDA were soft segments. ODA with APPS was used to form the polyimide hard block; polysiloxane soft block samples

were synthesized using APPS and BTDA. Thus, poly(imide siloxane) block copolymer samples were synthesized using ODA with APPS and BTDA.

Characterization of the samples was performed by using FTIR (Fourier Transform Infrared Spectrophotometer) analysis to evaluate the structure of flexible and pelletized high-performance copolymer forms. It was understood that the characteristic chemical structure of the block copolymer samples was generally composed of two parts as siloxane Si - O and carbon chain-type structure through FTIR analyses. Then, the structure of the PIS samples was formulated.

TGA (Thermo Gravimetric Analysis) and DSC (Differential Scanning Calorimeter) analyzes of the BI and BII copolymer structures were performed. Characterization results were determined. It was seen that poly(imide siloxane) PIS copolymers had high thermal resistance properties. The TGA analysis was done under a nitrogen atmosphere at a heating rate of 20°C min^{-1} from 38°C to 800°C. 18% weight loss of the BI block copolymers and 11% weight loss of the BII block copolymers occurred in the range of 400 to 500°C. Poly(imide siloxane) block copolymers were not solved in a large number of organic solvents.

The structures were mechanically tested with uniaxial hydraulic press test to determine elastic recovery properties. After the uniaxial hydraulic press test, an X-ray radiography test was used for flexible rubber samples. The deformation and radiographic contrast of nonpressed and pressed polymer samples, which were pressed in uniaxial hydraulic press tests by compressing samples at 10, 20, and 30 tons pressing values were examined. It was seen that the structures exhibited elastic rubber (elastomeric rubber) properties so that the structures return to their original form after the applied tension was removed.

Dynamic Mechanic Analysis (DMA) measurements for the BI block copolymer was carried out by creep-recovery and stress relaxation testing. According to the creep-recovery graph, %95 of the sample came back to its original value and %5 of the sample was recovered after 170 minutes removing the force. Applied constant stress was 0.005 MPa. Constant strain rate was %20 according to the stress- relaxation test analysis. After removing the applied load, it was not observed a considerable creep rupture at poly(imide siloxane) block copolymer.

It was seen that the crystallinity in BII PIS block copolymer was higher comparing to PIS block copolymer BI via XRD characterization. Differences in the synthesis process were analyzed via SEM images of the block copolymer samples. The flexible form of poly(imide siloxane) samples (BI) had more homogeneous surface morphology than the pelletized grainy form of polyimide siloxane) samples (BII). It was realized by AFM analysis that the grainy nature of the BII sample related to the heating time of the BI sample. It was resulted that surface roughness will be corrected by increasing the molecular weight and amount of the APPS segments.

The poly(imide siloxane) powders were pelletized to obtain the pelleted form. It was pelleted as BII to compare performance changes in radiation shielding, to protect against ionizing radiation and to produce a difference in production.

Copolymer samples were pelletized to compare the radiation shielding properties of two differently produced samples, granular structure (BII), and flexible rubber sheet structure (BI), to optimize the shielding capacity against gamma rays. The behavior of flexible and pelletized poly(imide siloxane) block copolymer samples against gamma rays was investigated by the gamma transmission technique. Comparing the linear

attenuation coefficient increase in flexible and pelleted samples showed that flexible samples (given two different radioisotopes, such as Cs-137 and Co-60) perform better for the gamma shield.

In poly(imide siloxane) block copolymers, beta and neutron attenuation properties were compared to evaluate radiation penetration for flexible sheet form BI and pellet form BII. Modifications in the BII polymer because of pelleting the poly(imide siloxane) block copolymer improved radiation-shielding properties. The half-value layer (HVL) for negative beta particles was detected as ~9.5 cm. For neutrons, the half-value layer of the BII copolymer sample was obtained at 14.74 cm. Structural changes in the poly(imide siloxane) block copolymer, depending on the critical parameters of production, were found to lead to variations in beta and neutron attenuation. By pelletizing the granular structure in the BII sample, it was found to provide better beta and neutron shielding properties in poly(imide siloxane) block copolymers for use in medical applications.

Block copolymer samples were exposed to gamma radiation through the same irradiation plane at room temperature. The Co-60 Radioisope was used in this study and the activity of the source was ~ 10^6 Ci. The half-life of Co-60 radioisotope is 5.3 years. Gamma irradiation was carried by using Co-60 radioisotope and the applied dose rate is 10 kGy/h. The gamma irradiation was performed at 2.1 kGy/h by using Co-60 radioisotope. The irradiation dose time of PIS samples is 4.76 hours. Absorbed dose level of copolymer samples was selected as 10 kGy to examine the cumulative dose effect to investigate the absorbed dose-effect on irradiated material. Then, the irradiation effect on poly(imide siloxane) block copolymers was examined. The changes in gamma transmittance of the irradiated BI PIS samples were evaluated to examine the variations in the irradiation effect of gamma-rays at the irradiated sample. The gamma transmittance of the irradiated copolymer samples was performed at the same measurement conditions with the unirradiated samples by using the same experimental settlements and the same Cs-137 and Co-60 radioisotopes. The changes in HVL values of the unirradiated and the irradiated specimens were compared at two different gamma energy such as 0.662 MeV (emitted from Cs-137 radioisotope) and 1.25 MeV (emitted from Co-60 radioisotope). HVL results indicated that there was a decrease in HVL of the irradiated samples and this change was distinguished more clearly by using Cs-137 radioisotope. The same results for HVL values for irradiated poly(imide siloxane) samples were observed in beta and neutron transmissions, too. The decrease of the HVL of the irradiated poly(imide siloxane) samples indicated that the radiation shielding was enhanced by the formation of crosslinks of the irradiated poly(imide siloxane) samples at 10 kGy.

This study aimed to achieve the best results for the commercialization of the material and to make the material suitable for use in various industrial areas. Characterization of samples allowed us to examine flexible substrates for use in biomedical, solar technology, aerospace applications, and flexible microelectronic devices. Due to their characteristics, these materials have potential use in flexible organic microelectronic devices, solar cells as flexible substrates, biomaterials, medical devices, and aerospace applications. It has been concluded that these structures, which can be produced in any desired form and adapted to different configurations, are important and suitable for a wide variety of industrial applications.

POLİ (İMİD) SİLOKSAN BLOK KOPOLİMERİNİN SENTEZİ, ESNEK LEVHA VE PELLETLENMİŞ FORM HALİ İÇİN RADYASYON ZIRHLAMA ÖZELLİKLERİNDE IŞINLAMA ETKİSİNİN KARŞILAŞTIRILMASI

ÖZET

Esnek polimerler, esnek malzemelerin gerekli olduğu radyasyona bağlı çok çeşitli uygulamalarda, polimerik malzemelerde radyoizotopların etkili bir şekilde kullanılabilmesine imkan sağlamaları sağlamaları bakımından önemli role sahiptirler. Poli(imid siloksan) (PIS) blok kopolimerleri esnek bir biçimde kullanılabildiğinden, uyumlu polimerler olarak çok çeşitli endüstriyel malzemelere uygulanabilir.

Bu malzemeler biyomedikal ürünler, biyouyumlu malzemeler gibi çeşitli uygulama alanlarında ve güneş pili teknolojileri, havacılık ve uzay uygulamaları ve esnek organik elektronik cihazlar gibi çeşitli endüstriyel uygulamalarda kullanılmaya uygundur. Esnek polimerler, polimerik malzemelerde etkili kullanım sağladıkları için birçok uygulamada önemli bir rol oynarlar. Yüksek performanslı polimerlerin verimli hale getirilmesi ve geliştirilmesi, radyoizotop içeren radyofarmasötiklerin ilaçlarda, teşhislerde ve tıbbi ürünlerde kullanılmasını sağlar.

Bu çalışmada elektronikte, tıbbi uygulamalarda, havacılık teknolojilerinde ve güneş enerjisi teknolojisinde kullanılabilecek esnek altılıklar üretmeyi amaçladık. Üretilen poli(imid siloksan) (PIS) kopolimerleri, güneş pillerinde kullanım için gerekli olan esnek substratların özelliklerine sahiptir. Bunun yanısıra, elastomerik kauçuk poli (imid siloksan) blok kopolimer malzemeleri elektronikte geniş uygulama alanlarına sahiptir. İstenilen formda üretilebilen ve farklı konfigürasyonlarda uygun hale getirilebilen poli(imid siloksan) bu alanlarda önemlidir.

Kopolimer yapıları ve bu kopolimerlerin birçoğu yumuşak blok segmentlerinin ayarlanması ve arttırılmasıyla elde edilir ve kopolimerler yumuşak ve sert segment uzunluklarının ayarlanmasıyla sentezlenir. Bu sentetik yaklaşım, kopolimerlerin imid birimleriyle rastgele biçimde bağlanmış siloksan blokları ile sentezlenmesini destekler. Bu çalışmada, poli(imid siloksan) blok kopolimerleri, yapısal özelliklerdeki değişiklikleri incelemek için aminle sonlandırılmış APPS kullanılarak sentezlendi. Esnek poli(imid siloksan) blok kopolimerleri (BI), esnek kauçuk (elastomerik kauçuk) formunda üretildi.

Yapının esnek formu, ODA artırılarak ve APPS azaltılarak değiştirildi ve ayarlandı. Esnek poli(imid siloksan) blok kopolimerleri bu teknikle üretildi. Böylece, yeni poli (imid siloksan), diaminer ve aromatik dianhidritler olarak aminopropil sonlandırılmış siloksandan üretildi. ODA (4,4'-oksdianilin) ve BTDA (benzofenon -3 3′-4 4′-tetrakarboksilik dianhidrit) sert segmentlerdir, APPS ve BTDA yumuşak segmentlerdir. Poliimid sert bloğu oluşturmak için APPS ile ODA kullanıldı; polisiloksan yumuşak blok örnekleri APPS ve BTDA kullanılarak sentezlendi.

Böylece poli(imid siloksan) blok kopolimer örnekleri APPS ve BTDA ile ODA kullanılarak sentezlendi.

Numunelerin karakterizasyonu, esnek ve peletlenmiş yüksek performanslı kopolimer formlarının yapısını değerlendirmek için FTIR (Fourier Transform Kızılötesi Spektrofotometre) analizi kullanılarak gerçekleştirilmiştir. Blok kopolimer numunelerinin karakteristik kimyasal yapısının FTIR analizleri ile genel olarak siloksan Si-O ve karbon zincir tipi yapı olmak üzere iki kısımdan oluştuğu anlaşılmıştır. Daha sonra PIS örneklerinin yapısı formüle edildi.

BI ve BII kopolimer yapılarının TGA (Termo Gravimetrik Analiz) ve DSC (Diferansiyel Taramalı Kalorimetre) analizleri yapıldı. Karakterizasyon sonuçları belirlendi. Poli(imid siloksan) PIS kopolimerlerinin yüksek termal direnç özelliklerine sahip olduğu görülmüştür. TGA analizi azot atmosferi altında 38°C ila 800°C arasındaki 20°C min^{-1} ısıtma hızında yapıldı. BI blok kopolimerlerinin %18 madde kaybı ve BII blok kopolimerlerinin %11 madde kaybı 400 ila 500°C aralığında meydana geldi. Poli(imid siloksan) blok kopolimerleri çok sayıda organik çözücü içinde çözülmedi.

Yapılar elastik geri kazanım özelliklerini belirlemek için tek eksenli hidrolik pres testi ile mekanik olarak test edilmiştir. Tek eksenli hidrolik pres testinden sonra esnek kauçuk numuneler için bir X-ışını radyografi testi kullanıldı. Tek eksenli hidrolik pres testlerinde 10, 20 ve 30 ton presleme değerlerinde numuneler sıkıştırılarak preslenen preslenmemiş ve preslenmiş polimer numunelerinin deformasyon ve radyografik kontrastları incelenmiştir. Yapıların elastik kauçuk (elastomerik kauçuk) özellikleri sergilediği, böylece uygulanan presleme giderildikten sonra yapıların orijinal biçimlerine döndükleri görülmüştür. BI blok kopolimeri için Dinamik Mekanik Analiz (DMA) ölçümleri, sünme geri kazanımı ve stres gevşeme testi ile gerçekleştirildi. Sünme geri kazanım grafiğine göre, numunenin % 95'i orijinal değerine geri döndü ve 170 dakika sonra kuvvet kaldırıldıktan sonra numunenin %5'i geri kazanıldı. Uygulanan sabit stres 0.005 MPa idi. Stres-gevşeme testi analizine göre sabit gerinim oranı %20 idi. Uygulanan yükün kaldırılmasından sonra poli(imid siloksan) blok kopolimerinde önemli bir sünme ve kopma gözlenmedi.

BII PIS blok kopolimerindeki kristalinitenin XRD karakterizasyonu yoluyla PIS blok kopolimer BI ile karşılaştırıldığında daha yüksek olduğu görülmüştür. Sentez işlemindeki farklılıklar blok kopolimer numunelerinin SEM görüntüleri ile analiz edilmiştir. Poli(imid siloksan) numunelerinin (BI) esnek formu, poli(imid siloksan) numunelerinin (BII) peletleştirilmiş granüllü, toz formundan daha homojen bir yüzey morfolojisine sahipti. AFM analizi ile BII numunesinin granüllü, toz yapısının BI numunesinin ısıtma süresi ile ilgili olduğu anlaşıldı. Yüzey pürüzlülüğünün APPS segmentlerinin moleküler ağırlığı ve miktarı arttırılarak düzeltileceği sonucuna varılmıştır.

Poli(imid siloksan) tozları, pelet haline getirilmiş formu elde etmek üzere pelet peletleştirildi. Radyasyona karşı zırhlamada ki performans değişikliklerini karşılaştırmak, iyonlaştırıcı radyasyona karşı koruma ve üretim farkı yaratmak için BII olarak peletlendi.

Kopolimer numuneleri, gama ışınlarına karşı zırhlama kapasitesinin optimizasyonu için, granüler yapı (BII) ve esnek kauçuk levha yapıda olmak üzere (BI) iki farklı fiziksel biçimde üretilen numuneler, radyasyon zırhlama özelliklerinin karşılaştırılması amacıyla pelet haline getirildiler. Esnek ve peletlenmiş poli(imid siloksan) blok kopolimer numunelerinin gama ışınlarına karşı davranışı, gama iletim

tekniği ile incelenmiştir. Esnek ve pelet haline getirilmiş numunelerdeki lineer zayıflama katsayı artışının karşılaştırılması, esnek numunelerin (Cs-137 ve Co-60 gibi iki farklı radyoizotop göz önüne alındığında), gama kalkanı için daha uygun bir performans sergilediğini göstermiştir.

Poli(imid siloksan) blok kopolimerlerinde, BI esnek tabaka formu ve BII pelet formu için radyasyon penetrasyonunu değerlendirmek üzere, beta ve nötron zayıflama özellikleri karşılaştırıldı. Poli(imid siloksan) blok kopolimerinin peletlenmesi nedeniyle, BII polimerindeki modifikasyonlar radyasyon zırhlama özelliklerini geliştirdi. Negatif beta parçacıkları için yarı değerli katman (HVL)~9.5 cm olarak tespit edildi. Nötronlar için, BII kopolimer numunesinin yarı değerli tabakası 14.74 cm olarak elde edildi. Poli(imid siloksan) blok kopolimerindeki yapısal değişikliklerin, kritik üretim parametrelerine bağlı olarak, beta ve nötron zayıflamasında değişikliklere yol açtığı bulundu. BII örneğindeki granüler yapının peletlenmesiyle, tıbbi uygulamalarda kullanım için poli(imid siloksan) blok kopolimerlerin daha iyi beta ve nötron koruyucu özellikler sağladığı bulundu.

Blok kopolimer numuneleri, oda sıcaklığında aynı ışınlama düzleminden gama radyasyonuna maruz bırakıldı. Bu çalışmada Co-60 radyoizotop kullanıldı ve kaynağın aktivitesi ~ 10^6 Ci'dir. Co-60 radyoizotopunun yarı ömrü 5.3 yıldır. Gama ışıması Co-60 radyoizotop kullanılarak yapıldı ve uygulanan doz oranı 10 kGy/s idi. Gama ışıması Co-60 radyoizotop kullanılarak 2.1 kGy/s'de gerçekleştirildi. PIS örneklerinin ışınlama doz süresi 4.76 saatti. Işınlanmış materyal üzerindeki absorbe edilen doz etkisini araştırmak için kümülatif doz etkisini incelemek için kopolimer numunelerinin absorbe edilen doz seviyesi 10 kGy olarak seçildi. Daha sonra poli(imid siloksan) blok kopolimerleri üzerinde ışınlama etkisi incelendi. Işınlanmış BI PIS örneklerinin, gama geçirgenliğindeki değişiklikler, ışınlanan örnekte gama ışınlarının ışınım etkisindeki değişimlerini incelemek üzere değerlendirildi.

Işınlanmış kopolimer numunelerinin gama geçirgenliği, aynı deney yerleşimleri ve aynı Cs-137 ve Co-60 radyoizotopları kullanılarak ışınlanmamış numunelerle aynı ölçüm koşullarında gerçekleştirildi. Işınlanmamış ve ışınlanmış örneklerin HVL değerlerindeki değişiklikler 0.662 MeV (Cs-137 radyoizotoptan yayılan) ve 1.25 MeV (Co-60 radyoizotoptan yayılan) gibi iki farklı gama enerjisinde karşılaştırıldı. HVL sonuçları ışınlanan örneklerin HVL'sinde bir azalma olduğunu gösterdi ve bu değişiklik Cs-137 radyoizotop kullanılarak daha net bir şekilde ayırt edildi. Işınlanmış poli(imid siloksan) numuneleri için HVL değerleri beta ve nötron iletimlerinde de gözlenmiştir. Işınlanmış poli(imid siloksan) numunelerinin HVL'sinin azalması, radyasyon zırhlanmasının, 10 kGy'de ışınlanmış poli(imid siloksan) örneklerinin çapraz bağlarının oluşturulmasıyla arttığını gösterdi.

Bu çalışma, malzemeninin ticarileştirilmesi için en iyi sonuçları elde etmeyi ve malzemeyi çeşitli endüstriyel alanlarda kullanıma uygun hale getirmeyi amaçlamıştır. Numunelerin karakterizasyonu, biyomedikal, güneş enerjisi teknolojisi, uzay-havacılık uygulamaları ve esnek mikroelektronik cihazlarda kullanım için esnek substratları incelememizi sağladı. Karakteristik özelliklerinden dolayı, bu malzemeler esnek organik mikroelektronik cihazlarda, biyomateryal olarak tıbbi cihazlarda, havacılık ve uzay uygulamalarında ve esnek altlıklar olarak, güneş pillerinde potansiyel kullanıma sahiptir. İstenen herhangi bir biçimde üretilebilen ve farklı konfigürasyonlara uyarlanabilen bu yapıların, çok çeşitli endüstriyel uygulamalar için önemli ve uygun olduğu sonucuna varılmıştır.

1. INTRODUCTION

There have been a lot of materials in the industry, and new ones are being added to them every year. Examining them separately is impossible so, they are divided into classes of similar structure and characteristics and introduced commonly[1]. There are different classifications in the old sources. However, the most consistent and most appropriate classification is based on interatomic bond types by making use of significant advances in material science. According to this, the materials are divided into three classes: a) metals b) ceramics and c) plastics [2-3].

Plastics are one of three important materials and these materials are also called polymers, organic materials, or resins because the basic element C (carbon) in the composition is the main element C atoms bonded by chain covalent bonds to each other form the backbone of the polymers [1-4]. They belong to the group of polymers chemically. Plastics or polymers are materials, which generally contain covalent bonds of non-metallic elements. C fibers with the tensile strength of around 3100 MPa are considered to be one of the highest strength materials. The most important of the side atoms attached to C chains is H (Hydrogen). In addition to the C atom, it is usually H, and some may contain Cl (Chloride), F (Fluoride), O (Oxygen), N (Nitrogen), and S (Sulphide) [1]. Hundreds of structural polymer types have been developed depending on the type and arrangement of the side atoms such as Cl, F, N, O, and S. That is why polymers are substances made of large molecules[5-7].

Small molecules that are connected by chemical bonds to form polymer molecules are called monomers [1-2, 6]. Molecular individuals, called monomers, are transformed into very large, giant molecules when covalent bonds are attached when a large number of replicates become available. Thus, solid-state polymers of large giant molecules are obtained and are therefore called polymers [1]. In a polymer molecule called macromolecule, hundreds, thousands, sometimes more, of these structural units are interconnected [1,2]. Reactions that convert to polymer molecules starting from monomer units are called polymerization reactions[1,2]. The structural units of the polymer are equal to or substantially equal to the monomer[1,2]. The large size and

complexity of their molecules cause them to have these substances extremely different and superior properties [1,2]. They exist in the gas, liquid, and solid-state forms depending on the number of units in the molecular structure obtained by the addition of small molecular units (monomers) to each other. Paints, varnishes, adhesives, and similar materials in liquid form are also considered as polymers. Such materials have been named plastic since they are softened at a certain stage of their production and they are shaped by injecting plastic into a mold. Plastics are lightweight and easily shaped, making the most complex geometric shapes easily available [1,3]. Therefore, they have a wide range of applications. Some of the materials classified as plastics are natural and some are synthetic. Wood, leather, wool, and similar fibers, which are used by humans long before metals, are natural polymers. Most of the plastics used in the industry today are synthetic polymers [1,2].

Degree in polymerization is measured by "mere" numbers in a polymer chain[1]. Linear polymers which are one of the two main groups of polymers are divided into two main groups as vinyl and butadiene. If there is the same kind of "mer" along the molecular chain, linear polymers are called "homopolymers" or "polymers" and [1,2]. These have the same bond angles and bond lengths along chains, and atoms in these polymers are arranged symmetrically, thereby increasing the tendency to form a crystalline structure by matching between adjacent chains. Some polymers have more than one type of "mer" and these are called "copolymers" and are considered to be a kind of solid melt. The copolymers can be of two types. The first consists of a mixture of different types of polymer chains containing the same type of mer. In the second type of copolymer, there is more than one kind of "mer" in the same chain, so the structure of all chains in the whole mass is the same[1, 3, 7].

Copolymers in different proportions and different types of "mers" are arranged in different ways to form a very different structure [1]. The "mers" may be sequenced sequentially or randomly along the chain or may be attached to a chain containing the same type of "mere" in the form of another type of chain branch. Copolymers are irregular in structure, hard to deform, and have high saturation. For example, it forms a copolymer of vinyl chloride with vinylidene chloride (PVC). This copolymer has high strength and modulus of elasticity, as well as high toughness, good impact resistance [1,2].

In the synthesis of several copolymers, immense commercial success was gained by repeating units with different combinations [1,2]. Synthesis of copolymer supplies the capability for homopolymer properties in the desired direction by properly chosen repeated the second unit. For changing some polymer properties such as thermal stability, toughness, crystallinity, and flexibility, the copolymerization technique has been utilized [3].

The addition of flexible polysiloxane components to the thermally suitable polyimide made it possible to obtain several attractive polymeric materials [5-6]. In this way, they exhibit suitable material behavior at high and low temperatures. These polymeric materials are resistant to oxidation and radiation and their electrical properties are sufficient for many applications [2].

The block copolymers have low water sorption, well processability, low dielectric constants, and a perfect adhesion property [2-3]. Therefore, these materials have become appealing materials in microelectronic, printed circuits, medical and aerospace applications. The present and developing technology in this important class of polymers have been described by review articles that have appeared [4-9].

This introduction will center first on the areas nearly related to the research topic. This thesis is divided into seven sections. The first two sections tell about polymers and polymer types, copolymers, their structure, and types. These first two sections also discuss common synthetic techniques, which were used in the preparation of polyimides and poly(imide siloxane) in the literature and also discusses some general aspects and the synthesis of poly(imide siloxane) block copolymers. The third section is about radiation, radiation types, and interaction with the materials. The fourth and fifth sections cover techniques for the production of the samples, characterization in poly(imide siloxane) block copolymers, and application of radiation transmission technique with irradiation effect on the radiation shielding properties of poly(imide siloxane) block copolymer samples. The sixth section covers the discussion part on experimental results and the seventh section is the conclusion part of this study.

2. POLYMERS

The polymer industry began in 1839 when Goodyear found the vulcanization process. Artificial polymeric substances were obtained for the first time in the early 19th century. Such materials were made on an industrial scale for various purposes at the beginning of the 20th century. However, the basic scientific principles governing the formation of synthetic high polymers were found between 1925-1935 [2]. Although, Hevea rubber has some uses it has become an important raw material with the vulcanization process. The demand for rubber increased rapidly with the growth of the automobile industry [2]. For the first time, Staudinger gave formulas for polystyrene and polyoxymethylene (paraformaldehyde) and explained the inability to crystallize polymers such as polystyrene through the lack of stereoregular structure in a monograph published in 1932. The Staudinger theory was the beginning of important studies in that it suggested that chain length could be identified, although later proved to be wrong. The investigation of polycondensations continued with Carothers' work in 1928, which was initiated by Dupont laboratories. In these studies, it was investigated that the formation of dimers or cyclic monomers can be compared with those of chain molecules. Depending on the ring size of stability in cyclic components was emphasized and researchers at Corning Class Works were working on the production of the heat-resistant polysiloxane. This study was completed by a synthesis of polydimethylsiloxane at General Electric Co. Polyurethanes are described by Bayer at World War II as crosslinking was found to increase elasticity and polyethylene was used in the isolation of radar cables during World War II. The tacticity of chain molecules in semi-crystalline polymers, degradation of polyacrylonitrile, and mercerization of cellulose were monitored in 1956 by IR spectroscopy. The first detailed polymerization was carried out about the crystalline vinyl monomer in 1960. In the 1950s, very high molecular weight polypeptides began to be produced. Dupont's patents show that highly elastic polymers can be obtained without cross-linking compositions of soft and crystallizable hard polymers that are not crystallized [10].

Poly(imide Siloxane) Block Copolymers

The chemistry, physical chemistry, and technology of polymeric materials showed great improvements especially towards the end of the 20th century and at the beginning of the 21st century [2]. In particular, research has intensified on engineering plastics, polymeric blends, and elastomers, which are defined as high-tech materials [2]. Many studies have been carried out on engineering applications of high-tech materials. Synthetic fibers (fibers), plastics, and synthetic rubbers (elastomers), known as synthetic polymers, are a wide variety of applications in the industry [2].

The usage of flexible substrates presents new probabilities in the application for solar cells, such as in building integration by application on rough surfaces as tiles. Besides, flexible substrates are thin and lightweight, which makes them more flexible than rigid cells. Furthermore, flexible solar cells in space applications are very appealing, which saves weight and so decreases launch expenses considerably [11].

The advantage of flexible solar cells and even the most important is that they allow low costs in production costs. Roll–to–roll covering is thought more appropriate from a manufacturing point of view than operation at rigid (glass) substrates. Moreover, the energy and expenses necessitated for manufacturing solar cells on the glass are mostly utilized for substrates and lid glasses [12].

Affordable, glassless, and subtle substrates jointly with a flexible and thin encapsulant, assemble the utility of flexible solar cells in cost-effective production. Lastly, ecological utilities benefit originate from assumed lower energy pay-back time and lowered module weight if assembled on cars, caravans, or RVs. Smaller batteries (e.g. for cars, products of the user) can be utilized and the lifetime of the battery will be increased when it was recharged and backed up by PV sources [13].

Copolymerization is one of the most important and successful polymerization reaction types that enables to produce new materials with intended properties during the connection of two structures with different chemical and physical properties in the same polymer chain [2]. It is also of great technological importance [2] to understand the effect of chemical structure on reactivity and useful to know the behavior of monomers in copolymerization. A polymeric product of the desired properties can be designed and prepared with greater freedom of movement by using this method. It is possible to make an almost unlimited number of different polymers because the

relative amounts of the monomers entering the polymer can be altered. Producing is also possible, which change from plastic properties to elastomer properties by varying the amounts of the second or third components from the reacting components.

The application areas of multi-component copolymers are extremely wide. The model outlines developed in the copolymerization technique can be summarized as follows: Important basic properties such as heat resistance, flexibility, resistance to solvents, and strength are provided by the proper selection of the two components introduced into the copolymer in large proportions. On the other hand, the third monomer introduced into the copolymer is used where highly specific behavior, such as vulcanisability, dyeability, fluidity properties, etc., becomes important. Block copolymer synthesis is based on reacting polymers with various end groups under various conditions to react to these groups. The application of this method is extremely simple in step (condensation) polymerization reactions. Suppose that two polyamides of various types are prepared separately. One of them contains amine groups at both ends and the other contains carboxyl groups at both ends. If we mix these simple polymers and further polymerize them, it is obtained the block copolymer. Schematic of block copolymer architectures and reaction mechanisms that is occurred at solution imidization are presented in Figure 2.1 and Figure 2.2 respectively [9].

A-B diblock copolymer

The addition of a third block produces an A-B-A or B-A-B triblock copolymer.

Coupling blocks together gives rise to [A-B]$_n$ multi-block copolymers where n is greater than 1.

Three or more diblock copolymers may be coupled at a single junction point to form radial or star block copolymers.

Sequences of one monomer "grafted" onto a "backbone" of a second monomer result in graft copolymers. Copolymerization results from the formation of active sites at points on the polymer molecules other than the ends, followed by exposure to a second monomer.

Figure 2.1 : Formation scheme of different block copolymer types [9].
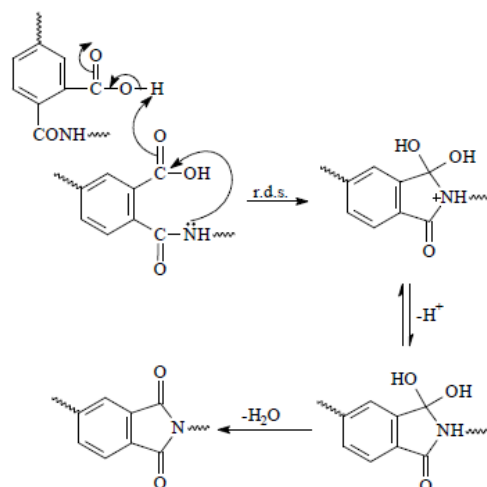
Figure 2.2 : Possible reaction mechanism for the solution imidization process [9].

Technological progress is needed for the development of flexible, lightweight, and economic substrates for using these substrates in many industrial application areas like energy storage systems and electronics. Medical applications, which consist of nanotechnology and polymeric materials present attention to scientific and industrial areas.

Polyimides have become one of the most considerable and sophisticated types of high-performance polymers with their excellent mechanical and thermal properties [2-8]. Polyimides are the most proper materials to be utilized at high temperatures[3-5]. Polyimides have thermal resistance and stability. Their surfaces are smoother than metal substrates [15,16]. These polymers appear to find a growing application in several fields. The polyimides present great resistance to irradiation, mechanical deformation, solvent effects. A balance is observed between the mechanical and electrical properties of these polymers. These polymers were used as adhesives, sealants, foaming agents, and as electronics, films, and fibers by extensive and detailed research on polyimides. Polyimides containing aromatic units in their main chains are generally prepared by polycondensation reactions carried out in two steps [2]. In the first step, the dianhydride of tetracarboxylic acid and a diamine are converted to the polyamic acid by acylation reaction in a suitable polar solvent. In the second step, the polyamic acid is thermally or chemically subjected to a dehydrocyclization reaction

called imidization. Polyimides with superior thermal, physical, and mechanical properties are among the interesting engineering plastics[1].

The main applications in polyimides are aerospace technology, automotive, and electronics industries through their long-term use at high temperatures. Processing problems limit the use of these wonderful polymeric materials [2].

The usage area of polyimides also contains nanotechnology with pharmaceutical technology and drug delivery. All these usage areas show that polyimides are quite attractive material in biomedical technologies and clinical trials, too.

Flexible substrates are accepted interesting materials depending on their properties like being lightweight, multiform, and nature-friendly. Energy systems in the future require for developing advanced materials, which include flexible substrates [3-6]. In today, polyethylene terephthalate (PET) substrates are used in solar cell technological applications as flexible substrates. However, PET has low heat and mechanical resistance. Finding an alternative substrates material such as poly(imide siloxane) (PIS) is very necessary. Depending on high physical performance against aggressive environmental conditions, PIS can be used as alternating material to PET. PIS contains polyimide and it is a multipurpose material with insulating, lightweight properties, high mechanical, and thermal resistance [2,7-8,14-18].

Polymers are important materials in the application of nanoparticles for medical devices. Success factors are taken notice for the quality assurance to guarantee success criteria about the biocompatibility applications in high-performance polymers. Biocompatibility applications include excessive heat and vibration of poly(imide siloxane) (PIS) block copolymers because of its ability to proceed with mechanical properties under the harshest conditions.

Within this work, producing poly(imide siloxane) polymer substrates in order to use in flexible solar cells, flexible electronic devices to use in aerospace and medical applications are aimed. Poly(imide siloxane) hybrid polymers have higher mechanical properties, higher heat resistance, and high radiation resistance than other polymer types. Through this property of poly(imide siloxane), it was planned to contribute to the higher efficiency of flexible solar cells by increasing properties of polyimide which are used in solar cells, medical, and also in aerospace technologies. Poly(imide siloxane) which was produced from the combination of flexible polysiloxane and

polyimide made it easier to be processable by this technique. Poly(imide siloxane) has high flexibility, high mechanical and temperature properties, and resistance to decompose under any aggressive oxygen environment.

We have studied for key factors of project success in the production and application of PIS block copolymers (for example; to get a suitable material in the usage of positive bacteria, which has a lack of immunogenic properties). PIS block copolymer samples are derived in two forms as flexible (BI) and granular (BII) samples by the combination of soft and hard blocks [2]. When polyimide forms the hard block segment, polysiloxane forms the soft block segments. PIS block copolymer shows more suitable thermal stability and chemical inertness than polyimide. PIS block copolymer also has high resistance against mechanical effects such as impact resistance and oxygen degradation effect. PIS owns high hydrophobicity and humidity barrier. These excellent properties are also enough to apply these materials for storage systems in the energy field. Also, PIS block copolymer samples show features of thermoplastics or thermoplastic elastomers [4,5,19-21]. Many studies are seen in the literature, which is synthesized by arranging block copolymers [17-19,21-28]. PIS copolymers can entrap metal salt. The polymer micelle can provide the microenvironment and the polymer contributes as a reactor in the production of metallic particles. The core of polymeric micelles is capable to behave as a microreactor and a drug [29-32].

The researches on different production processes for polymeric nanostructures develop the important industrial areas for the polymer applications at drug/gene delivery in the future trend [33-36]. The drug/gene delivery systems with a nanoscale-sized feature carry great potential at the effective biological systems and the drugs/genes. This study also aims to assess the produced polymeric structure which controls gamma radiation emission from the PIS block copolymer surface for the drugs including gamma radiation emitters. For this purpose, the mechanical degradation of the PIS block copolymer was examined by using two different radiation test techniques. One of them is the X-ray radiography technique and the other is gamma transmission techniques (by using Cs-137 and Co-60 radioisotopes) in this study. In the X-ray radiography technique, the radiographic examination clarified that there was not a considerable difference between the radiographic contrasts of the unpressed and the pressed BI

samples after the samples have been compressed at three different pressing values such as 10, 20 and 30 tons by using the uniaxial hydraulic press test.

Radiopharmaceuticals having radioisotopes in drug research and development, diagnostic and therapeutic utilizations have developed based on the improvement in high-performance nonrigid polymers. Flexible polymers commit a remarkable part in radiation relevant medical utilizations since these polymers enable to ensure efficient usage with the radioisotopes for polymeric biomaterials [18,22-23]. Poly(imide siloxane) (PIS) block copolymers can be practicable for biocompatible smart polymers as they can be utilized in a flexible form within nervous system restoration and reducing bacterial adhesion [33-35].

Besides, high-performance polymers (such as PIS) have been enhanced for utilizing in new generation cancer cure by encapsulating radiation emitters like Yttrium-90 radioisotope in the center of the polymer [36]. Polymer reaction versus irradiation can be considerably vary depending on the parameters of synthesis in the polymer. As a consequence, responses in the flexible polymers and polyimide materials versus the ionizing radiation are analyzed significantly for using them in the radiation process [33-35]. Gamma irradiation and beta particles can be utilized in medical sterilization and they possess an alike anti-microbiological impact comparing to each other. The impact of polymers mainly depends on the penetration depth in the radiation and thereby can be utilized by radiation transmission techniques. On PIS copolymers having microspheres, penetration depth can be changed through insignificant alterations in the microsphere wall thickness of the polymer, and may finally cause a deficient absorbed dose level. The irradiation may be applied on both sides of the copolymer to lap over the penetration depth as a possible solution. Efficiency in radiation treatments (such as sterilization utilizations) is connected to the microsphere double-side effect through insignificant alterations in the polymer thickness [18,22-23]. If radiation treatment efficacy is thought of as insufficient, two overlapping doses are thought of as a resolution in double-sided radiation exposure [18,22]. On the other hand, density or the trivial thickness changes in the polymers can alter the efficiency of the radiation transmittance in the therapy.

Radioactive additive (the precursor isotope) can be put into or onto the system of the medical device. Also, neutron activation can be fulfilled with the addition of the radioactive isotope in medical utilization [37]. However, the radiation attenuation of a

11

polymer can alter the effectiveness of the radioactive isotope for the medical utilisations. Increasing thickness in the polymer wall can negatively influence the reduction in radiation transmission. For this reason, this can not ensure sufficient radiation transmittance to the other side to provide proper sterilization in the polymer medical products as in treat balloons and balloon catheters [38].

Various polymers are utilized in medical applications [18,22-23,33-34]. Many polymer materials like polyethylene are used usually as flexible polymer substrates in several applications (in medicine and radiopharmaceutical science). Nevertheless, low thermal and mechanical resistances of polyethylene are needed to be developed the alternative flexible polymer with high physical performance (such as PIS) and to utilize them in the aggressive environmental conditions [35-38]. In this regard, polyimide materials are multi-purpose, versatile, important, and high-performance polymers through its great thermal and mechanical features [4,6-7]. Polyimides with lightweight, insulating, and flexible features are polymers that resist high temperatures and they possess excellent mechanical performance comparing to other polymers. Surfaces of the polyimides and poly(imide siloxane)s are smoother than the other flexible polymers. Also, the thermal resistance and mechanical performance of poly(imide siloxanes) are higher than the thermal resistance and mechanical performance of polysiloxane [15]. There is some information in the literature about the beta attenuation coefficients of plexiglass and several polymer composites [8-39].

There are several pieces of information about the neutron attenuation of polymer composites [40-42]. Also, some information is present about the neutron attenuation of polydimethylsiloxane composite [43] and the macroscopic cross-section of polydimethylsiloxane [44]. The mean free path in the neutron is detected as the average distance of the neutron traveling between two consecutive scatterings at ethylene propylene diene monomer as flexible polymer [45]. Polyethylene and polyvinyl chloride pellets are added into concrete to increase its neutron attenuation in medical applications [46]. Alternative smart polymers show some performance for the radiation shielding in irradiation fields in neutrons and gamma rays. On the other hand, broad comparison like the half-value layer (HVL) in PIS block copolymers between neutrons and beta particles is not existent. Negative beta particles are needed to be used in many medical utilizations.

The human body can be acknowledged as corrosive and antagonistic ambiance because the body includes complex organics and water. However, PIS block copolymer presents impact resistance, great adhesion, and resistance against decomposition under oxygen. PIS block copolymer also shows the properties of thermoplastic elastomers and thermoplastics [4,8]. Such properties as high humidity barrier and hydrophobicity properties in the PIS block copolymer make these materials suitable for use in medical devices in the body. Also, its humidity barrier and high hydrophobicity features can be assisted to solve energy consumption problems within energy storage systems in the smart wearable body or as sub-skin devices. PIS block copolymers possess the biomimetic features (like the human body) depending on its high contents of carbon and hydrogen. For that reason, the interactions of neutrons and negative beta particles with PIS block copolymers were utilized to identify the ionizing radiation behavior in PIS block copolymers within biocompatible devices. A comparison in the changes of HVL within PIS block copolymers was utilized for neutrons and negative beta particles to peruse the decrease of the radiation intensity by one half in this study. BI sample was synthesized as a flexible sheet form and the BII sample was synthesized in the grainy form of PIS block copolymer. Synthesized BII grains were pelletized to get proper shielding against beta and neutrons. For that purpose, the results of the flexible form (BI) and pelletized grains of PIS block copolymers (BII) were examined regardful the radiation attenuation. Applications of Sr-90 radioisotope (for negative beta particles) and ^{241}Pu-Be (for neutrons) for the radiation transmission method in air enabled to examine the structure of poly(imide siloxane) block copolymer and its radiation shielding property. Therefore, beta and neutron transmissions were analyzed for the use of poly(imide siloxane) block copolymer in wound healing, drug delivery, and several medical engineering applications, etc.

3. RADIATION AND INTERACTION OF RADIATION WITH MATERIALS

3.1 Definition of Radiation, Types and Radiation Sources

Radiation is the propagation and emission of energy in the waves, particles, or rays form. By another saying, radiation is formed by energy moving through space in the particles or waves form. Energy is sent off by the light form, X-rays, nuclear particles, or heat in radiation. Heat, light, microwaves, and radio waves are familiar with radiation types. Sunshine is one of the radiation forms. Light, suntans, and heat are delivered by the sun [48].

Figure 3.1 : Background radiation [48].

Radiation consists of the electromagnetic spectrum and releasing of particles. People who live in the granite regions or on mineralized sands get more terrestrial radiation and also people who live or work at high altitudes get much more cosmic radiation [48].

Sun rays, X-rays, which are used to diagnose diseases, from radio waves used for communication to microwave ovens, which are used to heat food in the kitchen are some of the many natural radioisotopes that we are exposed our daily lives. It is understood that the energy source does not need to be in the form of light or magnetism to be called radiation. Because radiation is derived from the waves radiating (moving outward in all directions) from a source, the intensity in all types for radiation from a

point source is computed by using an inverse-square law concerning the distance from its source. Natural radioisotopes are natural sources of radiation. Heavy elements (those with more than 83 protons in their nuclei) transform into smaller atoms to become more stable, emitting particles and energy waves from their nuclei. Elements that become more stable and give energy in this way are called "radioactive elements."

Electromagnetic radiation mostly exhibits "wave-like" behavior like radio waves, visible light, and so on. When electromagnetic radiation interacts with matter, transmission, diffraction patterns, detection of radio signals, and like these occurrences happen. The best definition was done by the name of a photon, which is thought of as a wave packet. According to this definition, neutral bunches of energy, which travel in a space at the light velocity, which is 300000 km/sec. is called as photons [47]. Radiation is divided into two groups depending on the energy of the radiated particles: Non-ionizing radiation and ionizing radiation. In non-ionized radiation, there is no enough energy to ionize molecules and atoms. On the other hand, ionizing radiation possesses enough energy to eject electrons from an atom or molecule, and ionizing radiation is known as ion-forming radiation in the particle it strikes.

The longer wavelength, lower frequency waves (like heat and radio waves) have less energy than the shorter wavelength, higher frequency waves (like gamma and X- rays). All of electromagnetic (EM) radiation isn't ionizing radiation. The waves with high frequency and the short wavelength in the electromagnetic spectrum are only ionizing, which contains X- rays and gamma rays [47].
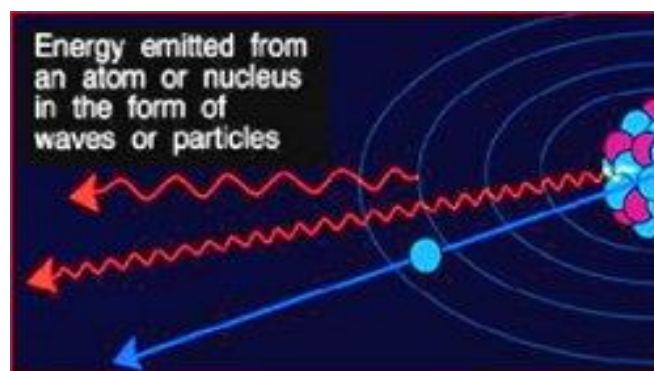
Figure 3.2 : Energy emitted from an atom or nucleus in the waves or particle forms [47].

Non-ionizing radiation: Energy is released from the lower-energy region of the electromagnetic spectrum. Non-ionizing radiation has longer wavelengths and lowers energy levels than ionizing radiation. Non-ionizing radiation isn't powerful enough to

change the structure in atoms when it touches with the atoms in matter. On the other hand, it can cause harmful biological effects. It is powerful enough to heat tissue. Microwaves, radio waves, visible light, and infrared (heat) waves from a heat source and ultraviolet light are the examples for non-ionizing radiation. Those are types of the electromagnetic spectrum. Radio waves are derived in two ways, either they are radiated by stars or produced by the human to transmit audio data. Stars and galaxies generate microwave radiation. It is mostly used to heat food or transmit data. Warm bodies, including living organisms, emit infrared radiation. Infrared radiation is also generated by gases and dust between stars, too. The visible spectrum is the most narrow part of the spectrum sensed by human eyes. It's radiated by lamps, stars, and some chemical reactions. Ultraviolet radiation is radiated by stars (and the Sun). The non-ionizing lower energies in the lower ultraviolet spectrum don't ionize atoms but can break the inter-atomic bonds that form molecules. It destroys molecules rather than atoms. For instance, if anybody is overexposed, it causes sunburns, skin cancer (long-wavelength solar ultraviolet causes sunburns and skin cancer), and cataracts [47]. Infrared and microwaves don't have a longer wavelength than UV in visible light, so they do not destroy bonds but reason oscillations in the bonds, that is perceived as heat. Radio wavelengths and any other non-ionizing radiation types usually are not accepted as destructive to biological systems [49].

Ionizing radiation:

Ionizing radiation derives from the nuclei of atoms. If one or more electrons are added to or removed one or more electrons from atoms or molecules, in this way ions are obtained. Ionization can be derived from electrical discharges, high temperatures, or nuclear radiation. If radiation removes electrons from atoms and produces ions, it is called ionizing radiation. Ionizing radiation with high doses can produce tissue or skin detriment intensely.

While most atoms are stable, some are unstable. Certain atoms alter or disintegrate into new atoms. Those types of atoms are called as 'unstable' or 'radioactive'. An unstable atom contains excess internal energy, so the nucleus alters spontaneously. It is referred to as 'radioactive decay'. Excess energy as radiation is radiated from an unstable nucleus in gamma rays form of sub-atomic particles in a fast-moving way. The hydrogen atom is the simplest. It contains one electron, which orbits around a nucleus on a proton. If an atom contains one proton in the nucleus, it is a hydrogen

atom as shown in Figure 4.3. Deuterium is Hydrogen-2 and tritium is hydrogen-3. On the other hand, while the chemical properties are the same, their nuclear features are very different (for instance, tritium is radioactive). Different models of an element can be stable or unstable (radioactive), but because they are models of the same element, they have identical chemical and biological features.
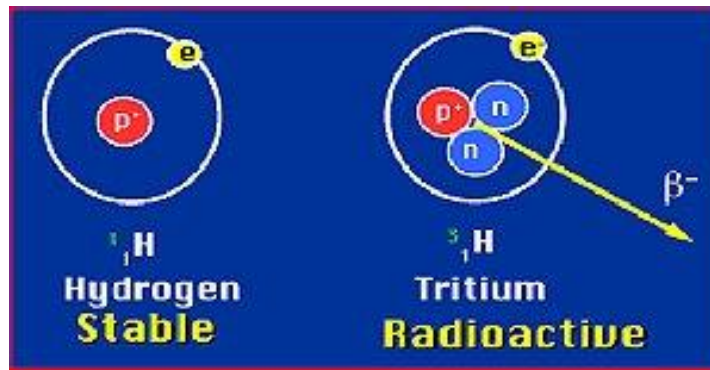
Figure 3.3 : Isotopes of hydrogen atoms [47].

If an unstable atom decays with radiation of an alpha or beta particle, it turns in to a new element and also can radiate gamma rays. These emissions are defined as gamma, beta, and alpha radiation. An unstable atom advances with one or more steps to turn in to a stable state form, which isn't radioactive anymore [48]**.**

Ionizing radiation consists of two parts as particle and wave type. Particle-type ionizing radiations are alpha particles, beta particles, and neutrons. Wave-type ionizing radiations are X-rays and gamma rays. Particle-type radiation consists of atomic or subatomic particles like electrons, protons, etc., that have the energy type as kinetic energy or mass in motion. The energy in electromagnetic radiation is transported by oscillating electric and magnetic fields by passing from space at the light speed. Alpha particles and beta particles are accepted as direct ionizing. They transport a charge and so, interact directly with electrons having to ionic forces (same charges push each other; opposite charges attract each other). The neutrons are indirect ionizing particles. They are indirect ionizing because they don't have an electrical charge. Ionization is derived from charged particles, that are generated on collisions with atomic nuclei. Gamma and X-rays are the waveforms of ionizing radiation. These are also accepted as indirect ionizing radiation because they are electrically neutral (as in all electromagnetic radiations). These types of radiation don't interact with electrons via coulombic forces. Figure 3.4 shows the transition of alpha, beta particles, and gamma-ray through three different materials [47].
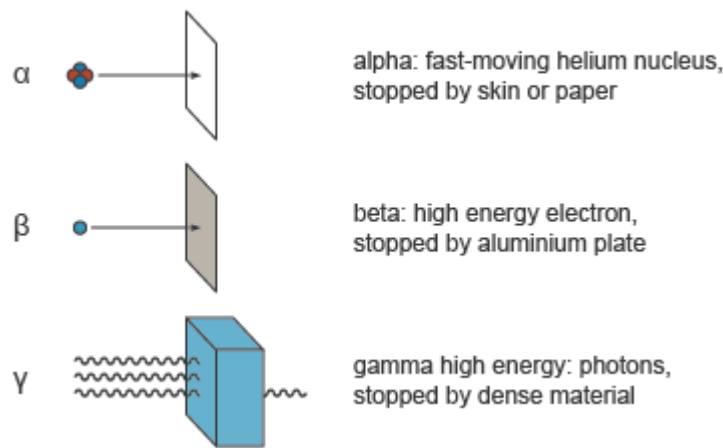
Figure 3.4 : Transition of alpha, beta particles, and gamma-ray through three different materials [47].

There are some important terms to be used in ionizing radiation. Those are activity, dose, and equivalent dose. Those are below:

Activity (Rdioactivity)

The number of decayed atoms per unit time shows the radioisotope activity and that is the feature of certain nuclides of radiating radiation by a spontaneous transformation of their nuclei. Several units in (radio) activity have been utilized containing curie (1 Ci = 3.7×10^{10} disintegrations per second) and becquerel (1 Bq = 1 disintegration per second) [50]. The decay rate of the radioactive source is known as activity A (t) and it is described as one radioactive disintegration per second. It is shown as 1 Curie $= 3.7 \times 10^{10}$ radioactive disintegrations/sec. (or the new unit Becquerel - Bq). The Becquerel (Bq) is used as the SI unit to measure the nuclear transformations rate. The radioactive material amount is gauged with Becquerel (Bq), which allows us to check against the typical radioactivity of some natural and other materials. Ionizing radiation is produced by atomic disintegration. The Curie (Ci) is an old unit. The curie is the activity of 1 gram of radium-226 [47, 51].

Dose

The gray (Gy) is the international (SI) unit measurement for absorbed dose, and it is described as 1 joule of energy deposited in 1 kilogram of mass. Gray (Gy) is the new international system (SI) radiation dose unit, that is described as absorbed energy per unit mass of tissue. "Gray" has replaced the older "rad" defined as the new SI unit. The rad is the old measure unit for this, and it is called "radiation absorbed dose."

1 Gy = 100 rad. If it is stated in short, that would be 1 Gy = 1 joule/kilogram = 100 rad. Gray is utilized for any form of radiation (gamma, alpha, beta, neutron), but it does not define the biological effects of different radiations [51].

Equivalent Dose

If any amount of energy of any type of ionizing radiation is absorbed by the human body, that can cause harm to health [51]. How much energy of the ionizing radiation is interacted with the body and deposited per unit mass of the part (or whole) of the body has to be known? Only by doing this, we can estimate biological effects. Biological effects of radiation are estimated in "Sievert" units. "Rem" is an older designation. If Gray is multiplied by the "radiation weighting factor" (also known as the "quality factor") associated with a specific type of radiation, Sievert is calculated. Sievert (Sv) (1 Sv = 1 Joule per kilogram) is used to calculate the health effects of ionizing radiation(both external and internal). Sievert is Standard International (SI) special name unit of dose equivalent (H), equivalent dose (HT), effective dose (E), weighted dose, and organ dose equivalent. Rem is also known as roentgen equivalent, man is a unit of equivalent dose. All radiation doesn't have the same biological effect (even in the same amount of absorbed dose). Rem is related to the absorbed dose in human tissue to the effective biological damage of the radiation. It is determined by multiplying the rads number by the quality factor (a number reflecting the potential damage caused by the particular type of radiation). The rem is a traditional equivalent dose unit, but it is replaced by the sievert (Sv), which 1 Sievert equals 100 rem. Dose equivalent is the product of absorbed dose, which is given to organ or tissue, and multiplied by a quality factor. It is sometimes multiplied by other parameters for accounting in the potential results from the absorbed dose as a biological effect (Quality factor). It is expressed in rem (traditional units) or sieverts (SI units). Quality factor (Q) is the factor by which the absorbed dose (rad or gray) is multiplied to obtain the biological damage (rem or sievert) to the exposed tissue on a common scale for all ionizing radiation. It is used because some types of radiation, such as alpha particles, are more biologically damaging to live tissue than other types of radiation when the absorbed dose from both is equal. The quality factor term has been replaced by the "radiation weighting factor" in the latest system of recommendations for radiation protection [51]. Neutron, proton, and alpha radiation are 5-20 times more harmful than the same amount of the absorbed dose of beta or gamma radiation [51]. The effective

dose of radiation is measured by the Sievert unit. Most of the doses are in millisieverts (mSv). 2 mSv per year from the natural background, and maybe more from medical procedures are received. 100 mSv or anything less than that value is harmless [48].

Sources of Radiation Exposure

Radiation permanently exists in the environment, in the air, water, food, soil, and living organisms. People receive a large proportion of the average annual radiation dose by results from natural environmental sources. Everybody is exposed, on average to 2.4 mSv/yr of ionizing radiation from natural sources. In some parts of the world, the natural radiation dose maybe 5 to 10-times higher [47]. Radiation can penetrate the skin and reach internal organs and tissues, and it is called penetrating radiation. Photons (gamma rays and X-rays), neutrons, and protons are penetrating radiations, but alpha particles and all but extremely high-energy beta particles are not considered penetrating radiation [51].

Ionizing radiation carries a very high-energy of electromagnetic radiation, so it can cause damage to matter and especially living tissue. Therefore, it is very dangerous at high levels and it is necessary to take under control the exposure. The exposure can be monitored easily by detecting and measuring even it is not felt.

Many people owe their lives and health to such radiation, which is produced artificially. For instance, hidden problems are detected by medical and dental X-rays. Other kinds of ionizing radiation are used to diagnose illnesses, and some people are treated with radiation to cure disease. Ionizing radiation is part of the environment and always has been so. At high levels it is hazardous, but it is harmless at low levels [48]. Alpha, beta particles, gamma rays, and neutrons are radiation sources [52].

3.1.1 Alpha sources

Alpha particle is the nucleus of a helium atom, made up of two neutrons and two protons with a charge of +2 and, so Alpha particles consist of two protons and two neutrons, in the form of atomic nuclei. Alpha particles, which are derived from the charge of the two protons are doubly charged. Alpha rays are formed by the propagation of these particles. Certain radioactive nuclei emit alpha particles [48, 51]. Natural radioactive heavy elements are mainly alpha active sources (uranium, thorium, etc.). Many elements formed by dividing heavy elements with atomic numbers greater than 83 by fission are also alpha emitters. More energy is generally carried in alpha

particles than gamma rays or beta particles and deposit that energy very fast while passing through tissue. Because alpha particles lose their energy very quickly in the environments they encounter, their penetration and range are very small. High-energy alpha particles can travel a few cms in the air, so relatively in slow speed and high mass of alpha particles also interact more easily with matter than beta particles or gamma rays and lose their energy fast. They, therefore, have little penetrating property and can be stopped by a thin layer of light material, such as a sheet of paper, 0.5 mm thick aluminum sheets or approximately 0.07 kg/m^2 thick human skin is sufficient to stop alpha rays below 7.5 MeV and cannot penetrate the outer, dead layer of skin. Therefore, they do not damage living tissue when outside the body. If alpha-emitting atoms are inhaled or swallowed, they give damage in that case because they transfer relatively large amounts of ionizing energy to living cells. On the other hand, they can inflict more severe biological damage than other types of radiation inside the body. Such high-energy particles can penetrate the skin sub-layers [48, 51].

3.1.2 Beta sources

The beta particle has the same mass and charges as the electron, but their center is different. Beta-decay occurs when the nucleus is released by negatron release (β-) or positron release (β +). That means beta particles are released during radioactive decay in the nucleus. In the β- process, the conservation of the electric charge requires the conversion of a neutron into a proton (ΔZ = 1), and the decay of β + and the capture of electrons requires the conversion of a proton into a neutron (ΔZ = -1). In short, when the number of neutrons in the atomic nucleus is high, the atom becomes stable by releasing beta particles. Carbon-14, tritium, sulfur-35, calcium-45, phosphorus-32, strontium-90 are the most important sources of beta known [53]. Especially, strontium (Sr), which is one of those important beta sources, is a silvery, soft metal that quickly turns yellow in air. Sr-90 is one of the radioactive fission materials, which was created within a nuclear reactor during its operation. Strontium-90 emits beta particles during radioactive decay [51].

Beta particles are fast-moving electrons, which are ejected from the nucleus of many kinds of decaying atoms (radioactive atoms). These particles are singly charged. Beta particles have a smaller charge (up to half) and lighter than alpha particles and so, they are ejected in much higher speed than alpha particles. Thus, beta particles having a

certain energy move at a relatively high speed compared to alpha particles of the same energy and can penetrate much deeper than alpha particles in any absorbing medium. They can penetrate till 1 to 2 centimeters of water or human flesh. They can be stopped by a thin sheet of aluminum a few millimeters thick. However, beta particles can penetrate the dead skin layer and cause burns potentially. They can cause serious direct or external radiation damage and can be lethal and depending on the amount received. If there are beta-emitting atoms, they also carry a serious internal radiation threat [48, 51,53].

3.1.3 Gamma sources

Gamma radiation or gamma rays are high-energy photons and high-energy electromagnetic radiation, which are emitted by radioactive decay of atomic nuclei. Gamma radiation is a very high-energy form of ionizing radiation, with the shortest wavelength and high frequency [47]. Gamma radiation (gamma rays) is in the part of the electromagnetic spectrum with the most energy and shortest wavelength. Gamma radiation is defined as any radiation with an energy above 100 keV by astrophysicists. Physicists define gamma radiation as high-energy photons released by nuclear decay. A lot of sources, which include gamma decay, lightning, solar flares, matter-antimatter annihilation, the interaction between cosmic rays and matter, and many astronomical sources release gamma rays by using the broader definition of gamma radiation.

Energy is transmitted by a wave without the movement of material, just like heat and light in Gamma rays. Gamma rays and X-rays are identical except that X-rays are produced artificially rather than gamma rays, which is derived from the atomic nucleus. These rays have great penetrating power unlike light and can pass through the human body. A block in the form of concrete, lead or water is used to obtain shielding against them [48].

Gamma rays are emitted by certain radionuclides when their nuclei transition from a higher to a lower energy state. All gamma rays emitted from a given isotope have the same energy, a characteristic that enables scientists to identify which gamma emitters are present in a sample. Gamma rays penetrate tissue farther than do beta or alpha particles but leave a lower concentration of ions in their path to potentially cause cell damage. Gamma rays are very similar to X-rays [51].

During the radioactive decay of a nucleus, the product core (offspring) is at the lowest energy level, etc., not in the basic state, but the product core is excited at an energy above the basic state. After about 10^{-4} seconds, the excited nuclei emit excess energy in the form of electromagnetic radiation called gamma rays. These rays are similar to X-rays, short wavelength, and input rays [54]. There is no change in the atomic and mass numbers of the semi-stable nucleus, which is degraded in this way, so it is called isomeric decomposition. The half-life of gamma emission is very short compared to other degradations, usually less than 10^{-9} seconds, but there is also a half-life gamma emission in hours, even days. The energy spectra are discrete.

Gamma rays are a type of electromagnetic radiation with high penetrating properties. Gamma rays penetrate much deeper than alpha and beta particles. Gamma radiation decreases exponentially as it passes through the shielding agent. Therefore, theoretically, gamma rays cannot be completely absorbed regardless of the thickness of the armor material. However, it is possible to choose a thickness, which can take the dose to an acceptable level [53].

Paul Villard discovered Gamma radiation in 1900. This type of ionizing radiation is used for studying the universe, treating gemstones, scanning containers, sterilizing foods and equipment, diagnosing medical conditions, and treating some kinds of cancer.

Health Effects

Gamma radiation has a significant health risk. These rays are a type of ionizing radiation, which means they have enough energy to remove electrons from atoms and molecules. However, they are less-penetrating than alpha or beta particles and less likely to cause ionization damage. They have high energy and that means gamma rays have high penetrating power. They pass through skin and damage internal organs and bone marrow.

The human body can repair genetic damage from exposure to gamma radiation up to a certain point. It seems that repairing mechanisms to be more efficient in a high-dose exposure than a low-dose exposure. The worst of all, genetic damage by gamma radiation exposure may be led to cancer.

Natural Gamma Radiation Sources :

There are numerous natural sources in gamma radiation. Those are:

• Gamma decay: Gamma radiation releasing from natural radioisotopes. Alpha or beta decay is usually followed by gamma decay where the daughter nucleus is excited and falls to a lower energy level with the gamma radiation photon emission. Gamma decay also results from nuclear fusion, nuclear fission, and neutron capture.

• Antimatter annihilation: an electron and a positron annihilate each other, by so extremely high-energy gamma rays are released. Besides gamma decay and antimatter with other subatomic sources of gamma radiation include bremsstrahlung, synchrotron radiation, neutral pion decay, and Compton scattering.

• Lightning: Lightning produces the accelerated electrons of what is called a terrestrial gamma-ray flash.

• Solar flares: Radiation across the electromagnetic spectrum by a solar flare may be released including gamma radiation.

• Cosmic rays: Gamma rays are released by the interaction between cosmic rays and matter from bremsstrahlung or pair production.

• Gamma rays bursts: When neutron stars collide or when a neutron star interacts with a black hole, intense bursts of gamma radiation may be produced.

• Other astronomical sources: gamma radiation is released from pulsars, magnetars, quasars, and galaxies [51, 55-58].

Ionizing radiation consists of two wave-type ionizing radiation. Those are X-rays and gamma rays. X-rays are one of those ionizing radiation wave-type.

3.1.4 X-Ray sources

X-ray is electromagnetic radiation, which caused by the deflection of electrons from their original paths, or inner orbital electrons that change their orbital levels around the atomic nucleus. X-rays can travel long distances through air and most other materials as gamma rays. More shielding is required to reduce the intensity of X-rays than do beta or alpha particles like gamma rays. X-rays and gamma rays differ in their origins mainly. X-rays are derived from the electron shell, but gamma rays are derived from the nucleus [51].

Both gamma rays and X-rays are forms of electromagnetic radiation. Their electromagnetic spectrum overlaps, so there is only one way to differentiate them. Gamma rays and X-rays are obtained from natural **sources** like radioactive elements and radon gas in the earth, and cosmic rays, which strikes to the earth from space. X-rays can also be produced from a cathode ray tube by heating a filament to generate electrons and accelerating the electrons to strike a target by applying a voltage, and bombarding the target material with those electrons. If electrons carry sufficient energy to pull off inner shell electrons of the target material, characteristic X-rays are obtained. Gamma rays are originated in the nucleus from decay, but X-rays are originated in the electron cloud around the nucleus. Gamma rays and X-rays are distinguished by their energy. While gamma radiation has photon energy above 100 keV, X-rays only have energy up to 100 keV [51].

Since all electromagnetic radiation, such as gamma and X-ray, behaves like particles in many events, the unit element of these radiations is called photons, which means very small energy packets. Electromagnetic radiation is considered X-rays, gamma rays, and Bremsstrahlung radiation. Since photons (X and gamma rays) do not have electrical charges, they are not subjected to Coulomb force as in charged particles. This does not mean that photons do not ionize atoms in matter. Photons are electromagnetic force carriers and interact with matter through ionization and storage of energy into the environment.

3.1.5 Gamma Interaction with Matter

The behavior of photons in the matter is quite different from that of charged particles. In particular, gamma rays can lose most of their energy, or even all, in a single event in their interaction with the electrons of the atom. Therefore, the range of gamma rays in the air is in the order of meters [52]. As X and gamma rays pass through matter, they interact in three main ways. Those are; Photoelectric effect, Compton scattering, and pair production (Figure 3.5).
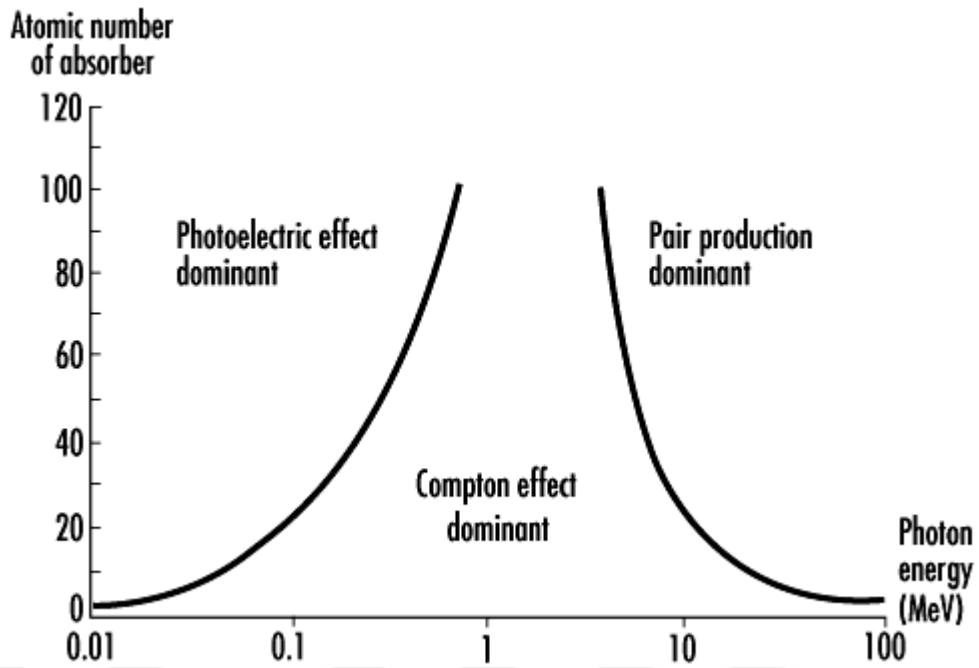
Figure 3.5 : The interaction modes of photons with matter[59].

As a result of these three events, two important properties of photons are determined. The first is that the penetration of the photons in the material is longer than the charged particles, and the second is that there is no change in the energy of the photons after passing the material with a certain thickness, but the intensity of the photons is reduced. This reduction in the intensity of photons is exponential as a function of thickness, as shown in equation 3.1.

$$I = I_0 e^{-\mu x} \tag{3.1}$$

Where "I_0" is the intensity of the incoming photons, "x" is the thickness of the absorber, and "μ" is the linear attenuation coefficient and depends on the material through which it passes and the radiation energy. Equation 3.1 applies to "narrow bundles" or "good geometry" situations where reflection and scattering effects are negligible. Otherwise, the determination of a build-up factor is required [54].

The fact that the density values in different phases of the materials can be different prevents the linear attenuation coefficient to be a material-specific value. Therefore, the materials cannot be compared with each other according to the linear attenuation coefficients. The mass attenuation coefficient, expressed as the ratio of the linear attenuation coefficient to the material density, allows the materials to be compared with each other. Equation 3.2 gives the formula of the mass attenuation coefficient (μ_m or μ / ρ).

$$\mu_m = \frac{\mu}{\rho} \tag{3.2}$$

The use of high atomic number materials such as iron, steel, tungsten, gold, concrete, and lead is suitable for gamma-ray shielding. However, for practical reasons, mostly lead and concrete is used [54].

Photoelectric effect :

A low energy photon generally releases all the energy of an atom in the K or L orbit of the atoms in which it passes through, releasing it from the binding force of the positively charged nucleus. This ejected electron is called photoelectron. The electron cavity formed as a result of this event is filled by another electron in the outer orbit and the X-ray is emitted [54]. This phenomenon is very important for the absorption of photons with energy less than 0.5 MeV by heavy elements. The photoelectric event is shown in detail in Figure 3.6.
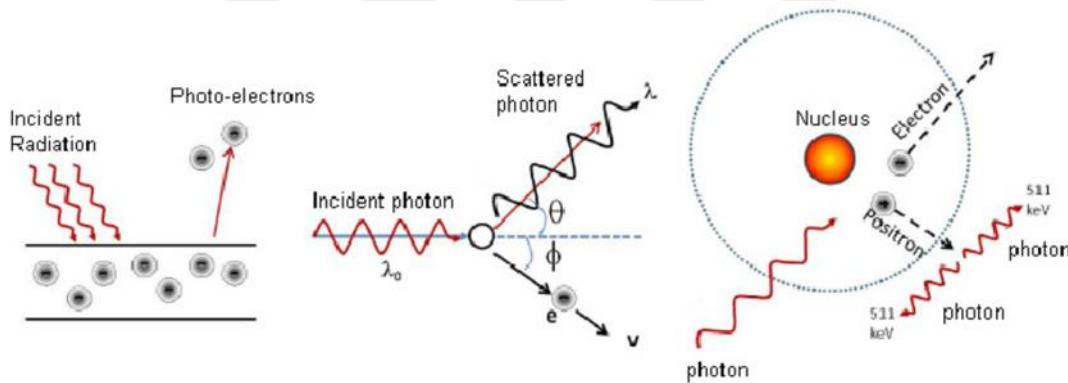
Figure 3.6 : The photoelectric effect [60].

During this event, some of the energy of the incoming photon is spent to break the electron out of the atom to which it is connected, and the rest is transferred to the severed electron as kinetic energy (Ke). I_B refers to the energy required to release an electron. This situation is expressed by Einstein's relation with equation 3.3.

$$hv = E_{Bonding} + E_{Kinetic} = I_B + K_e \tag{3.3}$$

This equation is important for substances with large atomic numbers loses their importance at values greater than 1 MeV energy [54].

Compton scattering :

The atom is loosely connected to an external orbital electron, a higher energy photon collision with the event that occurs as a result of Compton Scattering (Figure 3.7). The electrons are connected to the material. However, if the energy of the incoming photon is higher than the binding energy of the electron, the bonding energy is ignored and the electron is considered free. This incident cannot occur if the incoming photon has atomic bonding energy (below 100 keV) [54].
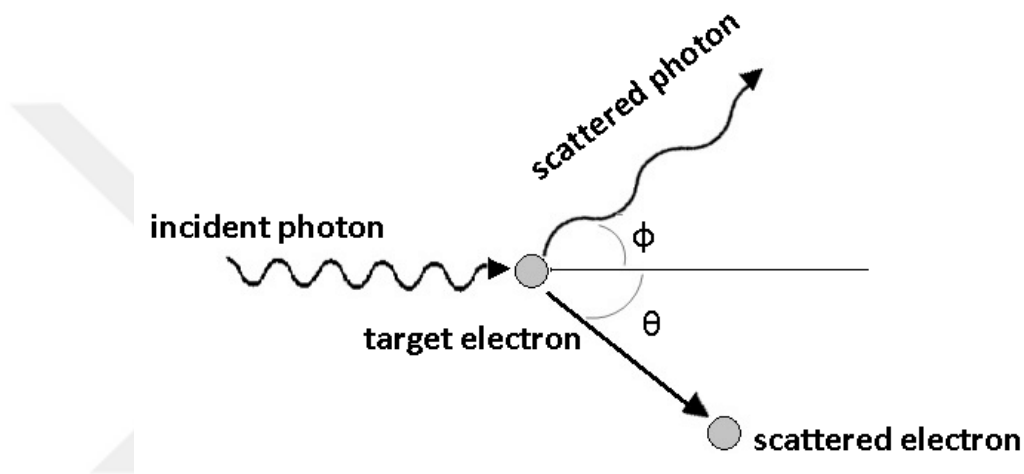
Figure 3.7 : The compton scattering [61].

Since it is an electron mass particle, it is not possible for the photon to absorb all its energy and to maintain the momentum. Therefore, the photon continues its path by transferring some of its energy to the electron and scattering. The angle formed between the photon and the electron depends on the energy of the photon. The difference between the wavelength of the incoming photon and the wavelength of the scattered photon is expressed in equation 3.4 below. Compton scattering is predominant in energy storage when photon energy reaches several MeV values [54].

$$\Delta \lambda = \lambda' - \lambda = h/m_0 c (1 - cos\theta) \qquad (3.4)$$

Pair production :

The formation of an electron-positron pair by losing the energy of a photon passing near the nucleus of an element with a high atomic number is called a double formation event. Considering that the masses of the electron and positron are equal and the

charges are opposite, no conservation laws are broken in this event that occurs near the nucleus. For that reason, the charge, linear momentum, and total energy are preserved. In short, the double formation is the conversion of the photon into an electron-positron pair.

This event occurs in the presence of a third object to provide momentum conservation [62]. Since the mass of the position is equal to the mass of the energy, the threshold energy for electron-positron pair formation will be $h\upsilon \approx 2m_e c^2 = 1.02$ MeV (Figure 3.8) [52].
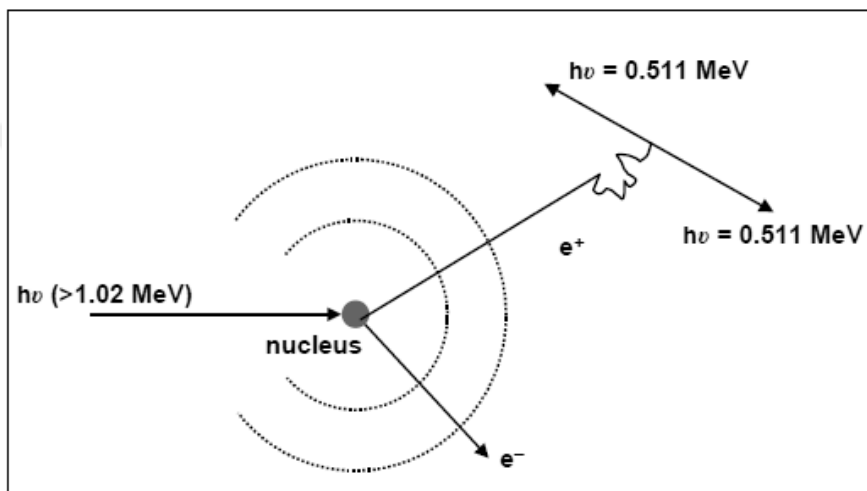
Figure 3.8 : The pair production [63].

The opposite of double formation is that an electron and a positron coincide and disappear after forming a photon pair. There is no requirement for this event to occur around the nucleus [52].

3.1.6 Neutron sources

Neutron is one of the particles that make up an atomic nucleus. The total charge of the neutron is zero and its atomic mass is 1.008656 (atomic mass unit) amu ($Mn = 1.6748 \times 10^{-27}$ kg). The symbol of the neutron is "n" and is shown in detail as $_0^1 n$. Naturally, the most known of the neutron emission materials are ^{252}Cf with a half-life of 2.65 years. Besides, neutron sources are generated by using some binary systems.

Neutrons can be classified according to their velocity or kinetic energy as thermal neutrons, epithermal neutrons, and fast neutrons. Interactions resulting from the collision of particles and nuclei are called nuclear reactions. These reactions result in many products. Uncharged neutron particles also interact with the nucleus through

these nuclear forces and do not interfere with the Coulomb barrier. Neutrons, which can be detected even at very low energies, are determined by producing charged particles as a result of their interaction with the atom. It is appropriate to use proton-rich materials to slow down neutrons. Neutrons can transfer most of their energies to them by colliding with a mass of materials and slowing them down. Neutrons can be divided into different classes according to their energy values. Neutrons can be divided into different classes according to their energy values [62]. These are;

- High energy neutrons;   E> 100 MeV,
- Fast neutrons;   10-20 MeV > E > 100-200 keV,
- Epithermal neutrons; 100 keV > E> 0.1 eV,
- Thermal / Slow neutrons;   E ~ kT ~ 1/40 eV,
- Cold and ultra-cold neutrons; E ~ meV ~ μeV.

3.1.7 Interaction of neutrons with matter

When neutrons meet with the matter, many interactions are produced, and as a result, the sum of the cross-sections of these interactions gives the value of the interaction of neutrons with the matter. The most important interactions between neutrons and materials; elastic scattering, inelastic scattering, neutron capture, nuclear reactions, and fission.

Elastic scattering :

High-energy ions continue along the linear path. However, in the low energy region, the effects of elastic nuclear collisions are more apparent. There is little or no energy transfer as a result of flexible collisions, but it can cause structural changes at low energies. Elastically scattered electrons can change direction but do not change their wavelength. When there is no energy loss in the primary electron, elastic scattering occurs. Coherent elastic scattering produces the electron diffraction effect, which is utilized to analyze crystal structure [64]. Kinetic energy is maintained during this collision. Figure 3.9 shows the elastic collision between the neutron and the atomic nucleus [65].
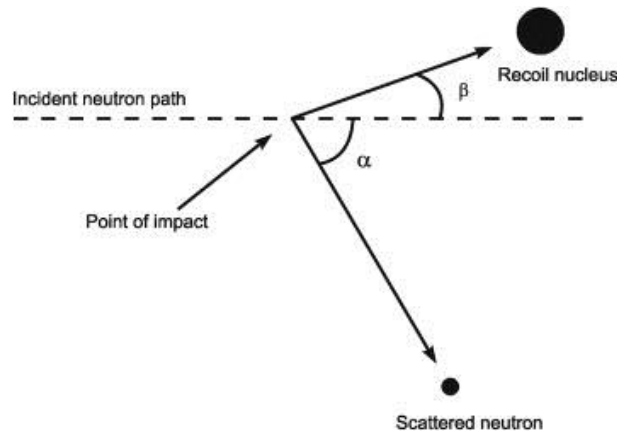
Figure 3.9 : Elastic scattering of the neutron from a nucleus [66].

Inelastic Scattering :

In inelastic scattering, the incoming neutron collides with the nucleus and the nucleus is excited, and then the nucleus emits a gamma-ray or some other kind of radiation and moves to its basic position. To stimulate the atomic nucleus in this reaction, the injection of the neutron must be greater than 1 MeV. Only elastic scattering is possible with neutrons below 1 MeV [62]. Figure 3.10 shows the inelastic interaction of neutrons with the atomic nucleus [65].
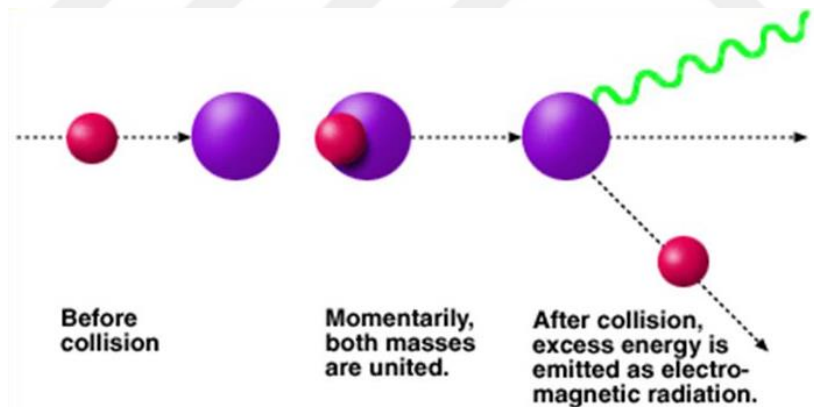
Figure 3.10 : Inelastic scattering of the neutron from a nucleus [67].

Neutron capture :

The neutron capture is captured by the nucleus of the neutron atom that reaches the target nucleus to form a unified nucleus. After a while, the combined core releases its excess energy by emitting sub-core particles or by dividing them into two. This situation is expressed by the reactions in equation 3.5.

$$n + (Z, A) \rightarrow \gamma + (Z, A + 1) \qquad (3.5)$$
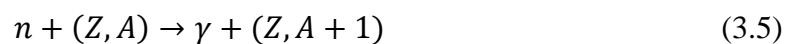
During neutron capture, neutron capture is likely to occur at low energy values because there is an inverse relationship between the speed of the neutron and the cross-section of the neutron. Figure 3.11 shows the capture of neutrons [65].
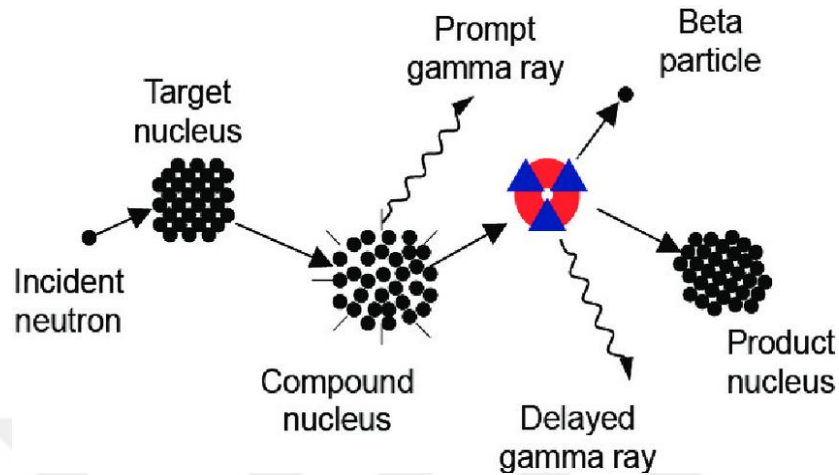
Figure 3.11 : Neutron capturing [68].

Nuclear reactions and fission :

Plutonium (Pu) is a heavy, man-made, radioactive metallic element. ^{239}Pu is the most important isotope, which has a half-life of 24,000 years. ^{239}Pu can be used in reactor fuel and is the primary isotope in weapons. One kilogram is equivalent to about 22 million kilowatt-hours of heat energy. The complete detonation of a kilogram of plutonium produces an explosion equal to about 20,000 tons of chemical explosives. All plutonium isotopes can be lethal if they are absorbed depending on the dose and exposure time. They are also absorbed by the bones, too [51]. Plutonium-239 is a good nuclear fuel and split by fast neutrons, it releases an average of 2.30 secondary neutrons per neutron captured. These secondary neutrons are required to maintain the chain reaction. Plutonium is the main fuel in a fast neutron reactor. It is progressively bred from non-fissile ^{238}U in any reactor that comprises over 99% of natural uranium. The fissile ^{239}Pu is the most common plutonium isotope, which was formed in a typical nuclear reactor by neutron capture from ^{238}U. Then, it is followed by beta decay. When it was fissioned, that yields much the same energy as the fission of ^{235}U. Plutonium-240 is the second most common isotope, which was formed by neutron capture by ^{239}Pu in about one-third of the impacts. ^{238}Pu Plutonium, ^{240}Pu, and ^{242}Pu emit neutrons despite at a low rate as a few of their nuclei spontaneously fission. They and ^{239}Pu also decay by emitting alpha particles and heat [69].

33
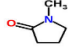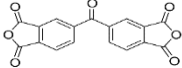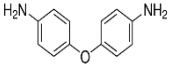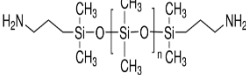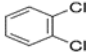
4. EXPERIMENTAL STUDIES

4.1 Used Chemicals

Poly(imide siloxane) block copolymers were synthesized using amine terminated APPS to study changes in structural properties. Flexible poly(imide siloxane) block copolymers (BI) were produced in the form of flexible rubber (elastomeric rubber) and BII poly(imide siloxane) block copolymers were produced in granular form. The flexible form of the structure was changed and adjusted by increasing ODA and decreasing APPS. Flexible poly(imide siloxane) block copolymers were produced by this technique. Thus, the new poly(imide siloxane) was produced from aminopropyl terminated siloxane as diamines and aromatic dianhydrides. ODA (4,4'-oxydianiline) and BTDA (benzophenone -3 3′-4 4′-tetracarboxylic dianhydride) are hard segments, APPS and BTDA are soft segments. ODA was used with APPS to form the polyimide rigid block; polysiloxane soft block samples were synthesized using APPS and BTDA. Thus, poly(imide siloxane) block copolymer samples were synthesized using APPS and BTDA and ODA. The used chemical materials were given in Table 4.1. They were supplied from Sigma Aldrich with high purity.

Table 4.1 : The used chemical materials and their properties.

Used Chemical Materials	Synonyms	Molecular Formula	Structural Formula	Molecular Weight (g/mol)
Methyl-2-pyrrolidinone	NMP (1 L)	C_5H_9NO		99,13
3 3' 4 4'-Benzophenone tetracarboxylic acid dianhydride	BTDA (5g)	$C_{17}H_6O_7$		322.23
4 4'-Oxydianiline	ODA (100 g)	$C_{12}H_{12}N_2O$		200,24
Poly(dimethyl siloxane)bis(3-aminopropyl)-terminated	PDMS (50 mL)	$H_2N(CH_2)_3Si(CH_3)_2O[Si(CH_3)_2O]_nSi(CH_3)_2(CH_2)_3NH_2$		27,000
1-2 Dichlorobenzene	ODCB (1 L).	$C_6H_4Cl_2$		147

4.2 Experimental Setup in The Synthesis Study

The experimental set up for the block copolymers synthesis was presented in the figure below Figure 4.1.
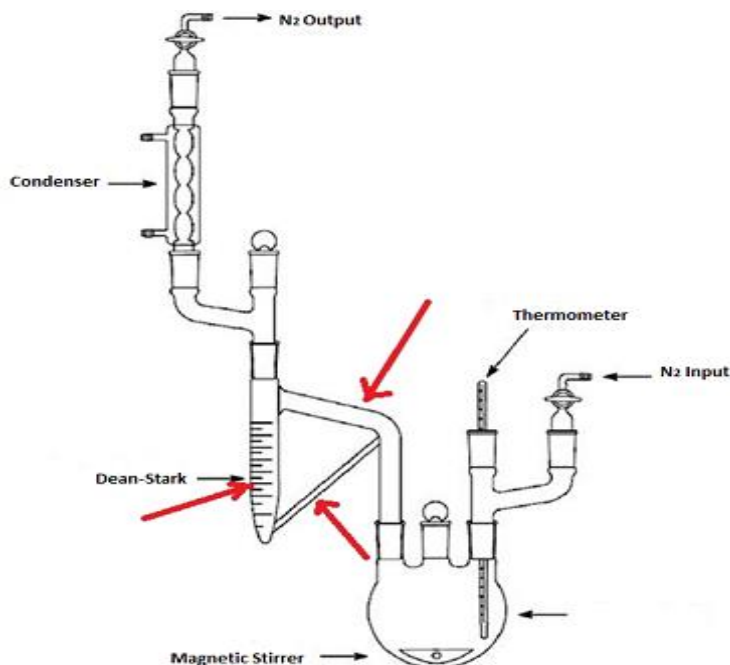
Figure 4.1 : Testing apparatus of synthesis [25].

4.3 Production of Material

The condensation polymerization technique was used to produce poly(imide siloxane) copolymer samples. This technique is the best technique that can be used in other polymerization techniques to synthesize to produce block copolymer material. Those polymerizations are also, in general, called stepped polymerization reactions. In these reactions, molecules with two or more functional groups bond by condensation reactions to form bigger molecules. On the reactions, a small molecule, such as a water molecule, is released [2]. Synthesis of poly(imide siloxane) block copolymers with the flexible sheet (BI) and pelletized (BII) were performed in this thesis. Besides, randomly segmented RI poly(imide siloxane) copolymers were synthesized at the viscous property, which have high adhesion property (its structural characterization details are available at Appendices).

4.4 Synthesis of Poly(imide siloxane) Block Copolymers

4.4.1 Synthesis of BI poly(imide siloxane) block copolymers

Synthesis of PIS block copolymers BI was explained at fourteen steps:

1. Polyimide hard blocks were formed by ODA and BTDA. APPS and BTDA formed soft blocks (as polysiloxane). BTDA was put into the three-necked flask and the flask was filled with (1.64 g), NMP (5 mL), and ODCB (5 mL) under inert gas (nitrogen).

2. The dianhydride was dissolved in the flask with APPS (3.53 g) in ODCB (5 mL) within another beaker. Then slowly was added into the three flasks, which contains BTDA and ODA.

3. The magnetic stirrer was inserted into the flask. The other necks of the flask were closed. The nitrogen gas was given to the flask from one of the necks of the flask. The total mixture was mixed for 6 hours at room temperature. The color of the mixture was white and in the liquid form.

4. The reaction temperature was increased to 185°C and stirred for 1 hour. The white color of the solution turned to yellow in the first 15 minutes. The water was collected in dean-stark (Figure 4.2 a-d).

(a)   (b)

(c)   (d)
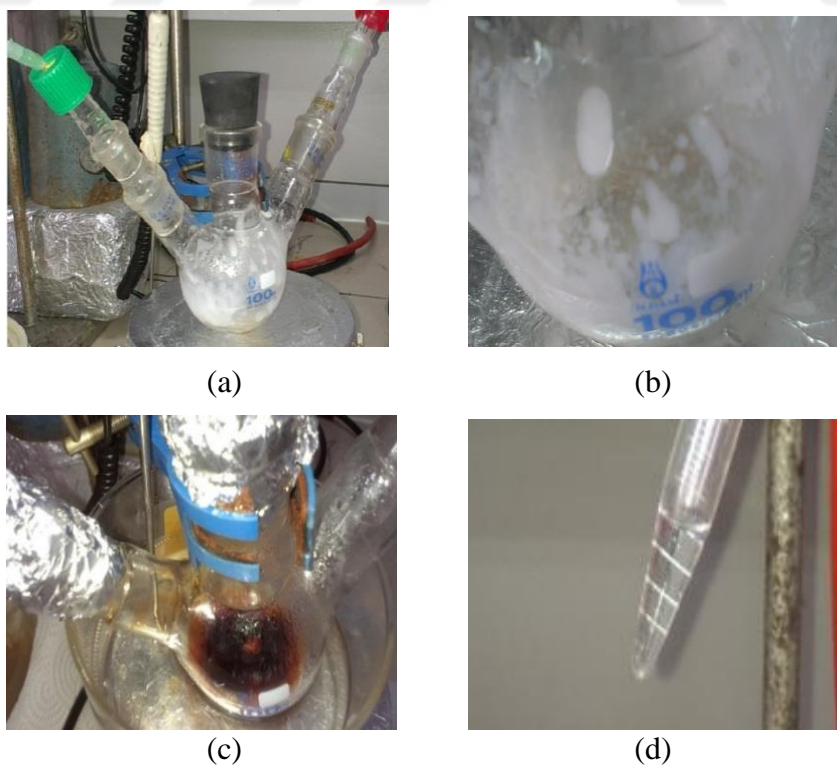
Figure 4.2 : (a-c) The white color of the solution turned to yellow in the first 15 minutes. (d) The water was collected in dean-stark.

5. Then, BTDA (1.62 g), ODA (1.24 g), and NMP (10 mL) were mixed within another flask for 6 hours at room temperature (in Figure 4.3).

6. The second mixture was mixed with the first mixture.

7. When the second mixture was added into the first one, ODCB (5 mL) was used (against any loss of the mixture).

(a)   (b)
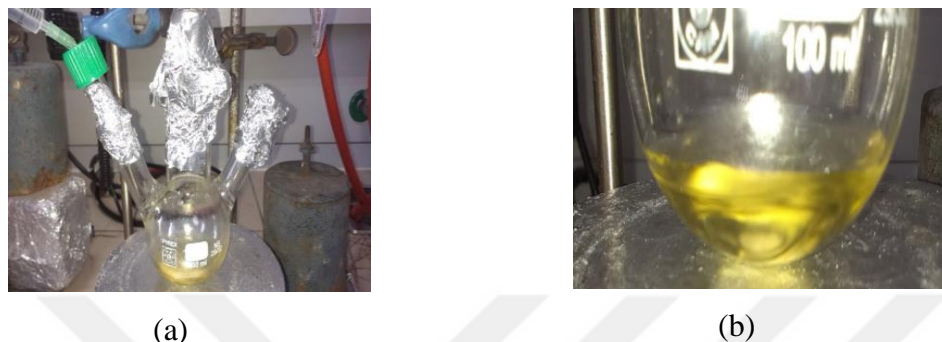
Figure 4.3 : (a) Addition of NMP (10 mL) in to BTDA (1.62 g) and ODA (1.24 g). (b) The total mixture of the block copolymer was stirred for 6 hours within another flask at room temperature under inert gas.

8. First, the last solution was mixed for 12 hours at room temperature. Then, it was mixed for 8 hours at 185°C (Figure 4.4 a-f).

9. The collection of water slowed down. The vaporization started to slow down and the chemical reaction was over. 22 mL of water was collected due to evaporation.

(a)   (b)   (c)

(d)   (e)   (f)
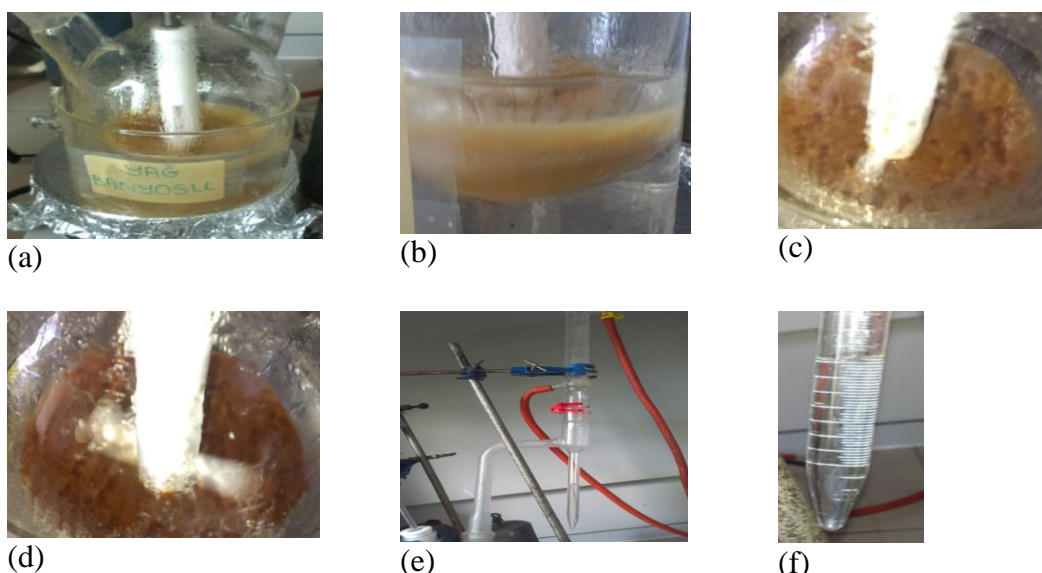
Figure 4.4 : (a) The started vaporization (b) The mixture started to turn in to a light brown color. (c) The vaporization started (d) Colour change due to chemical reaction happened (e) The water due to vaporization was collected (12 mL) within dean-stark (f) Extra water (10 mL) was collected later.

0.5 ml of water was collected at the last step in the dean- stark. Thus, the total amount of water reached 22,5 mL at the end of the synthesis. The mixture was in the creme form, jel-like at the end of the synthesis as in Figure 4.5.

• A sample like rubber was produced at the end of the synthesis.

• The extract was diluted with NMP.

• The copolymer sample was washed with ethanol.

• Lastly structure was dried for 12 hours at 120°C in vacuum to get the PIS block copolymer BI.

Figure 4.5 : The collected water slowed down in the dean-stark.

Figure 4.6 : Flexible poly(imide siloxane) block copolymer BI.

4.4.2 Synthesis of BII poly(imide siloxane) block copolymer samples

1. BTDA (1.63 g), NMP (5 mL), and ODCB (5 mL) chemicals were added to a three-necked flask and nitrogen gas was introduced into the medium.

2. After the dianhydride structures were completely dissolved, APPS (3.52 g) was slowly added to the ODCB solvent to dissolve in ODCB (5 mL) in a different beaker, and the resulting solution was mixed for 6 hours at room temperature under inert (nitrogen) atmosphere.

3. The temperature of the produced solution was increased. The temperature was kept for 1 hour at 185°C.

4. The second mixture obtained with BTDA (1.61 g) and ODA (1.3 g) was dissolved in NMP (10 mL) by stirring for 6 hours at room temperature by placing the mixture in another glass flask.

5. When the second mixture was put into the first mixture, about 5 mL of ODCB was used to prevent the loss of material.

6. The resulting mixture was mixed for 12 hours at room temperature.

7. The temperature of the solution was preserved for 10 hours at 165°C. The temperature of the mixture was maintained at 165°C for 10 hours. Thus, the temperature effect on the poly(imide siloxane) block copolymer BII structure was observed.

8. Then, the temperature of the mixture was increased to 185°C and mixed for 8 hours. The solution was preserved at 185°C for 8 hours.

9. In addition to 8 hours of mixing poly(imide siloxane), copolymer structures were heated at the temperature of 185°C 8 hours of mixing.

10. In the dean-stark apparatus, 8 mL of water was deposited as a result of evaporation during the reaction. Fewer water outlets were observed compared to the flexible material of the previous step.

11. After mixing the mixture 8 hours at 185°C, the product obtained was cooled to room temperature. Then, the extract was diluted with NMP.

12. It was seen that a granular, powder form of poly(imide siloxane) block copolymer was produced (in Figure 4.7). This powder form was washed in plenty of ethanol by mixing and filtered through a filter paper. The extract was obtained via a second wash with ethanol.

13. The filtrated product was deposited on filter paper and dried for 12 hours at 120°C in a vacuum oven. The product was then dried under vacuum at 120°C for 12 hours to obtain the PIS BII sample.

14. It was observed that the derived product maintained its granular appearance as it was before the vacuum was put into the oven.

Figure 4.7 : Poly(imide siloxane) block copolymer BII in granular form.

Generally, during the synthesis of copolymer structures, carbon and oxygen bonds in the structure of BTDA are derived by the addition of NMP and ODCB solvents by stirring 12 hours of BTDA, PDMS, and ODA under nitrogen gas at room temperature. Oxygen and hydrogen atoms are bonded to form new carboxylic acid structures with the addition of NMP and ODCB solvents to the opened chain structures. After 185°C heat treatment and 8 hours of stirring, nitrogen gas is bonded to the carbon atom, the polymer ring chain is broken off from 2 hydrogen and oxygen atoms carboxyl bonds to close the ring chain. During that time, water outflow occurs in the structure. The released water is collected in the dean stark and removed from the structure.

The polymerization reaction is completed by the extraction of water, which is a kind of weak acid. Therefore, if water outflow is observed towards the end of any polymerization reaction, this is the most important indication that the reaction is completed. The reaction continues until all of the monomers in the reaction are exhausted. Even if all the monomers have been exhausted in the reaction, the reaction is not fully completed unless the water is removed from the reaction.

The end of each polymer chain consists of carbon ring chains and unless the water is removed, which is considered to be a weak acid, the polymerization reaction will never be finished. Because the extraction of water from chemical reactions show that closure of carbon ring chains is completed. At the same time, the reaction is termed as "condensation reaction" since the monomers in the part of the reactants of the reaction were consumed and the reaction was completed with the exit of the water molecule.

It was found that the produced copolymers belong to the group of condensation polymers obtained by the copolymerization reaction due to the water outlet at the end

of the reaction. As a result of condensation reactions, the water molecule in the weak acid group is formed. Water extraction was detected for all products produced and water was collected at dean-stark. At the end of the reaction of the copolymer structures produced with different chemicals, it is determined that the type of copolymerization reaction is the step-growth polymerization.

In this study, the reactions in which the material is obtained are two-step. Thus, it is understood that it is also one of the stepped growth polymers called "Step-Growth". After all, two types of copolymer products were obtained by a condensation reaction, water outflow was detected. The completion of the reaction in all two types of products is determined by the water outlet. The water outlet indicates that chemical reactions occur, polymerization steps begin and aromatic carbonyl rings form and the chains of aromatic rings close.

4.5 Formulation of The PIS Block Copolymers

As a result of this study, the chemical formula of the poly (imide siloxane) copolymer structure was obtained using the ChemBio program. As seen in Figure 4.8, the first two blocks of the structure are produced first. These two blocks are then combined to give the final form of the PIS block copolymer samples. Also, the formulation of these examples shows that PIS block copolymer products exhibit rubber properties.
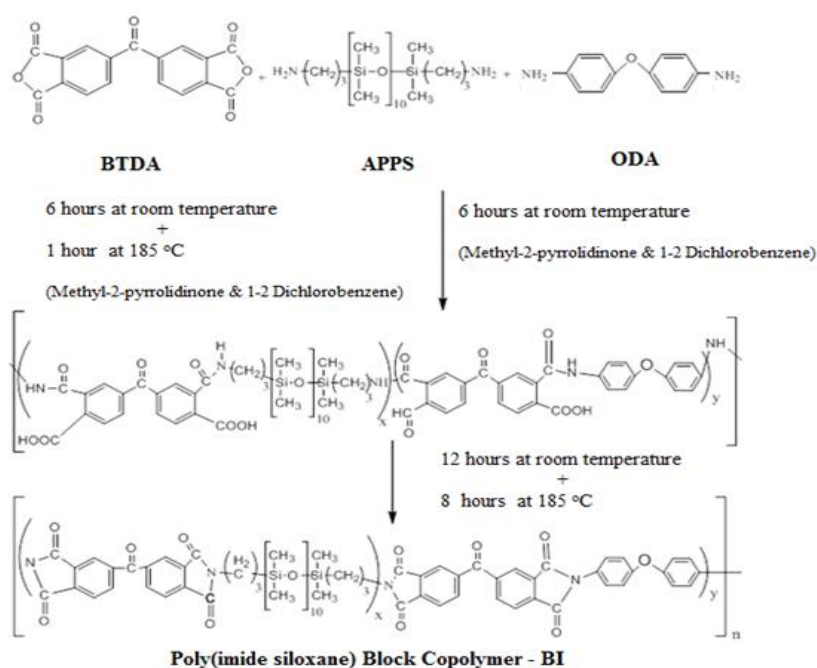
Figure 4.8 : Formulation of PIS block copolymers BI.

The chemical formulation for PIS block copolymer BII samples is shown in Figure 4.9. The only difference in this sample is the application of heat as seen in the formulation. For this purpose, an additional heat cure was applied during the synthesis. In addition to the heat cure applied at 185°C for 8 hours, the structure was applied 165°C for 10 hours (before the 185°C applied for 8 hours).
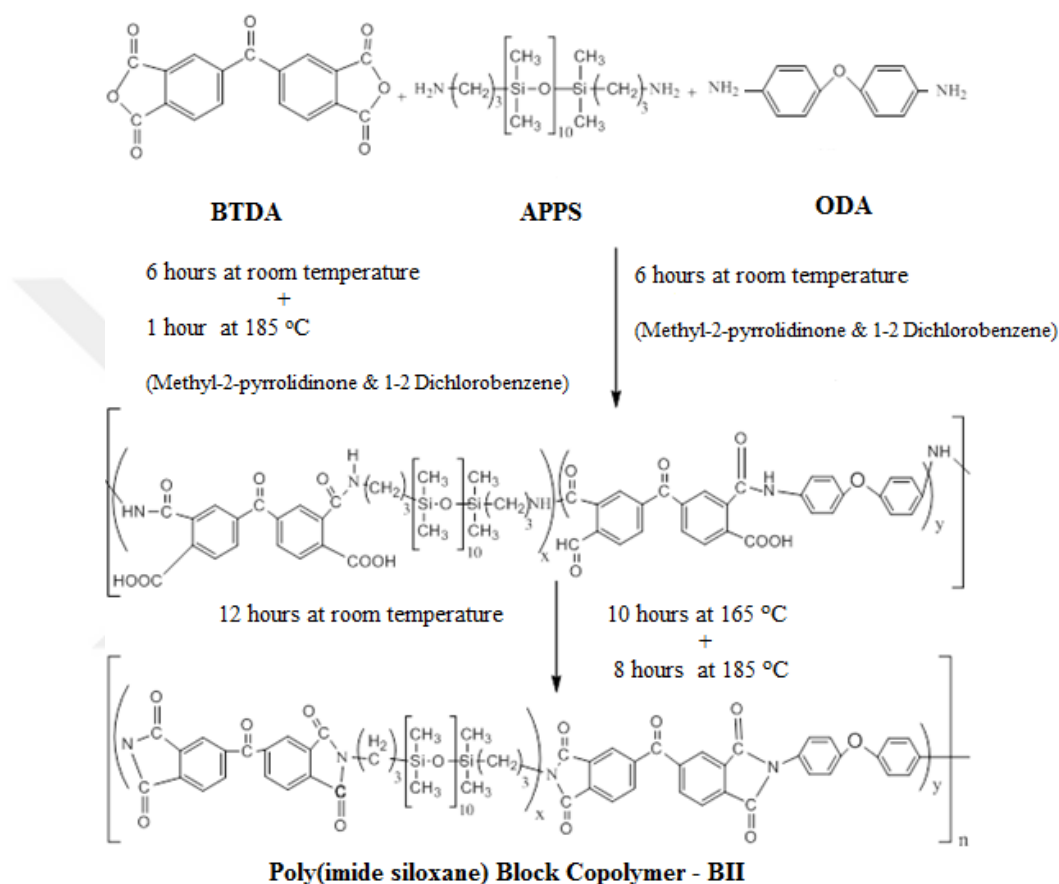
Figure 4.9 : Formulation of PIS block copolymers BII.

4.6 Pelletization Technique of Poly(Imide Siloxane) Block Copolymers

The produced block copolymer BII was in granular, powder form compared to the flexibility of the PIS BI sample. After the production of the BII structure, the powders were compressed by a manual hydraulic press in the stainless steel container. A stainless steel pelletizing mold with a radius of 10 mm was used to obtain a circular compact structure. The pelletization process of BII samples was done by applying 40 MPa pressing.

Both BI and BII samples were prepared to be 1 mm thick and 1 cm in diameter, and sample measurements were made by increasing the thickness by 1 mm. The mass of

the pelleted BI sample with 1 mm thickness and 1 cm in diameter was 0.944 grams. The mass of the pelleted BII sample with 1 mm thickness and 1 cm in diameter, was 0.967 grams.

(a)   (b)
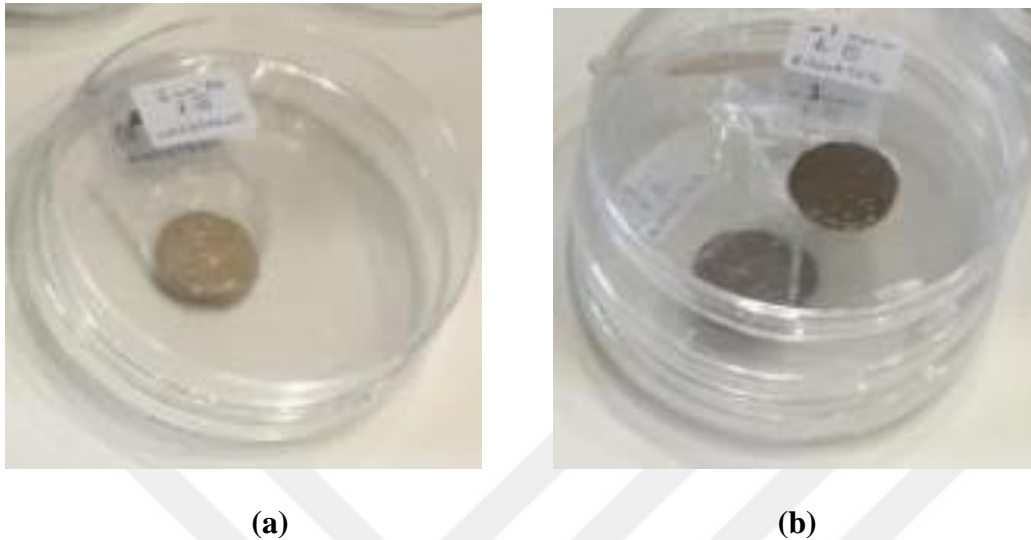
Figure 4.10 : Pelleted forms of poly(imide siloxane) block copolymers in (a) flexible sheet and (b) granular form.

4.7 Application of Radiation Transmission Technique

4.7.1 The settlement of gamma transmission method

Gamma's weakening was performed to measure and evaluate changes in gamma penetration in PIS. Radioisotope and detector were placed on the same axis. The gap between the gamma source and the detector was set to 12 cm. In experiments, suitable collimators were used for material properties. In order to limit radiation scattering, the use of collimators in experiments is necessary. A suitable gamma-ray beam was obtained in this way. The electrode collimator was used with a 3 mm electrode collimator bore radius.

The sample was placed between a gamma source and the detector. The scattering effect was reduced with a lead collimator. Cs-137 and Co-60 radioisotopes in ITU Energy Institute Radioisotope Laboratory were used as radioisotope sources. The Cs-137 radioisotope used (with 8.06 μCi) has a peak at 0.662 MeV and has a half-life of 30.1 years [70]. The Co-60 used (with 7.24 μCi) has two peaks at 1.17 MeV and 1.33 MeV (considered as the monochromatic energy peak at ∼ 1.25 MeV) and has a half-life of 5.23 years (seen in Table 4.2) [70 -71].

Table 4.2 : Properties of Cs-137 and Co-60 radioisotope sources.

Gamma Radioisotope Source	Half Life	Energy (MeV)	Activity
Cs-137	30,1 years	0.662	8.06 µCi
Co-60	5,23 years	1.17 1.33	7.24 µCi
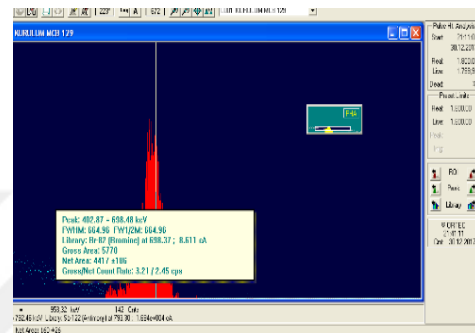
(a)   (b)

Figure 4.11 : (a) Cs-137 radioactive isotope source with 8.06 µCi activity and 30,1 years half-life. (b) Screenshot of Cs-137 radioactive isotope source in the user program (It has one energy peak at 0.662 MeV).
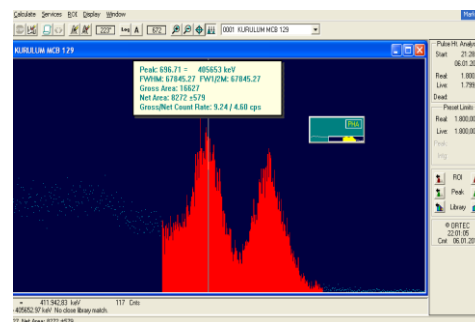
(a)   (b)

Figure 4.12 : (a) Co-60 radioactive isotope source with 7,24 µCi activity and 5,23 years half-life. (b) Screenshot of Co-60 radioactive isotope source in the user program (It has two energy peaks at 1.17 and 1.33 MeV).

A gamma spectrometer was used to determine the relative density of samples BI and BII by the NaI scintillation detector (Canberra Bicron Model with 802-2X2 Mark). 1024-channel Multi-Channel Analyser and Ortec Maestro software were utilized for counting the gamma-ray intensity coming from the source (I_0 initial radiation

intensity). The linear attenuation coefficient was determined from the I/I_0 ratio in Equation 5.1 [71].

$$I = I_0 . e^{-\mu x} \tag{4.1}$$
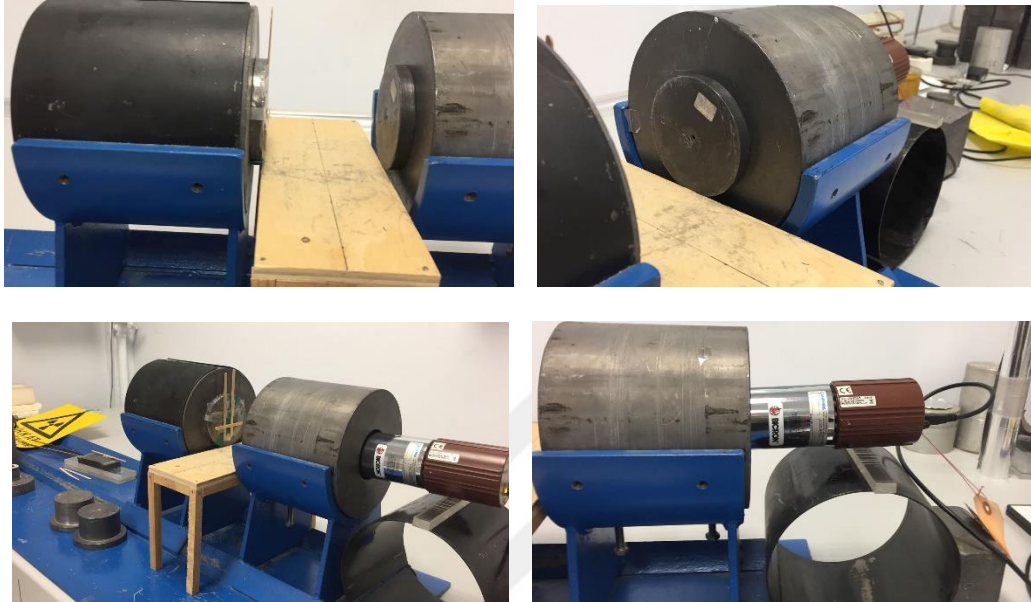
Figure 4.13 : View of the gamma test experimental setup.

"I" are counts transmitted to the polymer and detected in the detector. I is the transmission intensity, which passed from the material, "I_0" is the count detected in the detector without sample between the detector. "I_0" is the initial intensity and the source "x" is sample thickness. μ is the linear attenuation coefficient [72, 73].

4.7.2 Experimental setup of Sr-90 radioisotope for beta transmission

The polymer and plastic industry utilized the beta transmission technique at the control processes of material thickness. The beta transmission method enables the evaluation of the density changes [70].

In this study, the experimental setup for beta transmission was adjusted to measure the beta attenuation of the samples and Sr-90 beta radioisotope, which has been in Istanbul Technical University - Energy Institute Radioisotope Laboratory was used as the radiation source in our experimental studies. In this experiment, Sr-90 (with a half-life of 28.6 years and 2.86 mCi activity), with a maximum electron energy of 0.546 MeV with a radius of 0.015 cm, was used as a beta source.

The beta measurement process was performed in a plexiglass cell for shielding purposes against beta. In addition, the aluminum discs were inserted in the cell to preserve the laboratory ambiance against radiation. For radioisotopes, energy and half-life are very important factors for radiation penetration into the PIS block copolymer in the beta transmission method. If E>1 keV, electrons can be stimulated by the Compton Effect [36].

PM 1405 Geiger-Muller detector was used as a measuring device. This detector, which is given in Table 4.3, is used for high counting performance. The meter is suitable for radiation protection and health physics use. The device was effectively used to obtain optimal numbers of the local radiation source in polymeric materials. The measuring device used in the experiments is a high-quality detector and is also used to measure the transmitted gamma and X-ray [71].

Figure 4.14 : The Sr-90 radioisotope source used in the beta counts was inserted inside the experimental setup.

Besides, the drop-in appropriate screen filter allows estimating beta radiation in detail. Accelerated electrons lose energy as the producing bremsstrahlung radiation that consists of X-ray. Changes in radiation intensity within the PIS block copolymer structure allowed to investigate beta particles that had Coulomb interaction due to the acceleration of beta particles. A suitable collimator for polymer structures was used to obtain a suitable electron beam and to eliminate scattered electrons. The outer and inner diameters in the collimator were 13 cm and 6 cm, respectively. The properties of the beta particle detector are presented in Table 4.3 and Figure 4.15 [36, 70-71].

Table 4.3 : Technical properties of the measuring instrument for beta particles.

	The used detector for beta particles
Detector	GM Counter
Dose Rate	0.01 μSv/h - 130 mSv/h; (10 μR/h - 10 R/h), indicating a range of beta flux density; 0.1-104 $min^{-1}cm^{-2}$
Rate Accuracy of Dose	$\pm (20 + K / H)$ % (dose rate, μSv/h) K- coefficient 1.0 μSv/h.
Measurement of Dose	Indicating range (0.01 μSv – 10.0 Sv) - special configuration, supplied by individual order-
Accuracy of Dose	± 20 % - special configuration, supplied by individual order-
Range of Energy	0.1- 3.5 MeV, beta measuring
Dimensions	148 x 85 x 40 mm
Weight	290 g
Temperature	-10°C to 50°C.
Humidity	till 95% at 35°C.
Environmental Protection	IP 30.

Figure 4.15 : PM 1405 Geiger- Muller detector as the measuring device.

4.7.3 Experimental setup of Pu-Be Neutron Howitzer for the for neutron transmission

An experimental setup was set in order to investigate the material's structure against neutrons and to conduct relevant experimental studies, in accordance with the principle of neutron transmission technique. A suitable experimental setup was created by using the facilities of ITU TRIGA Mark-II Training and Research Reactor at ITU Energy Institute in order to examine the neutron transmission of the specimens (in Figure 4.16). Elements of the experimental setup included Pu-Be neutron source, neutron

detector, neutron collimator, and neutron shielding materials. Pu-Be neutron Howitzer-3 (NH-3) source was produced by Nuclear Chicago Corporation.

Figure 4.16 : Experimental setup of Pu-Be Neutron Howitzer for the for neutron transmission design.

Neutron Source containing ^{239}Pu-Be has been used because it is a suitable neutron generator that provides neutron emissions suitable for the neutron transmission method. Polimaster brand PM1401K model multipurpose detector is used as a neutron detector. The properties of the detector used are shown in detail in Figure 4.17 and the characteristics of the neutron detector are shown in Table 4.4. With the He-3 detector in the detector, neutron counting was done in the energy range of 0.025 eV - 14 MeV.

Figure 4.17 : PM1401K Model scintillation detector.

Table 4.4 : Technical characteristics of the used measuring instrument for neutrons.

Properties of Utilized Detector for Neutrons	
Dose equivalent rate (DER) measurement	0.1 - 105 μSv/ h
Dose Rate Correctness	± (15+ (K / H) % ,where DER value in mSv/ h, K - coefficient equal 0.0015 mSv / h
Dose Measurement.	Indicating range : 0.01 μSv – 10.0 Sv Special configuration, supplied by individual order.
Dose Accuracy.	± 20 % special configuration, supplied by individual order.
Energy Range.	0.015-1.5 MeV
Dimensions	240 x 57 x 55 mm
Weight	650 g
Temperature	-30°C to 50°C
Humidity	till 95% at 35°C
Environmental Protection	IP 65

The scintillation detector used in the experiments includes the multi-channel analyzer feature. The HP Brand IPAQ pocket computer, which works in harmony with the detector, was used together with the PM1401K scintillation detector. The pocket computer has the ability to establish remote wireless (Bluetooth) connection with the detector and this provides favorable conditions for nuclear safety during experimental work. It is possible to make measurements in a secure way with a wireless connection by establishing a remote connection with the detector. Figure 4.18 shows a pocket computer that can work in harmony with a scintillation detector (Figure 4.19).

Figure 4.18 : Pocket PC that can work compatible with the scintillation detector.
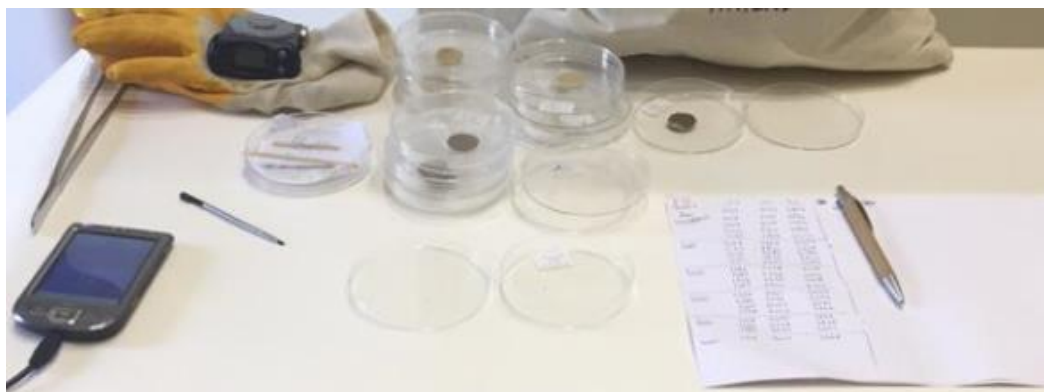
(a)
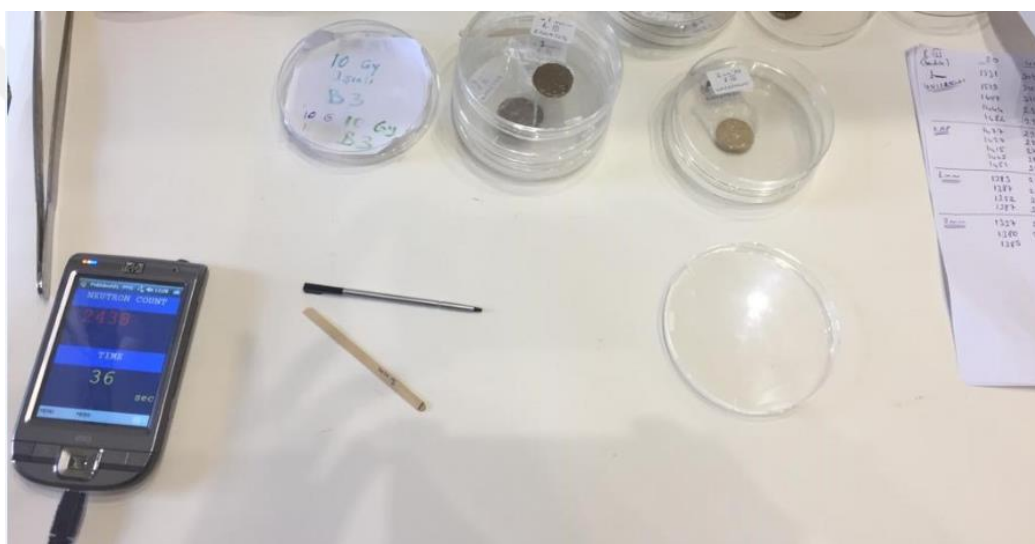
(b)
Figure 4.19 : Measurement of neutron transmission of pelleted PIS samples using
HP Brand IPAQ pocket computer (Pocket PC).

Properties for ^{239}Pu-Be neutron are given in Table 4.5. The length of the radial beam
port on Neutron howitzer is 25 cm and its diameter is 5 cm. Thermal neutron port (is
also known as first port) is proper for evaluating total macroscopic cross-section in
polymeric samples. The shielding of the neutron is connected with the energy of
neutrons. PIS BI and BII samples were utilized to slow neutrons with ~0.025 eV (at
20°C for Maxwellian distribution or thermal neutrons) because PIS block copolymer
samples did not affect the neutrons with high-energy.

Table 4.5 : Properties of Pu- Be Neutron Howitzer.

Properties	Value
Neutron Source	Pu-Be Neutron Source
Neutron Source Type	Nuclear Chicago Corporation
Neutron Production Reaction	(α,n)
Activity	2 Ci
Neutron Flux	10^4 n/cm^2 s
Average Neutron Energy	53.97 kJ/mole
Number of the Irradiation Ports	2
Sizes of the Howitzer	Ø 60 cm x 90 cm
Thickness of the paraffin	25 cm

The Pu-Be Neutron Howitzer (NH-3) port is well suited to evaluate epithermal neutrons. It is also suitable for examining the cross-section of denser materials about the effective way. The second port in the Pu-Be neutron howitzer is used due to epithermal neutrons.

Thermal neutron port in Pu-Be Neutron Howitzer was utilized to measure changes in total macroscopic cross-sections for both samples (in Figure 4.20). Negligible amounts of fast and epithermal neutrons were removed within the port. Besides, fast and epithermal neutrons were thermalized. Later, they were absorbed by the hydrogen and carbon contents of Neutron Howitzer in paraffin wax. The neutron transmission method was used by certified Pu-Be neutron howitzer. The Pu-Be neutron source owns the average neutron energy of 5 MeV (with 5 Ci activity). NH-3 produces neutron flux (at 10^6 n.cm^{-2}s^{-1}). Neutrons were thermalized within 2.5 cm paraffin wax [70, 74].

NH-3 detectors were utilized for measuring the number of neutrons. The distance between the source and PIS samples was 40 cm. Neutrons were adjusted to a restricted beam with a collimator, which is a 10 mm hole. The initial intensity (I_0) was measured, then a decrease in intensity (I) was observed by raising thickness (t). Radiation levels were reduced in the background. Thermal neutron transmission measurements were estimated by the generated data for both samples.
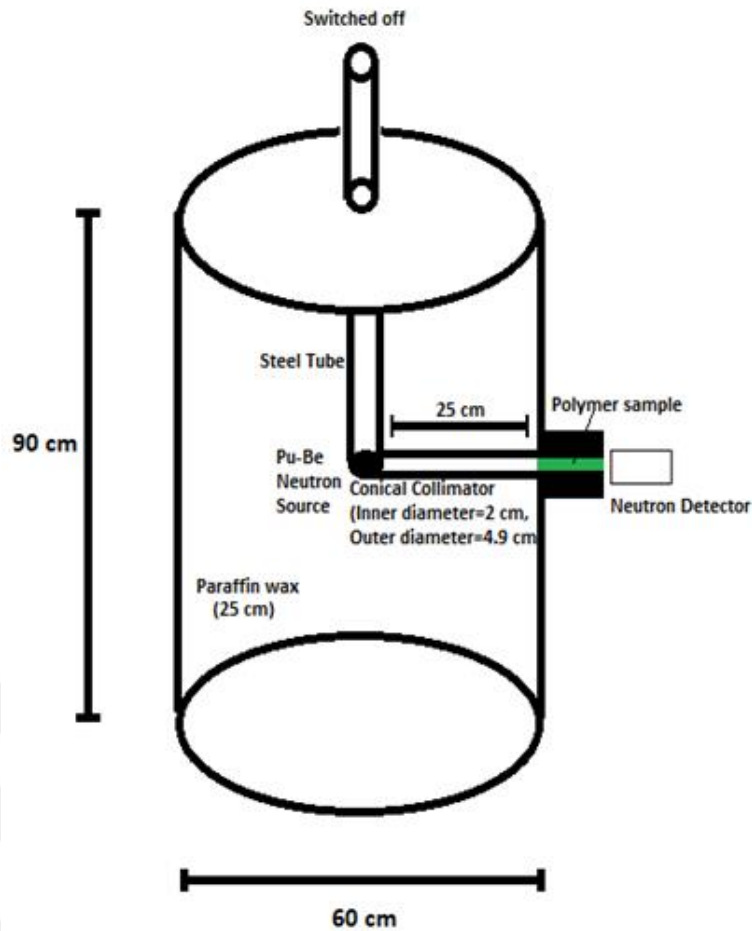
Figure 4.20 : Representation of thermal neutron port on the Neutron Howitzer.

4.8 Application of Irradiation Dose and Irradiation Settlement for Poly(imide siloxane) Copolymer Samples

Block copolymer samples were exposed to gamma radiation through the same irradiation plane at room temperature. The Co-60 Radioisope was used in this study and the activity of the source was ~ 10^6 Ci. The half-life of Co-60 radioisotope is 5.3 years. Gamma irradiation was carried by using Co-60 radioisotope and the applied dose rate is 10 kGy/h. The gamma irradiation was performed at 2.1 kGy/h by using Co-60 radioisotope at the Gamma - Pak Sterilization Company. The irradiation dose time of PIS samples is 4.76 hours. The absorbed dose level of copolymer samples was selected as 10 kGy to examine the cumulative dose-effect and to investigate the absorbed dose-effect on irradiated material. Because absorbed dose measured as the energy absorbed per unit mass was the quantity of ionizing radiation absorbed by the sample [40-41].

5. RESULTS

The structural characterization was performed by using several examination techniques. These techniques are FTIR, TGA-DSC, XRD, SEM, AFM, Gamma Radiography, DMA, Radiation transmission techniques.

5.1 Comparison of The Fourier Transform Infrared (FTIR) Spectroscopy Results for Poly(imide siloxane) Copolymer Structures

5.1.1 FTIR Analysis of Poly(imide siloxane) block copolymers BI

FTIR analysis of the PIS BI block copolymer is presented in Figure 5.1 and the structural details of the PIS BI block copolymer are evaluated in Table 5.1. FTIR analysis results showed that the poly (imide siloxane) block copolymer BI structure has a silicone, rubber-elastic structure according to the literature [83-86].
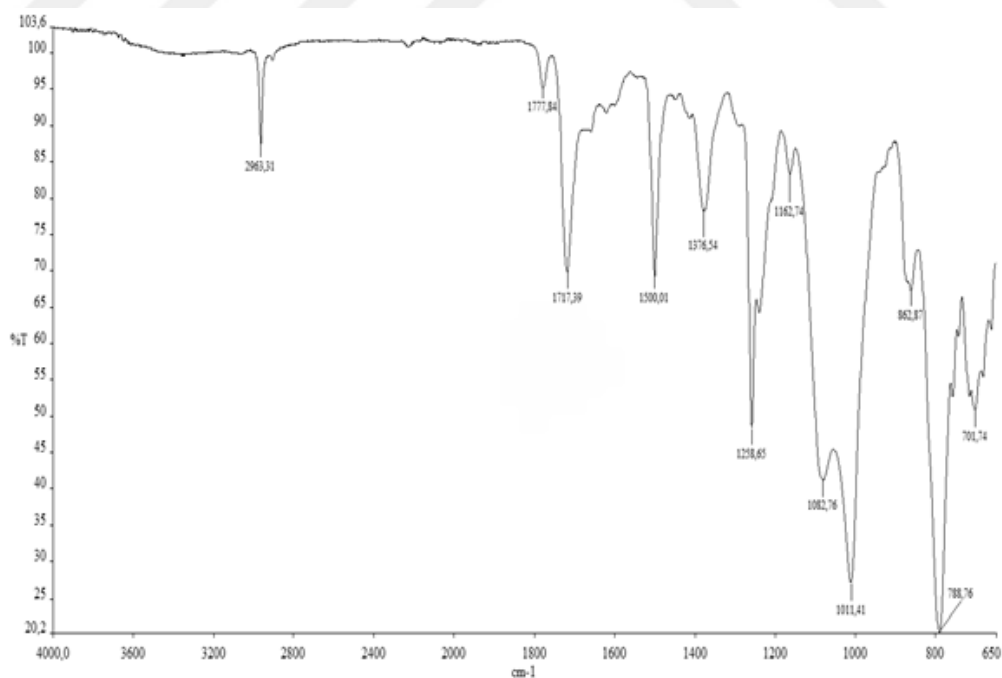
Figure 5.1 : FTIR analysis of PIS block copolymer BI.

Table 5.1: FTIR analysis of poly(imide siloxane) block copolymer BI.

Bound	Peak (cm^{-1})
aliphatic C - H stretching	2963
asym C = O stretching	1777
sym C = O stretching	1717
asym Si- O –Si stretching	1082
sym Si- O –Si stretching	1011
Si – C stretching	788

The characteristic chemical structure of BI copolymer samples consists of carbon and siloxane Si-O chains. It is also seen from the characterization interpretation of FTIR analysis with the "Euclidean Search" spectrum that the structure has an elastomeric structure in the silicone-rubber mixture.

The peaks in FTIR spectra at 1781 and 1722 cm^{-1}, are carbonyl amide groups (Figure 5.1). These absorption peaks of imide at 1781 cm^{-1} and 1722 cm^{-1}, evanesce at the end of capping via –COOH and indicates the formation of BI copolymers (Figure 5.1). Peaks of the BI structure at 1777 cm^{-1} and 1717 cm^{-1} were imide groups. The peak of the structure at 1500 cm^{-1} in BI is N-H imide.

Mechanical and thermal properties in PIS copolymers are influenced by the hard segmented content of the polyimide and the soft segment molecular size of APPS. This shows the elastomeric structures of polymeric materials in the rubber industry. This feature makes it possible to use the material at high temperatures. It also provides energy efficiency. Polysiloxane rubber structures have a Si-O-Si structure. These elastomeric properties show good electrical properties, thermal resistance, antioxidative properties, high-temperature resistance, abrasion, and radiation resistance in bad weather.

5.1.2 FTIR Analysis of Poly(imide siloxane) block copolymers BII

Structural characterization of the granular structure obtained by changing the temperature and time parameters to determine the temperature effect on the PIS block copolymer structures was analyzed by FTIR analysis. According to the FTIR results, amide or anhydride chemical chain rings, which are an excellent reaction indicator, were detected to be completed.

FTIR analysis of the PIS copolymer samples obtained by the effect of temperature change on the PIS block copolymer structure is shown in Figure 5.2. The characteristic

interpretation of the peaks were shown indicated by FTIR analysis in Figure 5.2 and in Table 5.2.

In this study, the change in the physical appearance of PIS block copolymers as a result of extra heat curing of 165°C for 10 hours was determined. The sample produced under an extra 165°C heat application was quite different from the sample obtained by keeping it at 185°C for 8 hours. While the solution was applied at 185°C for 8 hours, a hard rubbery structure was obtained. On the other hand, when an extra 165°C was applied to the solution for 10 hours, the products were obtained in a different, granular form. FTIR analysis of the BII PIS block copolymer showed similar results with the FTIR analysis of the BI PIS block copolymer. FTIR results are shown in Table 5.2 (and also seen in Figure 5.2).

Table 5.2 : FTIR analysis of poly(imide siloxane) block copolymer BII.

Bound	Peak (cm^{-1})
aliphatic C - H stretching	2962
asym C = O stretching	1777
sym C = O stretching	1712
asym Si- O -Si stretching	1091
sym Si- O -Si stretching	1014
Si - C stretching	799
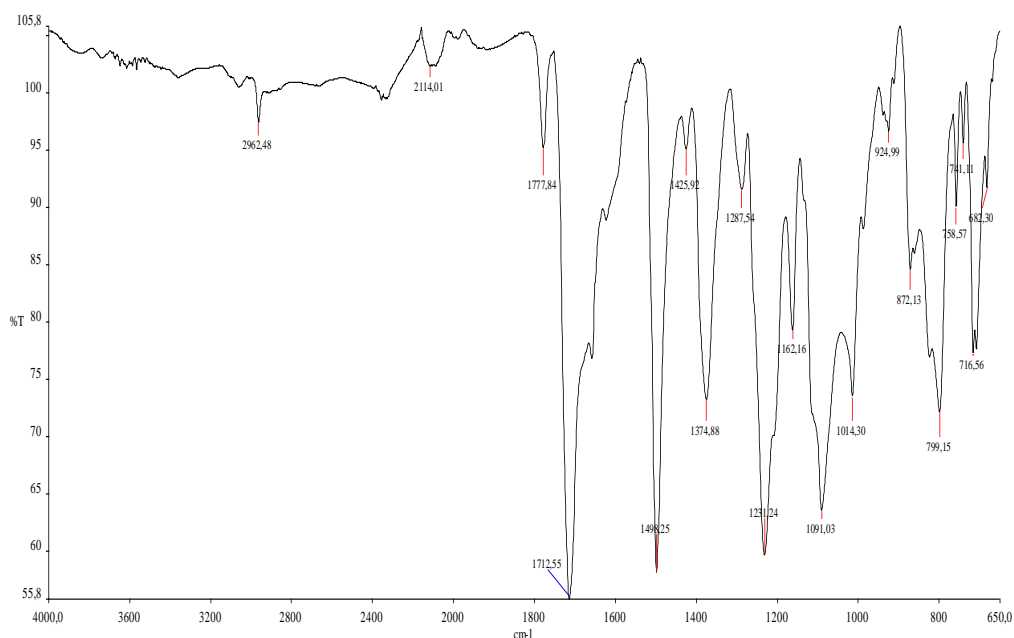
Figure 5.2 : FTIR analysis showing the extra heat-curing effect on BII block copolymers.

BI, BII samples were used in the same amounts to comparing the peaks at FTIR analysis (Figure 5.3). In the FTIR spectra of BI and BII copolymers, the peaks on 1781, 1777,1722, 1717, and 1712 cm^{-1} are because of carbonyl of amide groups. The peaks are those that indicate the carbonyl groups of the PIS structure (Figure 5.1-5.2). The peaks at 1501, 1500, and 1498 cm^{-1} are amide groups of N-H amide bonds. Those amide absorption peaks on 1781, 1777,1722, 1717, 1712 cm^{-1} indicates the development in the structure of BI and BII block copolymers by losing COOH at the end of the capping reaction (Figure 5.3). FTIR analysis of the samples confirmed the presence of siloxane segments in the polymer. C-H bond corresponding to the methyl groups is available with a peak ~2960 cm^{-1}.

The presence of detected diamine peaks by FTIR analysis shows that the polymer chain ring is completed and desired chemical synthesis is obtained. It is understood from these peaks that the anhydrite structure turns into diamine peaks by completing the aromatic ring chain. These peaks indicate the presence of ligaments that make the structure elastic.
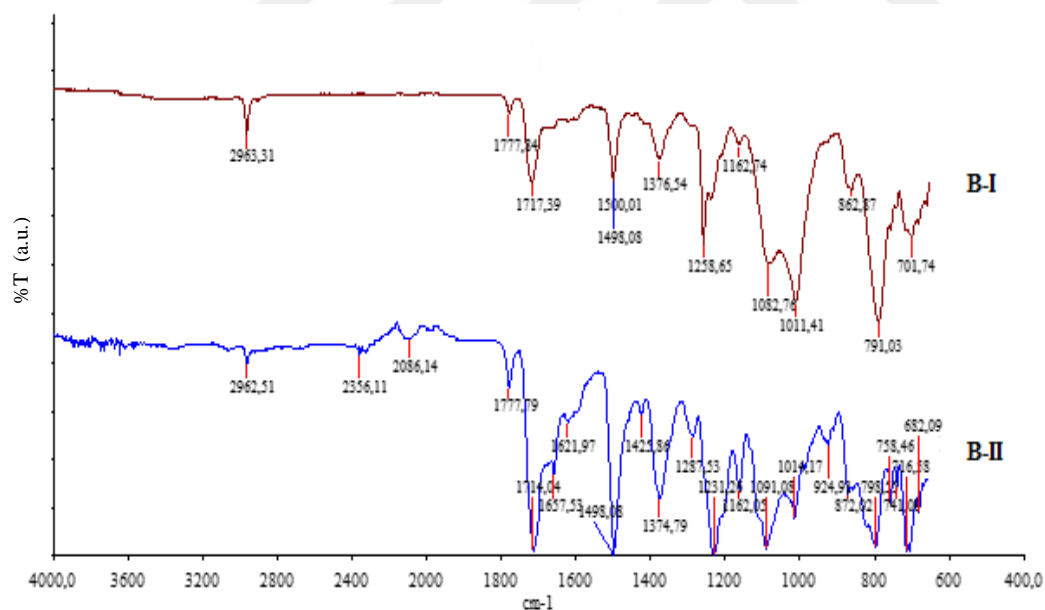
Figure 5.3 : FTIR analyses of the BI and BII PIS block copolymers.

FTIR analysis characterization interpretation shows the presence of silicone and rubber structures in block copolymer structures. Thus, it is understood that the samples produced using new chemicals with different anhydrides are made of silicone and rubber and have elastomeric properties. The results of the FTIR analysis show that the produced material by the new chemicals is also suitable for the formation of flexible

substrates. The chemical structure in copolymers usually consists of siloxane Si-O and carbon chain structures. Block copolymer synthesis using APPS occurs in chains where the anhydrous ring is completed by BTDA. The presence of diamine peaks seen in the FTIR analysis results indicates that the polymer chain ring has closed.

5.2 Thermal Analysis of Produced Poly(imide siloxane) Copolymers

TGA and DSC analyses were performed to determine the strength limit and the endurance of the obtained poly(imide siloxane) copolymer structures at high temperatures.

5.2.1 TGA analysis of produced poly(imide siloxane) copolymer structures

TGA was applied under inert gas(nitrogen) via heating rate of $20^{\circ}C$ min^{-1} from $38^{\circ}C$ to $800^{\circ}C$ for BI, and BII copolymer samples.

The loss of substance in BI PIS block copolymer was determined as 2.41% and 0.132 mg at $200^{\circ}C$; 7.81% and 0.428 mg at $400^{\circ}C$; 17.90% and 0.982 mg at $500^{\circ}C$; 62.79% and 3.446 mg at $600^{\circ}C$; 74.73% and 4.102 mg at $700^{\circ}C$; 76.41%and 4.194 mg at $800^{\circ}C$ (Figure 5.4 and Table 5.3). According to the results of TGA measurements, the BI PIS block copolymer maintains its thermal stability to a high temperature, such as $500°C$ (in Figure 5.4 and 5.5). On the other hand, it was detected that the composition of the BI block copolymer structure was significantly decomposed at $600°C$.
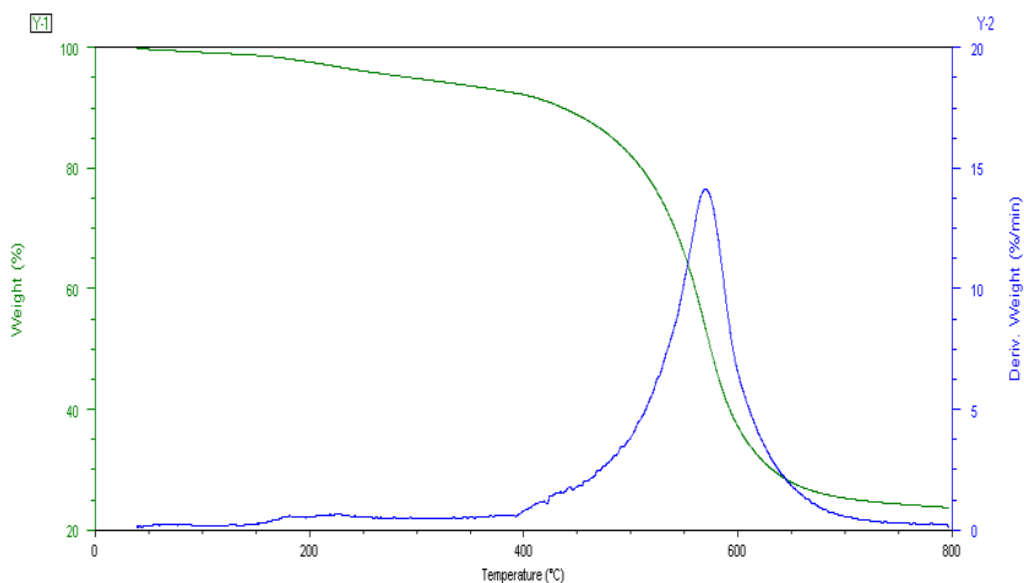
Figure 5.4 : TGA analysis of the BI PIS block copolymer.

TGA analysis of BII PIS block copolymers was presented in Figure 5.5. The loss of substance in PIS block copolymer BII was determined as 3.02% and 0.285 mg at 200ºC; 7.16% and 0.676 mg at 400ºC; 10.89% and 1.028 mg at 500ºC; 25.83% and 2.440 mg at 600ºC; 43.77% and 4.135 mg at 700ºC ; 48.25%and 4.559 mg at 800ºC (Table 5.3). Thermal degradation behaviors in BI and BII block copolymers were virtually identical. The weight loss of the copolymer BII was ~7-8 % in the range of ~ 400-450ºC as in BI block copolymer. Td as thermal degradation is an important index in discussing thermal stability of polymers and Td of the block copolymer samples were detected between 400-450ºC. The weight loss of the BII block copolymer was detected as 10% in the range of 500-550ºC. 25% weight loss was determined at 600ºC. The structure of the BII copolymer was decomposed mostly at 600ºC as seen in Figure 5.5.
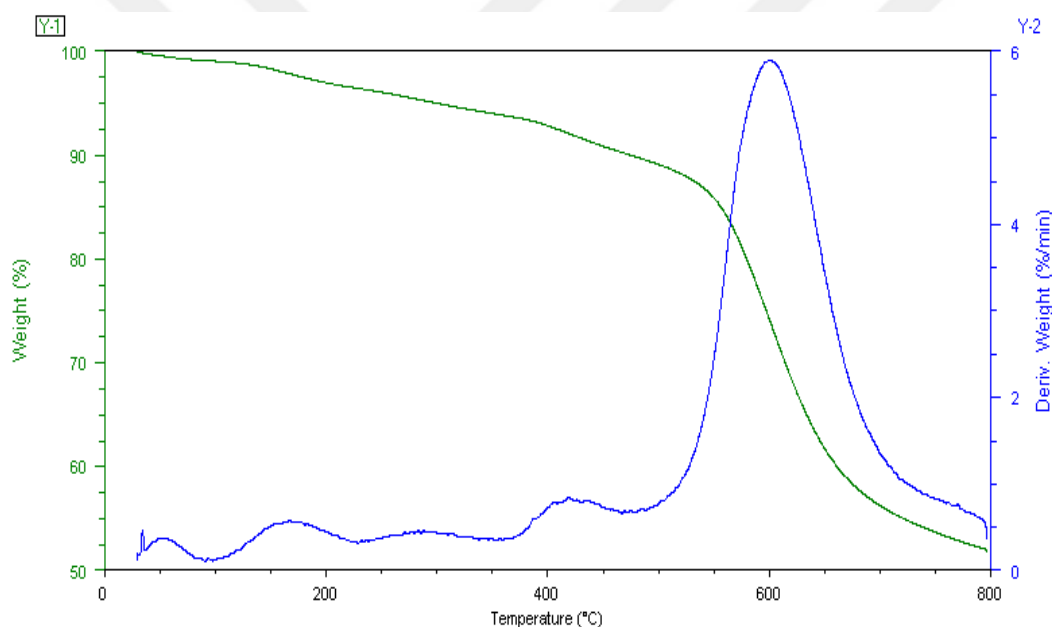
Figure 5.5 : TGA analysis of the BII PIS block copolymer.

The substance loss of BI and BII block copolymers was almost the same under inert gas (Table 5.3). It is caused by the diamine chains present due to the APPS content and that thermal degradation begins in the weak aliphatic n-propyl bonds in the PIS copolymers. The Td of the copolymers showing thermal degradation was tied to the APPS content more than the chain length contained in both block copolymer samples [25,26].

Td value was increased by increasing the hard segment content. Therefore, the thermal stability of the BII PIS block copolymer was better than the BI PIS block copolymer,

especially after 500ºC. The application of a higher temperature cure during the production of the BII sample has broken the linkages between the diamines faster, and this made to get a harder structure. This enabled to free dianhydride. Free dianhydrides capped polysiloxane and new, closed aromatic rings were produced faster and stronger in BII rather than in BI samples. Details about the values were given in Table 5.3. Thermal degradation was an important index for examining the thermal stability of polymers. According to Td results, it was resulted that the thermal stability of the PIS BII sample was better than the BI sample. It was assumed that thermal degradation in PIS developed with an increase in the hard segment contents. The BII block copolymer structure is considered to have better thermal resistance than the BI block copolymer structure due to the increase in the hard segment content in the BII block copolymer structure, and with this increase, the BII block copolymer structure had higher thermal resistance than the BI block copolymer structure.

Table 5.3 : Substance loss of PIS block copolymers.

Temperature Range (ºC)	BI		BII	
	Subst. Loss (%)	Subst. Loss (mg)	Subst. Loss (%)	Subst. Loss (mg)
200	2.41	0.132	3.02	0.285
400	7.81	0.428	7.16	0.676
500	17.90	0.982	10.89	1.028
600	62.79	3.446	25.83	2.440
700	74.73	4.102	43.77	4.135
800	76.41	4.194	48.25	4.559

5.2.2 DSC analysis of produced poly(imide siloxane) copolymer structures

Differential Scanning Calorimetry (DSC) is a useful method with its fast, easy to use, and very sensitive properties. It is generally abbreviated as DSC and it detects thermal transitions due to phase transitions (primary, as melting, crystallization of pseudo-secondary as glass transition) and chemical reactions (thermal decomposition or oxidation). Decomposition (and sometimes oxidation) is coupled with significant mass change and mass change is related to desorption or vaporization. The resultant heat difference is a temperature function. Sample and reference are kept at a constant

temperature during this procedure. These analyzes showed enthalpy changes in samples. The materials were characterized and defined by this technique. Enthalpy changes were determined where thermal decomposition was due to significant mass change. Changes prove that significant heat fluctuations occur within the bonds of the samples, and these fluctuations can be identified by enthalpy changes as a function of temperature where thermal decomposition occurs.

The function of temperature shows heat differences. DSC is also used for examining thermal analysis in polymers by monitoring the heat capacity (as a function of temperature). Differential Scanning Calorimeter was used as thermal analysis for measuring energy directly and gave certain results about the heat capacity of copolymers. Endothermic peaks were recorded in DSC not necessarily have to be related to the melting. The endothermic peak can stem from a phenomenon called enthalpy relaxation depending on the polymer and the experimental conditions.

This method was used for measuring the variation in the required heat quantity to increase the temperature of the copolymers. DSC information was used to complete TGA data in this work and to get precise results and it is performed TGA analysis along with DSC. The DSC curves of the copolymers are shown in Figures 5.6-5.7.

DSC analyzes of copolymer samples were applied in an inert gas (nitrogen) with a heating rate of $38^{o}C$ to $800^{o}C$ with a heating rate of $20^{o}C$ min^{-1} for all copolymer samples. Enthalpy changes in BI PIS block copolymers (Figure 5.6) and BII PIS block copolymers (Figure 5.7) result from the chemical composition of the copolymers as a function of temperature. Therefore, it was possible to identify and characterize the produced copolymers in this study.

There was a relation between the loss in mass and heat loss via the exothermic reactions which are determined from DSC analyses (in Figure 5.6-5.7). On the other hand, heat losses that were observed via exothermic reactions on DSC analyses are compatible with the loss in mass which was determined from TGA analyses (in Figure 5.4-5.5).

The changes in DSC analyses indicated that the thermal decomposition occurred with insignificant mass change. The insignificant mass change presented insignificant heat fluctuations. These fluctuations addressed enthalpy changes as temperature function resulted in thermal decomposition. Grey remainder was obtained at the end of the

thermal decomposition process, which was considered as SiO_2. The reason for this result was probably dependet on SiO_2 remained on the sample container of the TGA device [25,26].
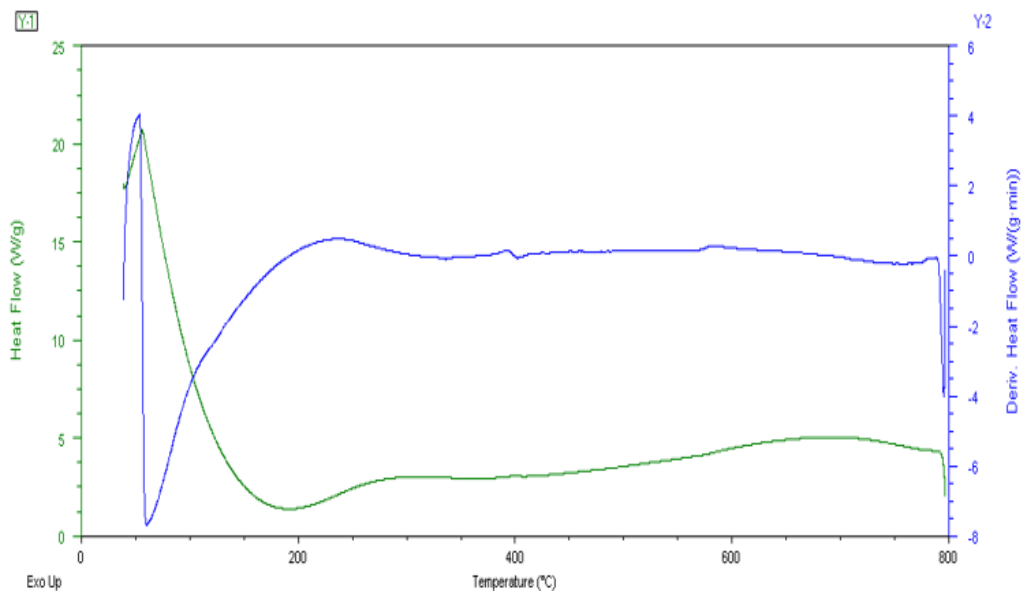
Figure 5.6 : DSC analysis of the BI PIS block copolymer.
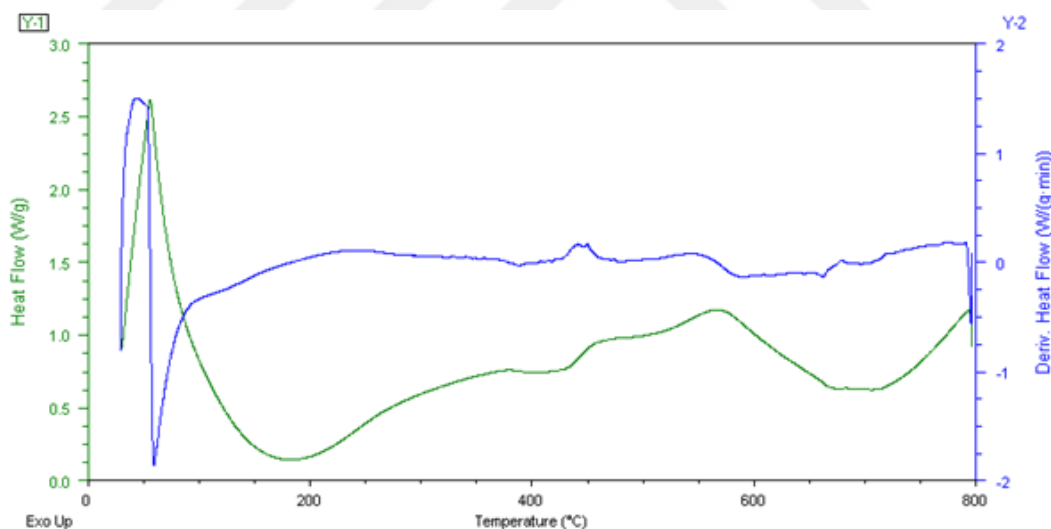
Figure 5.7 : DSC analysis of the BII PIS block copolymer.

BI copolymer structures maintain their softness and rubbery form as a result of the cooling process. The structures, which are produced in soft and rubbery form, can maintain its physical condition even in a cold environment. It was found from DSC results that siloxane segments were not crystallized. They are in an amorphous form. Hence, PIS copolymers have possed thermal plastic elastomer properties. According

to the detected TGA and DSC results, PIS copolymers have been observed to have high thermal resistance, flexibility, and adhesion. Due to these properties, these materials have very important usage areas as substrates in microelectronic devices, medical devices, aerospace applications, and solar cells [2-7]. TGA analysis showed that block copolymer materials have high-temperature resistance. These materials have potential uses as substrates in microelectronic devices, aerospace applications, and solar cell technology due to these properties [2-7].

5.3 XRD Analysis of Produced Poly(imide siloxane) Block Copolymer Structures

In the literature, there is no detailed structural characterization comparison for the diffraction planes of flexible BI and granular powder BII samples. The XRD diffraction (XRD) spectra of both samples are shown in Figure 5.8 and Figure 5.9. The crystallinity in the PIS block copolymer BII appears to be quite high compared to the PIS block copolymer BI. XRD patterns in all samples showed amorphous conditions. The line widths can be expanded for polymer diffraction and usually have an important amorphous peak as in poly (imide siloxane) block copolymers BI. The angles for XRD characterization was taken between 20° and 120°, and no vertex was determined. It is shown in Figure 5.8.
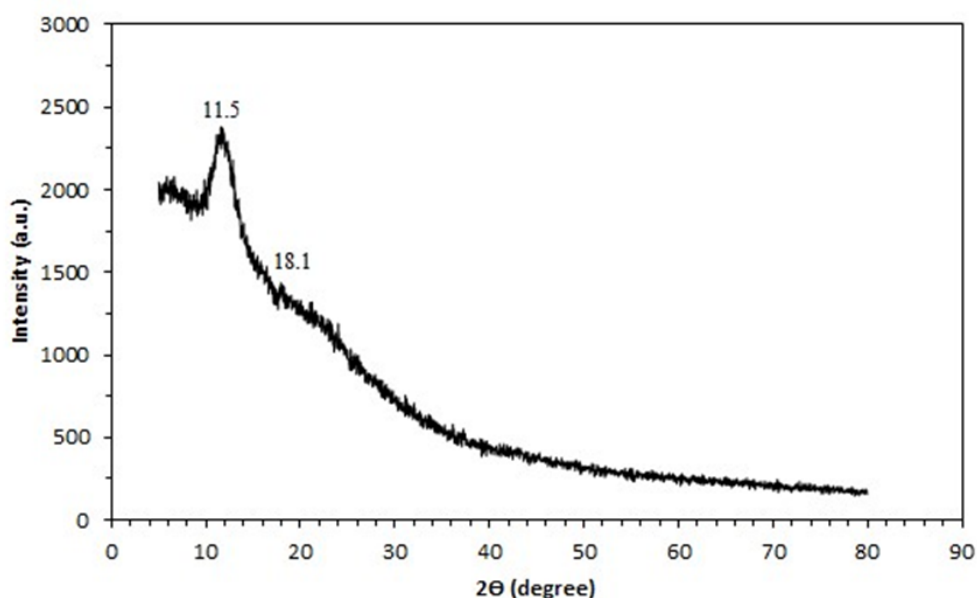
Figure 5.8 : XRD analysis of block copolymer BI.

64

The two diffraction peaks were distinguished at $2\theta = 11.50°$ and $18.1°$ in the BI sample. A violent peak was observed at $2\theta = 11.50°$. It demonstrated that APPS in the soft domain significantly reduced crystallization in poly (imide siloxane) block copolymer BI. The X-ray Diffraction (XRD) peaks of the BI sample corresponding to the diffraction planes (330) and (050) are seen in 11.5 and 18.1 (2 Theta), respectively (Figure 5.8).

The hydrogen bonds in the BI sample were predominantly affected due to the addition of APPS and the Si-O-Si crosslinking chains of the solution. It can be said that the crystallization direction of both soft and hard regions of PIS block copolymer BI structures is destroyed by the addition of APPS during the synthesis of the structure. It reduced the formation of Si-O-Si crosslinking chains, hard segments that cause crystallinity. Cross-linked chains of Si-O-Si are bonds that indicate the presence of amorphous structures rather than crystal structures. These results show that the tendency to crystallize in the BI sample was destroyed in both soft and hard blocks. Crystallization in the soft block decreased due to the rubber properties in the BI sample. FTIR analysis of the samples supports this (Figure 5.8). This study supports other structural characterization results. XRD analysis of the BI PIS block copolymer shows that the structure has an amorphous phase.

Poly(imide siloxane) block copolymers have crystal formation due to stronger hydrogen bonds between hard-soft and hard-hard parts. The formation and development of the crystal structure during the transition of the material from the BI structure to the BII structure is probably due to the fact that the fixed, smooth chain structures formed by hydrogen bonds begin to be arranged together. Therefore, there are strong hydrogen bonds in the hard-soft and hard-hard segments, which causes more crystal formation in the BII sample of the bonds, and this is the most important reason for crystal formation. Peaks showing the hard region crystallization present in the BII structure at $2\theta = 16.05°$, $21.04°$, $23.1°$, and $27.57°$, since the BI poly(imide siloxane) block copolymer contains more Si-O-Si cross-linked bond due to APPS, aren't seen in BI structure. In BII PIS block copolymers, peaks appear at 2 Theta = $16.05°$, $21.04°$, $23.1°$ and $27.57°$, and these peaks indicate various crystal sizes or BII structure tended to crystallize [29-31]. As the diffraction planes, (330), (730), (050), (550), (460) and (002 correspondings to 11.5, 16.05, 18.1, 21.04, 23.1 and 27.57 (2 theta degrees) on

X-ray Diffraction (XRD) patterns (in Figure 5.9) show that the BII block copolymer is at the semi-amorphous structure.
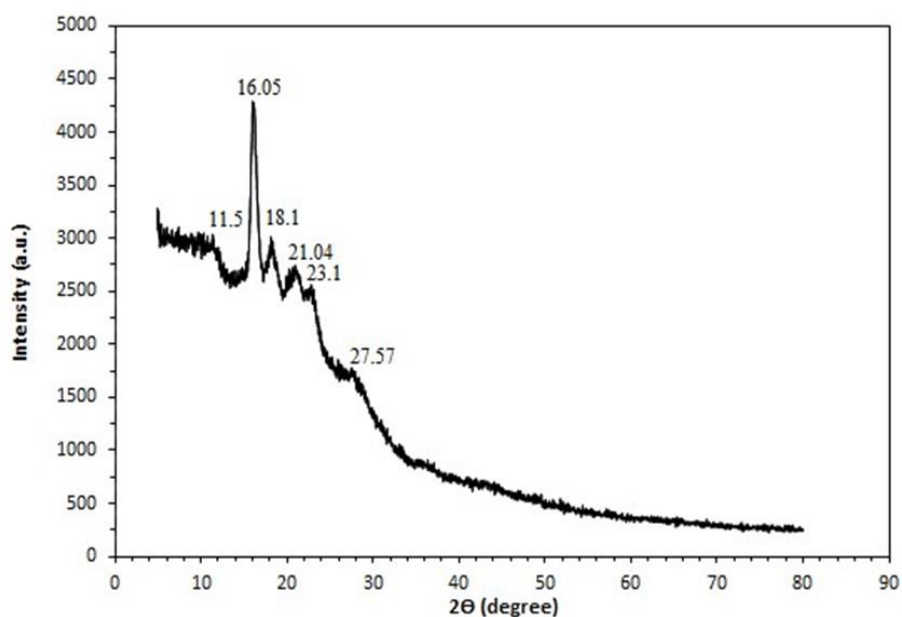
Figure 5.9 : XRD analysis of BII block copolymer.

XRD analysis of BI PIS block copolymers (Figure 5.8) and BII PIS block copolymers (Figure 5.9) supports these results. XRD results show that the BII structure has a solid and granular form. The density of the XRD peak in BII was more intense than the XRD density of the BI sample. The density of the XRD peak of the BII sample showed that the crystalline properties increased. The reason for the improvement in the properties of the crystal with the disappearance of its elasticity can be explained by the homogeneous chain alignment due to the hydrogen bond [31]. Similar XRD diffraction planes can be seen in the literature for cyclotetracyloxane [29] and methacryloxy propyl trimethoxy silane [30].

5.4 Examination The Surface Morphology of the Produced Polymer Structures

SEM (Scanning electron microscope) (VacMode ESEM) was used for analyzing the surface of the polymer. SEM images of the samples were coated by gold in a vacuum and mounted on aluminum mounts with carbon paste.

Surface topography in PIS copolymer samples was examined through Shimadzu SPM 9500 AFM (atomic force microscope) by operating in tapping mode. Images of AFM were taken on 10x10 μm^2 areas.

5.4.1 Surface morphology of the poly(imide siloxane) copolymers

The details on the surface morphology for the changes and several microstructural differences were determined at surfaces of the copolymers and SEM micrographs of copolymers with several hard segment contents were presented in Figures (Figure 5.10 - 5.11). Differences in the synthesis process were analyzed via SEM images of the block copolymer samples. Smooth surface morphology was seen in the BI sample (Figure 5.10).

The SEM micrograph of BI surface morphology showed separation of microspheres at 600x and 1000x magnification (Figure 5.10). The SEM micrograph of the BII sample is available in Figure 5.11. The flexible form of poly (imide siloxane) samples (BI) has a more homogeneous surface morphology compared to the lumpy grain form (BII) of poly (imide siloxane) samples. In the BI sample, the melted viscosity during imidization is directly affected by the APPS segment and showed similar results to the polyimide content depending on the rubber properties [31-32]. An increase in microphase resolution in the BI sample started with the addition of more ODA in this study. The imidized polyimide particles in BI and BII samples tend to aggregate and the slightly isolated microphase starts to grow. In this study, the heterogeneity (microphase separation) on the surface of the copolymer increased as seen in Figure 5.10-5.11.

The low polyimide content was dispersed into very small particles (in Figure 5.10-5.11) before imidization as an indicator of hard segments. It is assumed that the formation of polyimides occurs gradually during imidization and aggregation behavior. According to the results of SEM screening, the morphological structure was not homogeneous in the BI structure and was more intensely distributed in some regions. It is thought that APPS and BTDA structures form soft blocks of BI structure in some scattered regions consisting of random block distribution and this explains the flexibility in the sample.
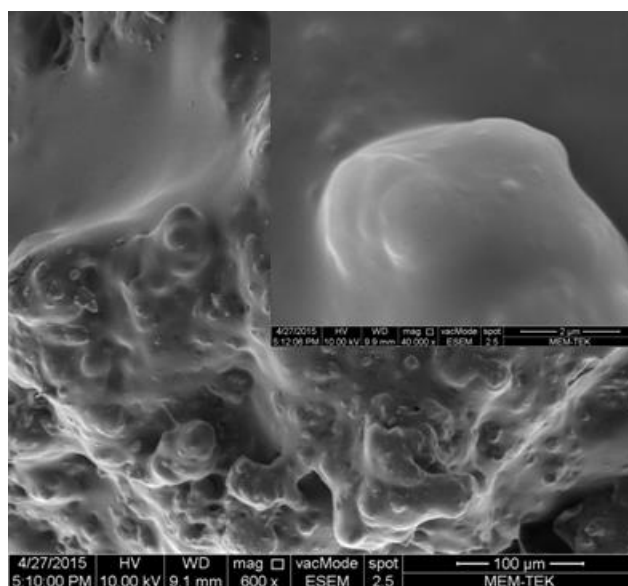
(a)
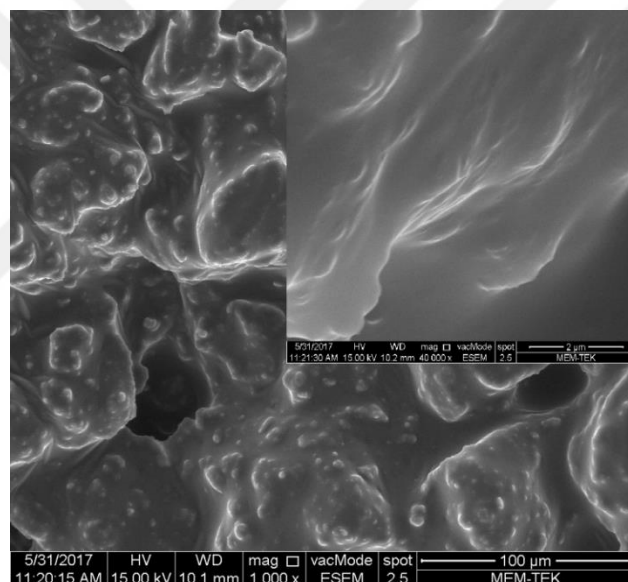
(b)

Figure 5.10 : SEM images of BI (a) for unpressed (b) pressed state (by 30 tons).

Polyimide formation in the BII sample gradually increased more comparing to BI samples by the increase of the heating time and the formed polyimide showed a tendency to aggregate in the bulk phase of block copolymer samples. The surface morphology examinations of the polymers are seen in the literature [32] and the details about the surface morphology of the pellet form of PIS are not mentioned in the literature.
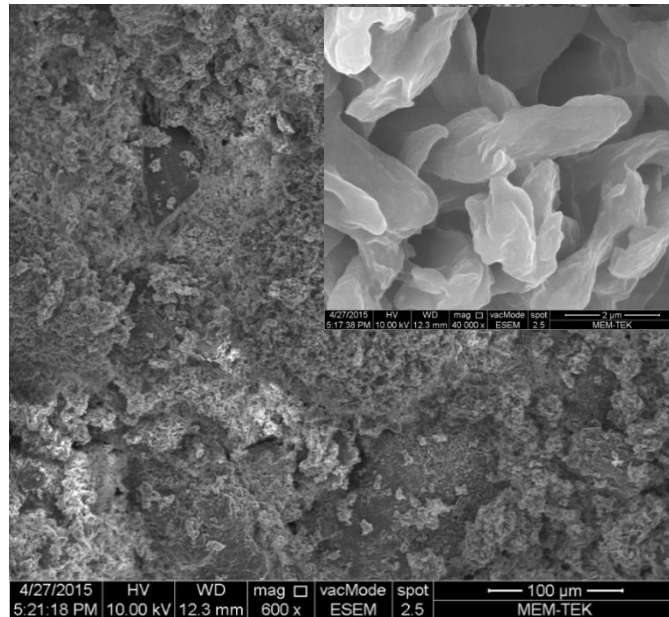
Figure 5.11 : SEM image for the BII surface of PIS block copolymers.

The details about the surface morphology of the pellet form of PIS was presented in Figure 5.11 in this study. The surface morphology of the BII structure exhibited a grainy, powder form because of the rise in heat cure of the synthesis. (Figure 5.11). The BII copolymer sample contains a highly hard segmented layer, and this content leads to improved microphase separation as seen in Figure 5.11. There appears to be an insufficient distribution in terms of compatibility between the two phases of the copolymers (soft and hard segments). The SEM micrographs shown in Figure 5.11 show the crystallite aggregation. It has been previously stated that the granular structure of the BII sample is related to the applied heat cure, and the SEM images confirm this. In microstructural images of copolymer samples, the comparison shows the effect of production parameters such as temperature and time on surface morphology (Figure 5.10-5.11).

5.4.2 AFM analysis of produced poly(imide siloxane) copolymer structures

Atomic Force Microscope (AFM) analysis is one of the methods of surface morphology analysis which allows obtaining three-dimensional microimages with resolution scale down to angstrom and micron ranges. Therefore, it is one of the preferred methods in surface imaging. The sample surface is scanned with the cantilever tip, which is one of the AFM components. The head is adjusted under a constant force and the surface homogeneity and height difference are detected by a

detector by scanning with the tip. The information received from the detector with the computer is converted into an image.

Softer parts in the image are observed in darker colors than those of the hard parts. Therefore, sections containing siloxane on AFM are darker than those containing imides. It is understood that homogeneity is not fully achieved due to the presence of dark and light areas on the surface of the block copolymer structures. The siloxane structures, which are dark regions, show the areas remaining in the pit in the surface topography. Thus, it was determined that there is a height difference between dark and light color regions. This indicates that the surface roughness will improve by reducing the molecular weight and amount of the APPS segments. This morphological difference is also affected by the compatibility between the APPS and polyimide segments. Images of AFM can be altered by changes in APPS content and molecular weight and are observed as it is in the form of islands in the sea in a kind of surface topography. The addition of more APPS means the formation of more peaks and valleys on the surface. Surface roughness is expressed as "Ra", which is defined numerically as a roughness factor. With this coefficient, information about surface roughness measurement for the structure is obtained by the nanometer size. Roughness value increases in proportion to the APPS content or molecular weight when the surface images are evaluated. The surface of the polyimide structure is flat and smooth when the surface roughness on the structure is less. Polysiloxane segments dissociate from polyimide state into wider regions named as islets. Thus, surface roughness in the structures is related to the intensity of the segment differences between two blocks. Such morphological difference is influenced by compatibility or difference between APPS and polyimide layers.

Therefore, imidization in the BI sample is directly affected by the APPS segments in the form of molten viscosity. In this study, the rubber properties of the structure are determined to depend on the polyimide content. The increase in microphase separation of the BI sample started with the addition of more ODAs. The imidized polyimide particles in BI and BII samples tend to accumulate and begin to grow as slightly isolated microphases. In this study, the heterogeneity of the surface in the copolymer increased as seen in Figure 5.12. The low polyimide content dispersed into very small particles (in Figure 5.12-5.13) as a precursor to the hard segments prior to the immidization. It is assumed that the formation of the polyimide occurs gradually

during imidization, and the formed polyimide BI and BII copolymer samples tend to accumulate in the bulk phase.
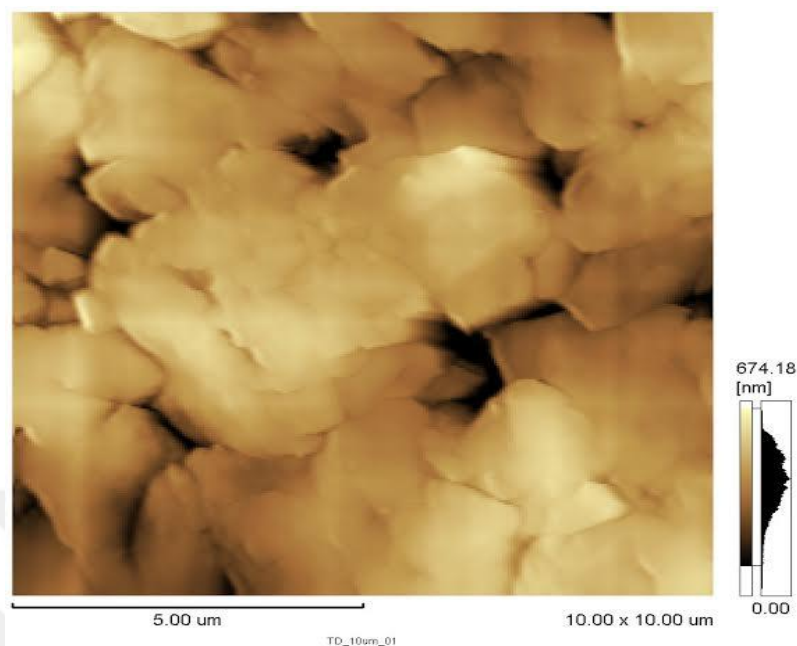
Figure 5.12 : Surface morphology of PIS block copolymer BII in 2D dimension.

The BII copolymer sample with a high hard segment structure exhibited greater microphase separation in Figure 5.13. There appears to be incompatible compatibility between the two phases of the copolymers (soft and hard segments). AFM micrographs show the crystallite aggregation in Figure 5.13. It is stated that the granular nature of the BII sample is related to the heating cure applied to the BI sample. Therefore, the details on the surface of PIS samples (BII) in pelleted granular form were analyzed by AFM. The surface roughness was analyzed in 2D and 3D images in Figures 5.12-5.13, respectively. AFM images were taken from 10x10 μm areas. The surface roughness was defined as a numerical "Ra" value as 674.18 nm (denoted as the Z value in Figure 5.13), defined as the roughness factor [75-80].
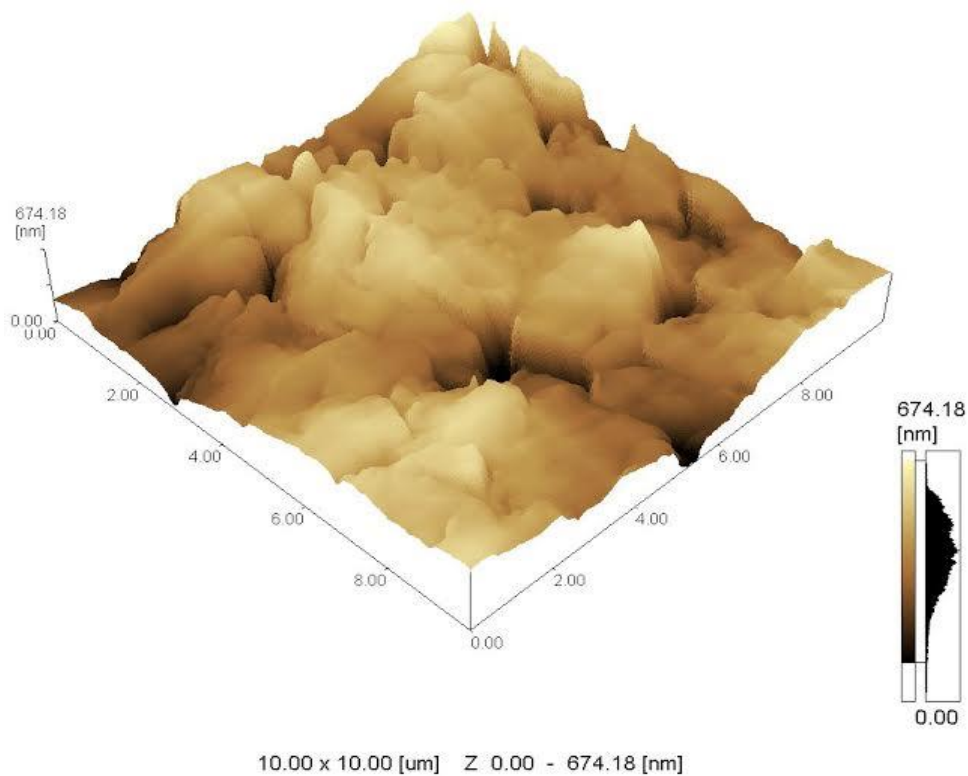
Figure 5.13 : Surface morphology of the PIS block copolymer BII in the 3D
dimension.

5.5 The Solubility of PIS Block Copolymer Samples

In the PIS block copolymer structure, the chain flexibility can be activated by
destroying the chains thanks to the solvent [27]. In this study, BI and BII copolymer
samples were examined by five different solvents as (N-methyl-2-pyrrolidinone
(NMP); 1,2-Dichlorobenzene (ODCB); Dimethyl sulfoxide, C_2H_6OS, (DMSO);
Chloroform ($CHCl_3$); 1,1,1,2-Tetrafluoroethane (CH_2FCF_3) (for 100 minutes).
Organic solvents are known to have the significant oxidizing capacity in polymers
[81]. Therefore, the copolymer solubility was examined by using 0.5 g copolymer
powder and 2 mL of organic solvent at room temperature for evaluating aggressive
media performances of the samples (eg. in the production stage of thin films on solar
cell substrates in acidic ambient). Copolymer samples in solvents remained insoluble
at room temperature. The temperature was raised to the boiling points of the solvents.
The solubility results of the copolymers are presented in the table below (Table 5.4).

Table 5.4 : Solubility in the PIS block copolymers.

Polymer	*Solvents*				
	NMP	**ODCB**	**DMSO**	**Chloroform**	**R134a**
BI	±	±	±	±	-
BII	±	±	±	±	-

Key : (+) soluble at room temperature;
(±) partly swelled at room temperature by mixing;
(-) nonsoluble on heating.

The BI sample wasn't dissolved in any solvents at room temperature. The BI block copolymer turned out to be soluble very little or partly swelled for 100 minutes at room temperature by stirring in Chloroform, DMSO, ODCB, and NMP and it was assumed that the reason of this was related to increases in the BI block lengths. On the other hand, PIS copolymer samples were not soluble within CH_2FCF_3 neither by mixing at room temperature nor by stirring with heating. Solubility was reduced and viscosity was increased by increasing the lengths of blocks. Poly(imide siloxanes) are extremely unpolar. They also have very low solubility comparing to other polymers. These copolymers can be used as compatibilizer with other organic polymers due to aromatic imide segments. For these reasons, it is possible using these samples as additives and as compatibilizing polymer in various technological applications [25,81].

5.6 Examinations for Mechanical Properties

The mechanical properties were investigated for the BI sample. As BII was synthesized as a granular structure, mechanical tests were not applied to BII samples in this study.

5.6.1 The uniaxial pressing results of flexible BI PIS Block Copolymers

Uniaxial pressing is one of the most used forming technologies in various materials. It allows the elastomer structure to be shaped on a wide surface. PIS block copolymer samples in various industrial applications, especially in areas where radiation effect is intensive and where applications are required as a light and flexible substrate or carrier were pressed by uniaxial pressing according to the standardization concept (European Union Standards). Companies are trying to develop standards on elastic structures suitable for uniaxial compression testing because uniaxial pressing test results show the reusability of the rubber structure (Si-O-Si structure). In addition, companies are

trying to produce uniaxial pressure testing standards for poly(imide siloxane) derivatives with good thermal resistance, high-temperature resistance, antioxidative resistance, and corrosion resistance (especially in rainy weather conditions).

In this study, the uniaxial hydraulic press was applied to examine the elastic recovery of the BI sample. In general, the press used in uniaxial hydraulic press tests was applied to examine the pressing performance of the PIS block copolymer sample in the range of several kilograms. A single-axis press test performed up to 950 kg. No significant difference was observed between unpressed and pressed samples until 950 kg was applied to the samples with the uniaxial press. Therefore, BI PIS block copolymers were pressed with 10, 20, and 30 tons, respectively, using Single Axis Hydraulic Press - MSE, which is usually applied to stainless steels, to test mechanical performance at 10, 20 and 30 tons. The elastic recovery of the sample was examined using this mechanical test. PIS block copolymers showed silicone-rubber properties. PIS block copolymers produced as a flexible plate showed a very flexible feature and silicone-rubber property. It was observed that BI samples returned to their original flexible forms after a few minutes and stabilized their elastic recovery. The tensile modulus of the BI sample was reduced by increasing the lengths of the segments (as a soft and hard block). Probably, elastic recovery in BI samples was raised by increasing lengths of both soft and hard blocks. There are some studies on elastic recovery in the produced block copolymer in the literature [15] and our results in this study are similar to the literature. PIS block copolymers can be produced in various siloxane segment lengths. The characterization of the samples reveals that mechanical properties decrease in longer siloxane segments [28]. The thermal resistance decreases by the length increase of soft blocks (APPS). Hence the effect of minimum block length in the mechanical and thermal properties of the copolymer was examined in this study.

5.6.2 Radiographic inspection of flexible BI PIS Block Copolymers

Several digital X-ray systems can supply fast and quick industrial studies by using advanced technology. These systems are quite sensitive to detect the defects in the polymer materials and it provides a permanent visual record of the pattern of the degradation [73]. The sensitivity of the radiographic image is a measure of the quality of the image in terms of the smallest detail or discontinuity in the examined material.

In this study, the radiographic images for the pressed BI copolymer samples were compared with the unpressed ones sensitively in the view of quality control. The

radiographic examination (as one of the major nondestructive testing methods) was performed to examine the homogeneity of the copolymer BI samples after the application of the uniaxial hydraulic press at three different pressing values such as 10, 20 and 30 tons. Homogeneity of the sample was analyzed thoroughly and non-invasively, as well as more sensitively and rapidly by using the radiography technique. The radiographic inspection technique by using digital X-ray systems was applied to research the differences in the main geometric image quality of the samples. The details on the radiographic images of the pressed samples were examined clearly by using digital X-ray radiography and changes in the mechanical performance of flexible BI copolymer following compressive strength tests were investigated. Radiographs were obtained applying 6 pulses by digital X-ray systems. The distance between the radiation source and the sample was 60 cm. Hence, the variations in the homogeneity of the copolymer samples were examined sensitively by using the radiographic test technique after block copolymer samples were compressed under three different pressing values such as 10, 20, and 30 tons by Uniaxial Hydraulic Press–MSE.

The variations on the contrast of the radiographic images indicated the degree of the discontinuity and the density difference between the unpressed and the pressed samples. In this study, changes in the mechanical performance of flexible poly(imide siloxane) copolymer by compressive strength test were investigated. There was no significant change in the homogeneity of the pressed (hydraulically) flexible samples in radiographic images compared to the unpressed sample at three different pressing values (10, 20, and 30 tons). Radiographic examination results indicated that elastic deformation corresponding to structural damage has not been occurred after three different pressing values. As a result, after three different presses applied to the flexible BI copolymer samples, the differences related to mechanical degradation in poly(imide siloxane) were compared with the X-ray radiography technique and no significant difference was found (in Figure 5.14).

Figure 5.14 : Radiographic examination of the flexible BI block copolymer.

5.6.3 Dynamic mechanic analysis of flexible BI sample

Dynamic Mechanic Analysis (DMA) measurements for the BI block copolymer was carried out by creep-recovery and stress relaxation testing. The testing results were presented for creep-recovery (in Figure 5.15) and stress relaxation testings (in Figure 5.16), respectively. The creep-recovery test for the block copolymer was carried out by DMA TA Instruments Q800. The specimen was compressed by using the compressive mode of deformation. The inverse of creep testing was used for stress relaxation testing. The sample was compressed quickly and the decay of the strain exerted on the material. In the creep testing, the sample was pressed with a set weight as constant stress and then watched the strain over time. BI block copolymer sample was pressed with a very low-stress level to hold the sample in the place and let to stabilize. The creep testing stress was applied, and the changes in the sample response were taken as a percentage of the strain during the test. The BI block copolymer was held under this stress 200 minutes until the sample reached equilibrium. After removing the applied press, the strain recovery was taken as a time function. After stress on the sample was lift up, the initial deformation was observed and the recovery part of the strain-time diagram occurs in common form. The strain recovery was recorded as a function of time. The curve was nearly linear in the initial deformation (in Figure 5.15).
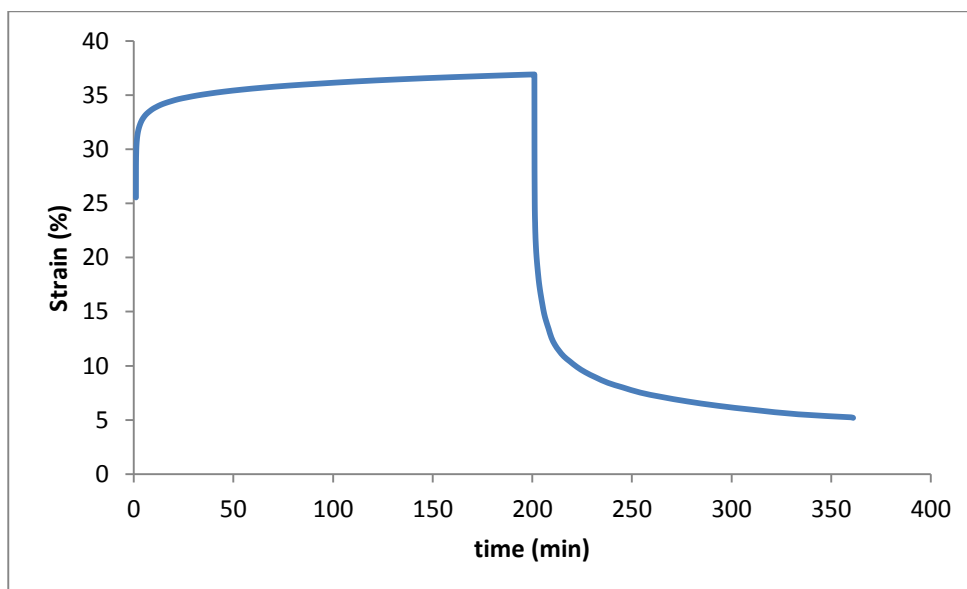
*: Constant stress is 0.005 MPa

Figure 5.15 : Creep-recovery test graph for the BI block copolymer.

After elastic recovery, viscoelastic creep and permanent flow were determined. After the initial deformation region, a transition zone was observed, and then the equilibrium region started. In this region, the material started to return to its original value in approximately 200 minutes (Figure 5.15). This region belonged to the characteristic feature of any viscoelastic material and the graph was typical. How much polymer came back after the stress was released could be detected by the percentage of the recovery. After the equilibrium region, the recovery region started and the amount of recovery was recorded. It was detected how the material relaxed when the press was lifted up by the recovery testing. According to the creep- recovery graph, %95 of the sample came back to its original value and %5 of the sample was unrecovered after lifting up the press in 170 minutes. Constant stress was 0.005 MPa. Stress relaxation testing is inverse of creep testing. The sample was compressed quickly and the decay of the stress exerted by the material was measured. The analysis of the stress relaxation graph is shown in Figure 5.16.
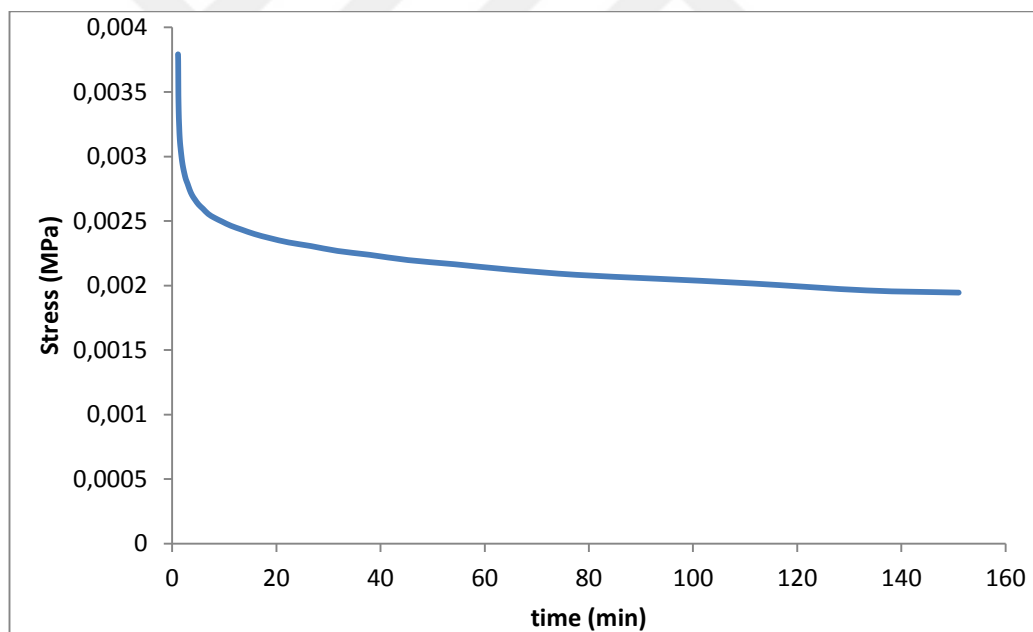
**: Constant strain is % 20

Figure 5.16 : Stress-relaxation test graph for the BI block copolymer.

Constant strain rate is %20 according to the analysis. After removal of the applied stress, there is not considered the creep rupture at poly(imide siloxane) block copolymer. Dynamic Mechanic Analysis (DMA) testing results of poly(imide siloxane) presented the importance of creep-recovery at the several application areas.

5.7 Application of Radiation Transmittance Technique

Radiation attenuations for gamma, beta, and neutron were measured to inspect shielding properties of BI and BII samples for different thicknesses.

5.7.1 Comparison of gamma-ray attenuation parameters between flexible and granular forms of PIS samples

The measurement results of the gamma transmission technique of the PIS block copolymer samples by the use of Cs-137 radioisotope was presented in Table 5.5. The variations in the relative intensity (I/I_0) were evaluated considering five different thicknesses of the PIS copolymer samples by using Cs-137 radioisotopes. Changes in the relative intensities in BI and BII samples were given in Figure 5.17 (for Cs-137 radioisotope). The measurement details about the decrease of gamma transmittance with the rise of the polymer thickness were presented in Table 5.6. Besides, the decrease of the gamma transmittance with the rise of the thickness was presented for Co-60 radioisotope in Figure 5.18.

Table 5.5 : The measurement results at the gamma transmission technique of the PIS block copolymer samples by the use of Cs-137 radioisotope.

Thickness (mm)	Count 1	Count 2	Count 3	Average	Standart Deviation	Relative Intensity (I/I_o)
BI Samples						
0	11526	10174	9578	10426	575	1
2	9714	8755	9443	9304	559	0,89
4	9838	8470	8629	8979	557	0,86
6	8897	8033	9551	8827	553	0,85
8	8100	7674	8157	7977	570	0,76
10	8492	7794	7036	7774	577	0,74
BII Samples						
0	4604	4615	4929	4716	184	1
2	4350	4736	4765	4617	188	0,98
4	4514	4568	4678	4587	184	0,97
6	4378	4475	4645	4499	190	0,95
8	4356	4455	4485	4432	187	0,94
10	4371	4383	4507	4420	184	0,94
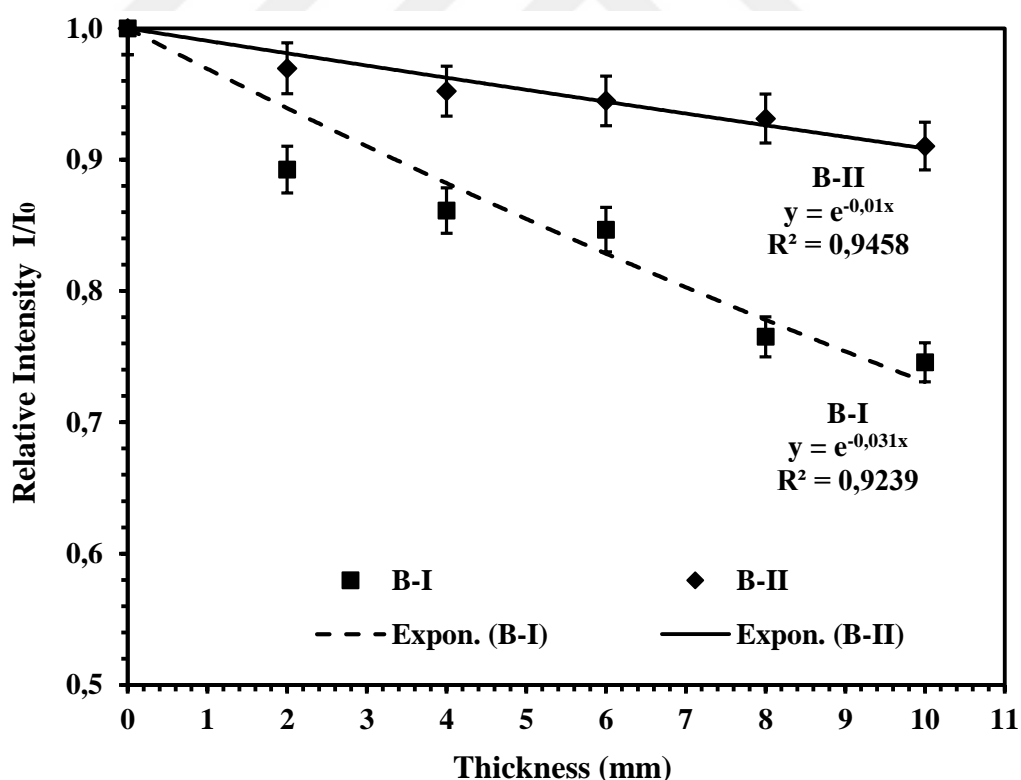
Figure 5.17 : Changes in relative intensity of block copolymer BI and BII samples for Cs-137 radioisotope.

Table 5.6 : Measurement results at the gamma transmission technique of the PIS block copolymer samples by the use of Co-60 radioisotope.

Thickness (mm)	Count 1	Count 2	Count 3	Average	Standart Deviation	Relative Intensity (I/I_0)
BI Samples						
0	5075	5032	5016	5041	187	1
2	5028	4769	5245	5014	183	0,99
4	5027	4802	4559	4796	189	0,95
6	4384	4854	5003	4747	187	0,94
8	4749	4671	4284	4568	187	0,91
10	4441	4662	4148	4417	186	0,88
BII.Samples						
0	9324	9707	8230	9087	592	1
2	9542	8037	8851	8810	582	0,97
4	8446	9172	8338	8652	583	0,95
6	8454	9084	8217	8585	582	0,94
8	8822	8781	7783	8462	576	0,93
10	8565	8298	7953	8272	579	0,91
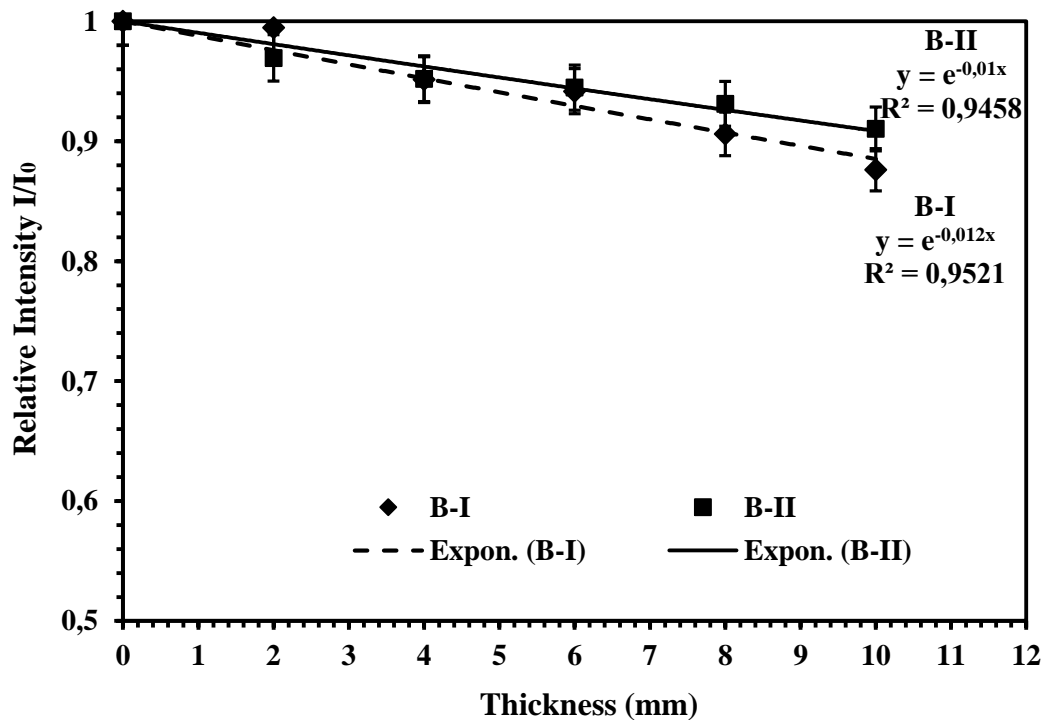
Figure 5.18 : Changes in relative intensity of block copolymer BI and BII samples for Co-60 radioisotope.

BII samples, which were pelleted 0.967 grams by a pelletizing device were inserted in front of the collimator hole used in the gamma transmission technique. The space

between copolymer samples and gamma source was 120 mm. The hole of the collimator that converts gamma photons into a narrow beam was 3 mm. Gamma attenuation features of BI and BII block copolymers were given in tables (in Table 5.5 for Cs-137 and Table 5.6 for Co-60).

The increase in the temperature of the poly (imide siloxane) block copolymer caused minor changes in its relative density (I/I_0). The reason for the changes in the I/I_0 result is thought to be due to the improvement in the aromatic chain rings of the poly (imide siloxane) matrix. Gamma transition properties in samples with different thickness values are given in Table 5.5 (Cs-137) and Table 5.6 (Co-60). Variations of linear attenuation coefficients (depend on the density in BI and BII copolymers. Comparing the results on attenuation coefficient values of PIS showed similarity between the PIS attenuation coefficients and the literature [82].

Comparisons of linear attenuation coefficients in BI and BII copolymers were done for two different photon energy values emitted from Cs-137 and Co-60 radioisotopes in Table 5.7.

Table 5.7 : The comparison in the linear attenuation coefficients and HVL of the PIS block copolymers by using Cs-137 and Co-60 radioisotopes.

Radioisotope	BI (flexible sheet form)		BII (pellet form)	
	μ_l (cm^{-1})	HVL(cm)	μ_l(cm^{-1})	HVL(cm)
Cs-137	0,031	22,359	0,007	99,021
Co-60	0,012	57,762	0,010	69,314

μ value of BII copolymer in the granular structure is lower than μ in the BI sample with the compact flexible form (for Cs-137 and Co-60 radioisotopes in Table 5.7). Besides, there was an increment in the coefficient of linear attenuation as BI was subject to the higher temperature at the production step. The increment of the linear attenuation coefficient indicated that the BI sample is in a more flexible structure comparing to BII. Applications in radiation transmission method for BI and BII samples were detected for a particulate radiation attenuation (such as beta radiation and neutrons considering total neutron macroscopic cross-section) in the previous study [18]. Pelleted PIS derived from the grainy form (BII) shows that BII has more effective radiation protection capacity than BI due to the scattering of neutrons and beta particles [18] from pelleted PIS grains (such as beta and neutrons). However, a detailed comparison between the flexible form and the pelleted grain form of the PIS

block copolymer is not available in the literature. In this study, in the flexible form (BI) PIS block copolymer, the linear attenuation coefficient is higher than the linear attenuation coefficient of the PIS block copolymer of the pelleted grain form (BII), (BI) PIS block copolymer material (including gamma) has a more effective radiation shielding property shows that it has the application of the radiographic test technique for compressed BI samples indicated that the results in the gamma attenuation coefficient of BI samples did not change considerably at the end of the compression tests. Results of the radiographic examination of the compressed BI samples (in Figure 5.14) supported the improvements of the linear attenuation coefficient in BI samples (Table 5.7) as the polymer properties were improved by the modification of the production process. The gamma transmission technique and radiographic test results of the BI sample show that this is more suitable for use as a light and flexible material in a variety of industrial applications, such as solar technologies and aviation applications. In addition, the BI sample is more suitable for use in a variety of industrial applications, such as the commercialization of bio-related polymers / bio-derivative materials. It is suggested that a flexible form of PIS block copolymer (BI) can be used as the mechanical resistant polymer in aggressive environments when it interacts with some chemical environments representing environment aggressiveness. The use of PIS block copolymer (BI) is suitable for harshest mechanical conditions of flexible microelectronic devices containing gamma radiation at medical applications, the several service areas for aerospace, solar technology applications, automotive and, cable industries.

5.7.2 Beta transmission technique of PIS samples

Bremsstrahlung radiation at a more intense level was produced by materials with high proton numbers through the interaction of negative beta particles with the material. Deceleration of electrons at Coulomb interaction yield Brems radiation. When radiation interacts with the electron of a material with a high number of protons, the Bremsstrahlung radiation is generated through the electron cloud surrounding the nucleus [40]. It seems that using a PIS block copolymer with a low Z number is appropriate for decreasing the intensity of Brems radiation [36, 70]. The relative beta intensity can be presented similar to the relative gamma intensity as (I/I_0) by Eq 5.1. Changes through the relative intensity by beta transmission technique (by using Sr-90 radioisotope) were showed for block copolymer samples in Table 5.8. An increase in

PIS thickness decreased the relative beta intensity of block copolymer samples (as in Figure 5.19 and Figure 5.20).

A test sample means compares the mean of a sample to a pre-specified value and tests for a deviation from that value. The reliability of the curves of the experimental results was examined to investigate the beta attenuation of BI and BII block copolymer specimens. The reliability of the curves was evaluated as a calibration curve by using a test sample for Sr-90 radioisotope in Table 5.8 and Table 5.10.

The changes in the relative intensity were determined with the rise of the thickness of the BI sample. A test sample with 4mm thickness was used in Figure 5.19 and another test sample for the BII sample was used at the same thickness in Figure 5.20. The details in the error estimation were determined by using the calibration curves of BI and BII samples in Table 5.9

Table 5.8 : The relative intensity results of BI and BII samples.

Thickness (mm)	Count 1	Count 2	Count 3	Average	Standart Deviation	Relative Intensity (I/I_0)
BI Sample						
0	1,44	1,39	1,28	1,37	0	1
2	1,17	1,16	1,12	1,15	0,032	0,841
*4	1,13	1,10	0,82	1,02	0,171	0,739
6	1,01	0,98	0,76	0,92	0,063	0,667
8	0,84	0,82	0,72	0,79	0,578	0,014
10	0,71	0,69	0,66	0,69	0,012	0,502
BII Sample						
0	1,41	1,30	1,28	1,33	0	1
2	1,20	1,15	1,12	1,16	0,017	0,870
*4	1,21	0,90	0,88	0,99	0,185	0,746
6	1,41	1,30	1,28	1,33	0,061	0,674
8	1,41	1,30	1,28	1,33	0,061	0,562
10	1,41	1,30	1,28	1,33	0,0531	0,467

* Test sample has 4mm thickness.
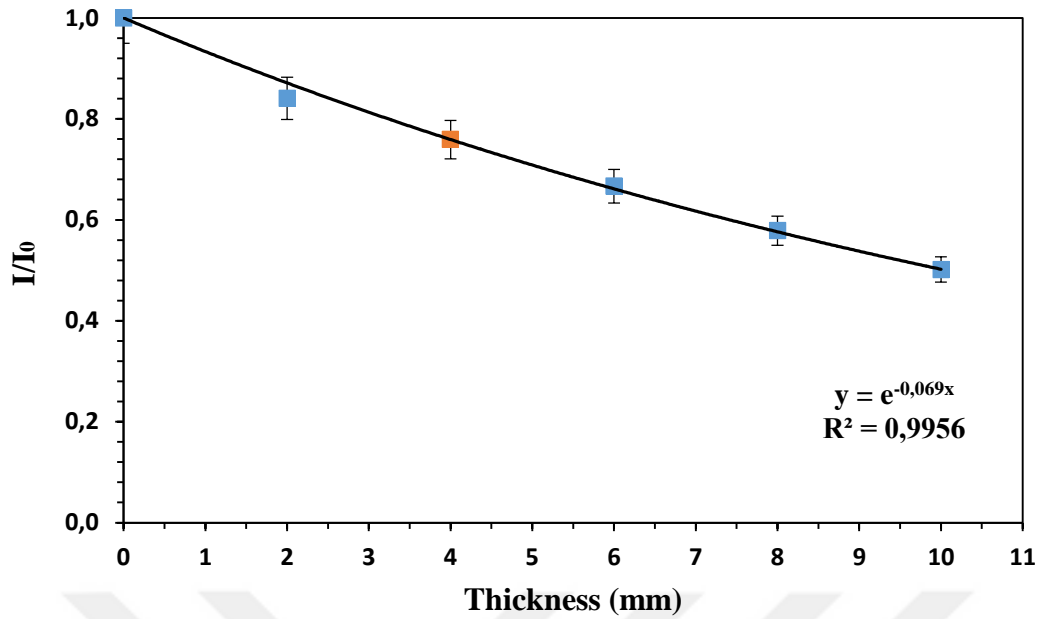
Figure 5.19 : Changes in relative intensity of the BI sample for beta particles.
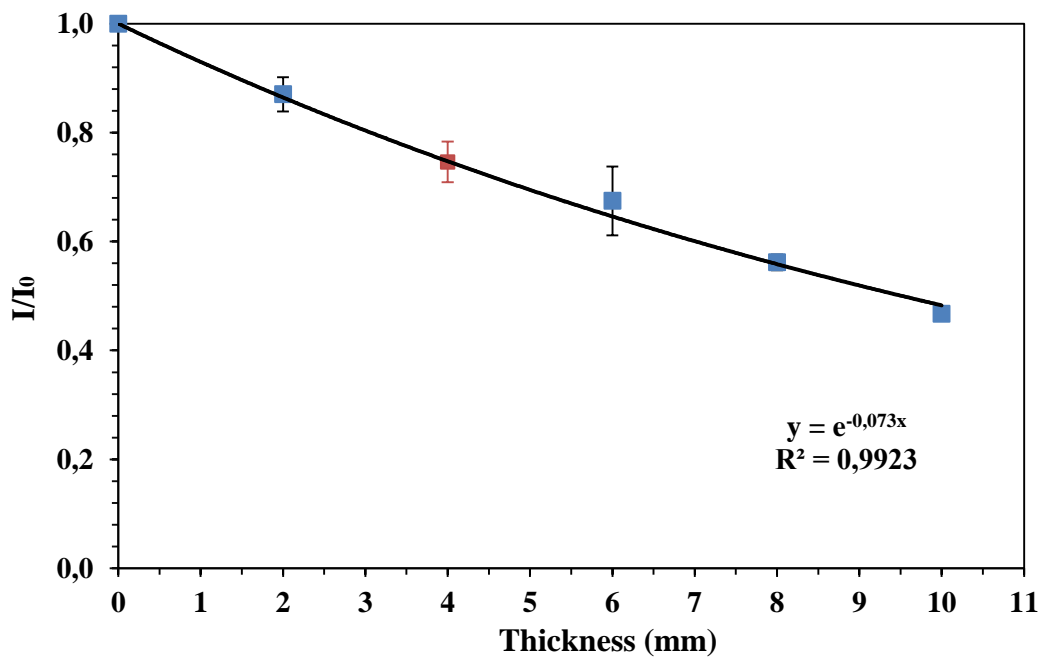
Figure 5.20 : Changes in relative beta intensity of the BII sample.

Reliability in the curves provided from the experimental results, which was inspected for beta attenuation of BI and BII samples was examined. Reliability in curves was measured as the calibration curve through a test sample. Table 5.9 presents results for the comparison of experimental results with test sample calibration curves.

Table 5.9 : Calibration curve details for BI and BII block copolymers.

Comparison of relative count on test sample	I/I_0, which is derived by experimental results	I/I_0, which is derived by calibrating of the curves	Error (%)
BI sample	0,759	0,760	-0,144
BII sample	0,746	0,756	-1,324

Changes in relative intensity were assigned by raising the thickness of the BI sample 4 mm thickness of the test sample was used (Figure 5.19). Another test sample of the BII block copolymer structure was utilized in the same thickness (Figure 5.20). Details of error estimation were detected through calibration curves for both samples (Table 5.9). The error was ~3% for the BI sample. On the other hand, the error was below 2% for the BII sample.

5.7.3 Neutron transmission technique of PIS samples

The high content of hydrogen and carbon atoms in the polymer provides good and suitable neutron shielding material with content rich in hydrogen and carbon [70]. On the other hand, materials rich in hydrogen and carbon have some negative aspects (such as soft form and low-temperature resistance) [74]. It contains high hydrogen and carbon originating from PDMS and BTDA in its PIS structure. Therefore, the PIS block copolymer material both provides high resistance against radiation and provides extremely good radiation shielding due to their elastomer properties and high-temperature resistance, thus ensuring extremely good radiation shielding. Some of the block copolymer structures have been used to detect neutron attenuation by raising the thickness (t) of the sample by thermal neutron absorption tests. The relative neutron density is shown in the equation below. The neutral attenuation feature has been discussed taking into account the total neutron attenuation, and this can be seen in Table 5.10.

$$I = Ioe^{-\mu t} \tag{5.1}$$

Some characteristic information about error estimation was detected via the calibration curves of BI and BII block copolymers (Table 5.11). The detected error was ~1% for BI. Moreover, the detected error was below 1% for BII.

BI and BII block copolymer samples were used to get the calibration curve and to measure relative intensity as I/I_0 of neutrons. Error comparisons of BI and BII samples were reported in Table 5.12.

Overlaps for matching curves of beta particles (Figure 5.19 - 5.20) and for neutrons (Figure 5.21 - 5.22) were shown for the calibration curves for BI and BII block copolymer samples. Comparisons of error showed an appropriate mean error. The maximum mean absolute error of calibration curves for all samples was ~ 1.5% in Sr-90 radioisotopes and ~0.5 in %Pu-Be NH-3 radioisotope. Calibration curves were produced through relative intensity and thickness.

Table 5.10 : Measurement results of BI and BII block copolymers through neutron transmission technique.

Thickness (mm)	Count 1	Count 2	Count 3	Average	Standart Deviation	Relative Count (I/I_0)
BI Sample						
0	4607	4629	4627	4618	0	1
1	4580	4554	4576	4567	0,005	0,989
2	4607	4629	4619	4618	0,002	0,973
3	4480	4458	4467	4468	0,005	0,968
*4	4366	4408	4248	4340	0,017	0,940
5	4245	4220	4232	4232	0,005	0,916
BII Sample						
0	4878	4836	4875	4857	0	1
1	4381	4799	4372	4518	0,054	0,930
2	4351	4350	4341	4350	0,004	0,896
3	4238	4188	4231	4213	0,002	0,867
*4	4142	4096	3828	4022	0,035	0,828
5	3930	3851	3881	3890	0,005	0,801

*Test Sample has a 4 mm thickness.

Table 5.11 : Calibration curves of error estimations for BI and BII to neutrons.

Comparison of relative count in the test sample.	I / I_0, which is derived from experimental results.	I / I_0, which is derived from curve calibration	%,the margin of error
BI	0,940	0,945	-0,535
BII	0,828	0,830	-0,235

Table 5.12 : Comparisons of error in BI and BII block copolymer samples.

Samples	%, the margin of error in Sr-90 radioisotope	%, the margin of error in NH-3
BI	-0,144	-0,535
BII	-1,324	-0,235
Mean Error	-1,469	-0,770
Mean Absolute Error	1,469	0,770
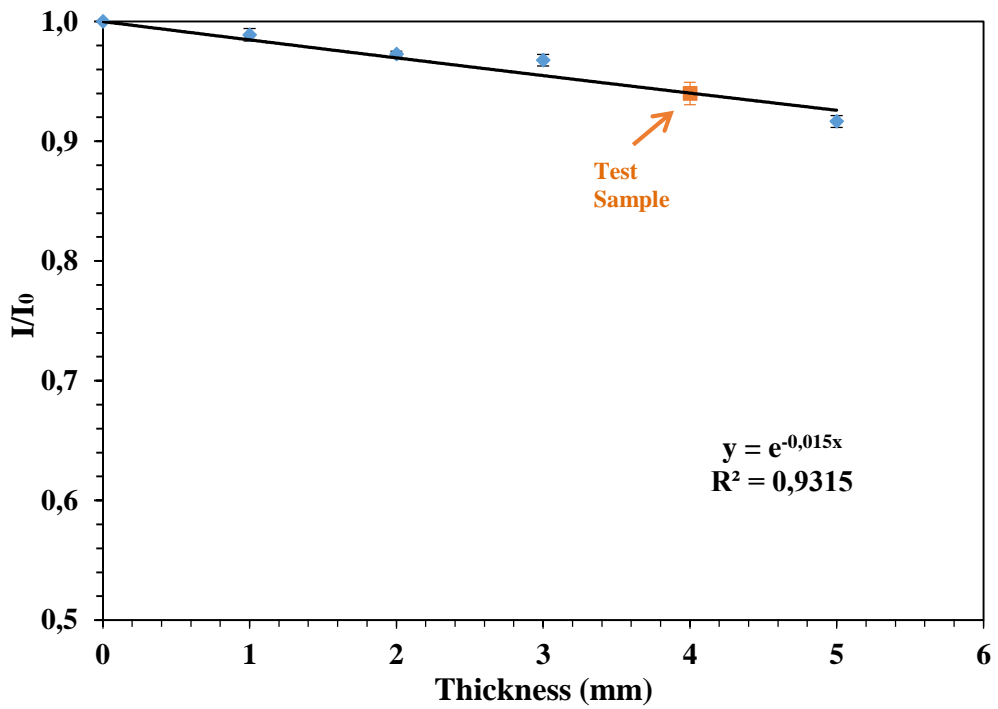
Figure 5.21 : Changes in relative intensity of neutrons in the BI block copolymer.
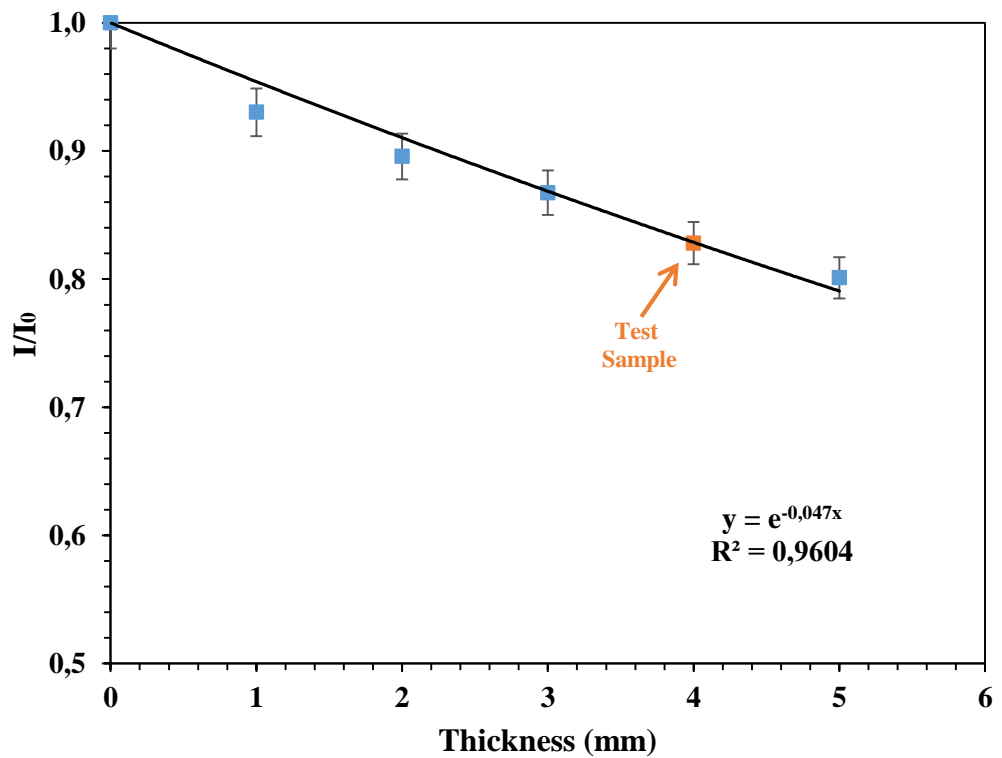
Figure 5.22 : Changes in relative intensity of neutrons in the BII block copolymer.

Figure 5.23 shows alterations in relative beta intensity for BI and BII block copolymers. A considerable difference between the relative intensity of BI and BII samples wasn't observed until 6 mm. On the other hand, differences in the relative intensity began to be recognized at 6 mm through the scattering effect of negative beta particles between BI and BII block copolymer samples.
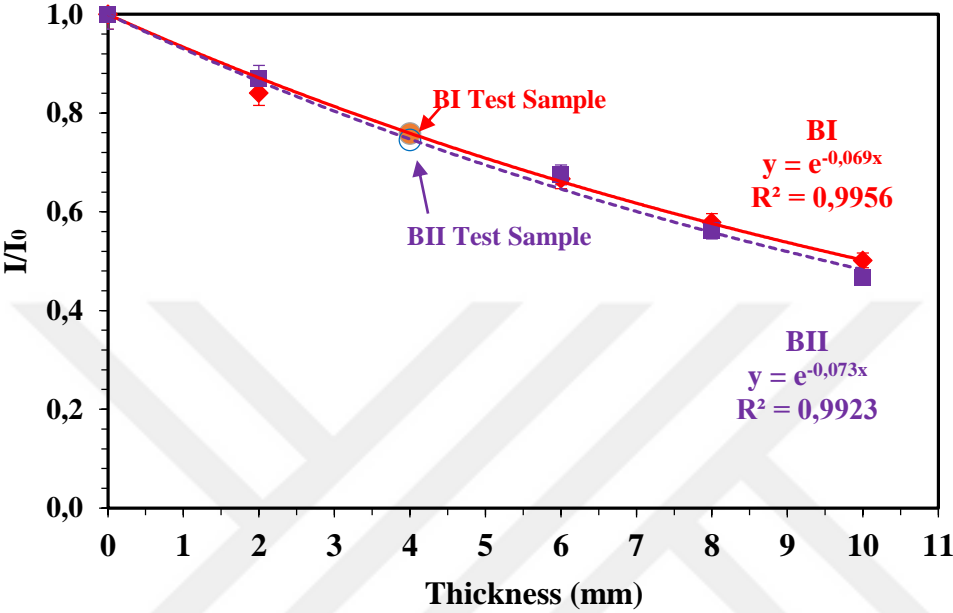
Figure 5.23 : Changes in the relative beta intensity of BI and BII block copolymer.
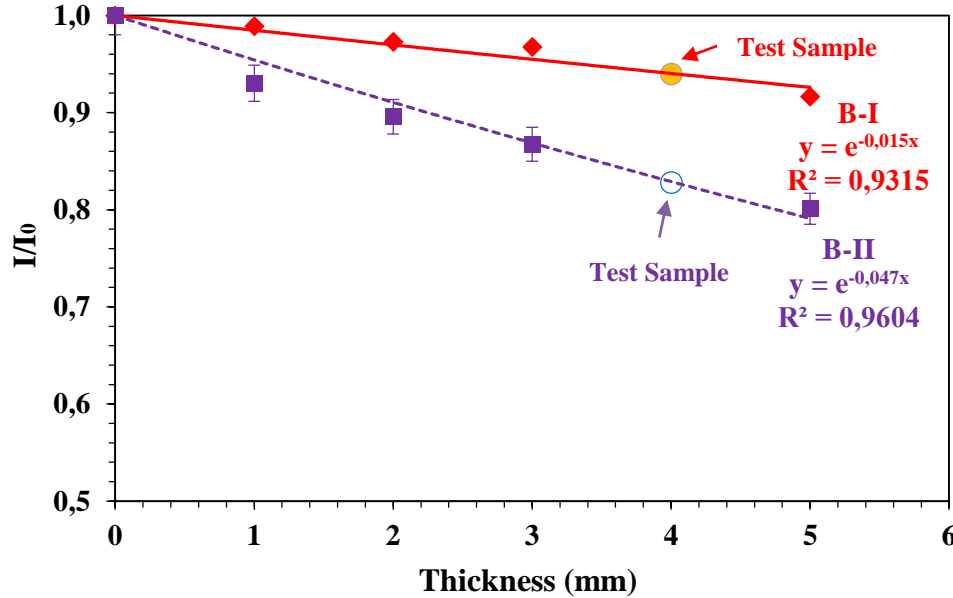
Figure 5.24 : Changes in relative intensity of neutrons for BI and BII samples.

The changes in the relative neutron intensity for BI and BII samples were indicated in. Figure 5.24. The neutron interaction mechanism with the materials showed clear

differences in the scattering effect of neutrons for BI and BII samples. Before the pelletizing, the voids dispersed in the material were improved by pelletizing the material. PIS block copolymer sample's shielding performance against neutron was also improved in this context.

Hence, pelletized BII grains were acknowledged more effective neutron intermediary material than BI flexible structure. Useful, sophisticated, and utilizable results were provided for studying easily in the irradiation area in this way.

5.7.4 The comparison of shielding properties of BI and BII samples

Consequences for neutron and beta attenuations showed changes in Half Value Layer (HVL) values for flexible structure BI and pelletized structure BII grains (as in Table 5.13). Comparison in changes for HVL values in block copolymer samples showed critical production parameter relations (as temperature and time). Pelleted BII grainy and porous structure enabled getting appropriate shielding against beta and neutrons. But the flexible sheet form of PIS caused a decrease in HVL depending on the development of the gamma radiation shielding (in Table 5.14 and Figure 5.25).

Table 5.13 : Comparison of radiation shielding properties of PIS samples for beta particles and thermal neutrons.

PIS Samples	Linear attenuation coefficient μ (cm^{-1}) for Sr-90 radioisotope	HVL (cm)
BI	0.069	10.04
BII	0.073	09.50
PIS Samples	Total macroscopic cross-section $\sum$ (cm^{-1}) for Pu- Be Neutron Howitzer	HVL (cm)
BI	0.015	46.20
BII	0.047	14.74

Table 5.14 : Comparison of gamma shielding properties of PIS samples.

Radioisotope	BI (flexible sheet form)		BII (pellet form)	
	μ_l (cm^{-1})	HVL(cm)	μ_l (cm^{-1})	HVL(cm)
Cs-137	0,031	22,360	0,010	69,315
Co-60	0,012	57,762	0,007	99,021
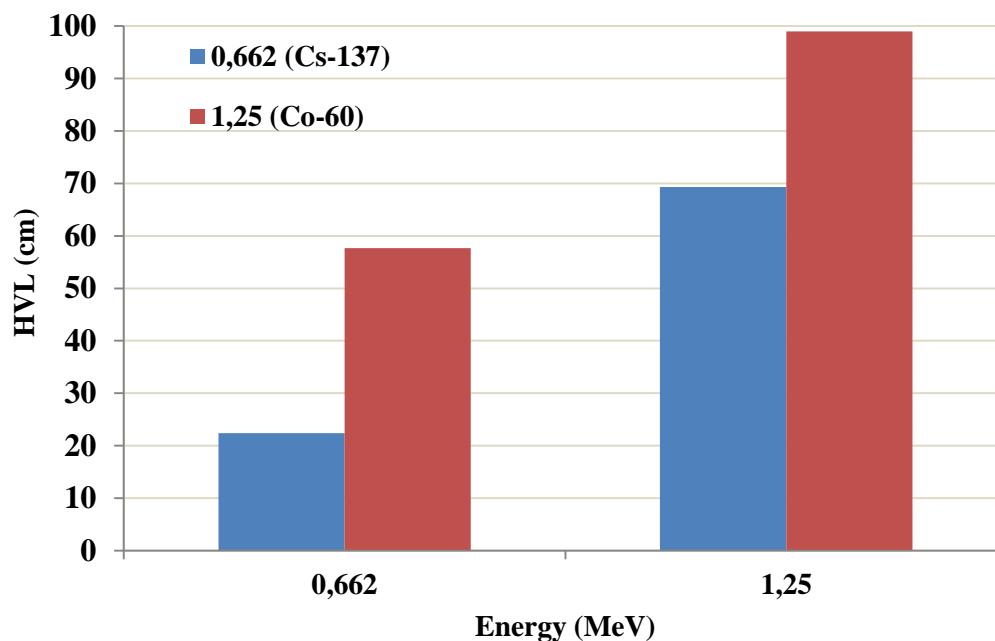
Figure 5.25 : HVL thicknesses of BI and BII samples for Cs-137 (with 0.662 MeV) and Co-60 (with 1.25 MeV) radioisotopes.

5.8 Irradiation Effect on Poly(imide siloxane) Block Copolymers

PIS BI flexible polymer has been irradiated at 10 kGy as the adaptness of the polymers to ambient presented the great significance at the irradiation area to use in several application fields such as biomedical and aerospace. The morphing feature of the flexible polymers has significant importance to use in the irradiation area depending on its ability to adapt to the ambient conditions (such as size, shape, and temperature) at the biomedical and aerospace industry [91].

PIS BI samples have been irradiated at 10 kGy (as a medical irradiation dose level) to use as a biocompatible polymeric material. Because polymeric biomaterials such as poly(imide) siloxane block copolymers are applicable for smart biocompatible polymers as they can be used in the flexible form in nervous system repair and minimizing bacterial adhesion [19]. The gamma sterilization of PIS BI was performed by using Cobalt 60 radioisotope which was a proper radioisotope to kill microorganisms [92]. The high dose range is defined from 5 kGy to 100 kGy for medical irradiation purposes as the high dose range covers the medical product sterilization by using radioisotopes at different medical products [92]. Radiation resistant polymer can be used in an optimum absorbed dose range until 10 kGy [92]. Hence, PIS BI samples were irradiated at 10 kGy dose level as radiation-resistant

flexible polymers have promised a significant role in radiation-related medical applications. The gamma sterilization of PIS BI was performed by using Cobalt 60 radioisotope which was a proper radioisotope to kill microorganisms.

The outer surface of the satellites at ISS orbit have exposed to a cumulative dose with 1 kGy during one year [93]. The aerospace technology materials have been used in the service area for ten years. In this study, the cumulative dose effect at PIS block copolymer samples was carried out at 10 kGy considering the service duty of the lightweight polymer samples to investigate the material deterioration considering the total dose effect at 10 kGy and to use as the flexible solar cell in aerospace applications[94-96].

5.8.1 FTIR results of the samples between unirradiated and irradiated ones

There is limited information about the FTIR spectra changes of the poly(imide) siloxane (PIS) block copolymers. The changes in the FTIR spectra of polymeric structures are explained by the irradiation effect in the literature. The FTIR spectra of unirradiated carboxymethylated chitosan vary after irradiation at 10 kGy by Co-60 radioisotope [83]. Besides, the FTIR spectra of the irradiated polyethylene grafted samples changed at 12 kGy in the literature [84]. The changes in the FTIR spectra of pyromellitic acid (PMA) was occurred by gamma irradiation at 10 kGy [85]. The variations of the FTIR spectra of the polytetrafluoroethylene sheet were distinguished at 10 kGy [86]. In this study, the comparison of the unirradiated and the irradiated (at 10 kGy) flexible poly(imide) siloxane (PIS) block copolymers indicated that there was not a considerable change at the FTIR spectra of the irradiated copolymer samples after irradiation process at 10 kGy (in Figure 5.26). The details about the comparison of the structural characteristics of the unirradiated and the irradiated BI samples were presented in Table 5.15. A comparison of the FTIR analysis results of BI flexible sheet samples for unirradiated and irradiated states indicated that the flexible sheet unirradiated BI sample showed characteristics of irradiated BI sample.
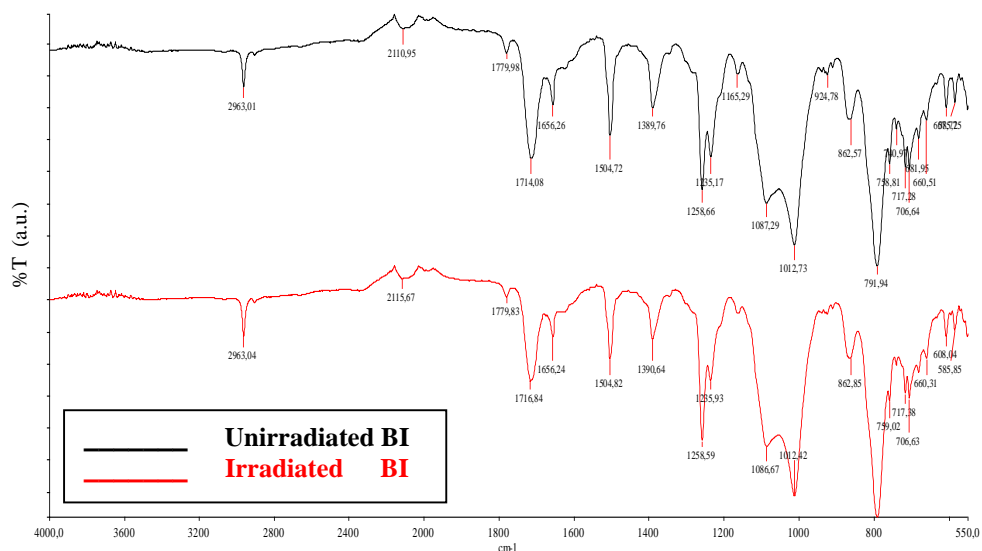
Figure 5.26 : FTIR analysis for unirradiated and irradiated PIS block copolymer samples.

Table 5.15 : FTIR analysis of characteristic peaks in PIS block copolymer BII.

BI samples for unirradiated state	Peak (cm^{-1})
aliphatic stretching	2963
asym C = O stretching	1779
sym C = O stretching	1714
asym Si- O -Si stretching	1087
sym Si- O -Si stretching	1012
Si - C stretching	791
BI samples for irradiated state	**Peak (cm^{-1})**
aliphatic stretching	2963
asym C = O stretching	1779
sym C = O stretching	1716
asym Si- O -Si stretching	1086
sym Si- O -Si stretching	1012
Si-C stretching	791

5.8.2 TGA results of the samples for unirradiated and irradiated PIS samples

The changes in TGA curves of the alginate/poly(N-isopropylacrylamide) graftcopolymers was determined at 0.5 kGy by gamma radiation [87]. The changes in TGA curves of the grafted vinyl acetate monomers were determined at 10 kGy [88]. But there are not the details about the changes in TGA curves of the poly(imide) siloxane (PIS) block copolymers in the literature. TGA analysis was applied for the irradiated copolymer sample and the changes in the total mass before and after the irradiation process were shown in Figure 5.27 a-b. The comparison of substance loss for the unirradiated and irradiated copolymers was presented as a percentage and mg

on a certain temperature range (in Table 5.16). The results indicated that a slight change in the mass loss ratio was determined between unirradiated and irradiated (at 10 kGy) samples. These results addressed that PIS samples were resistant to gamma radiation. The thermal stability of the unirradiated sample at ~80°C and the thermal stability of the irradiated sample by gamma-ray reached ~120°C in this study. The improvement of thermal stability of polyethylene and polyvinylchloride is determined depending on the cross-linking of the polymer structure when the polymer structure exposed to high-energy radiation [89]. The increase of thermal properties of the polymeric structure is possible by absorbed dose as cross-linking of the polymers support to improve structural properties by high energy radiation (polyethylene, polyvinylchloride).
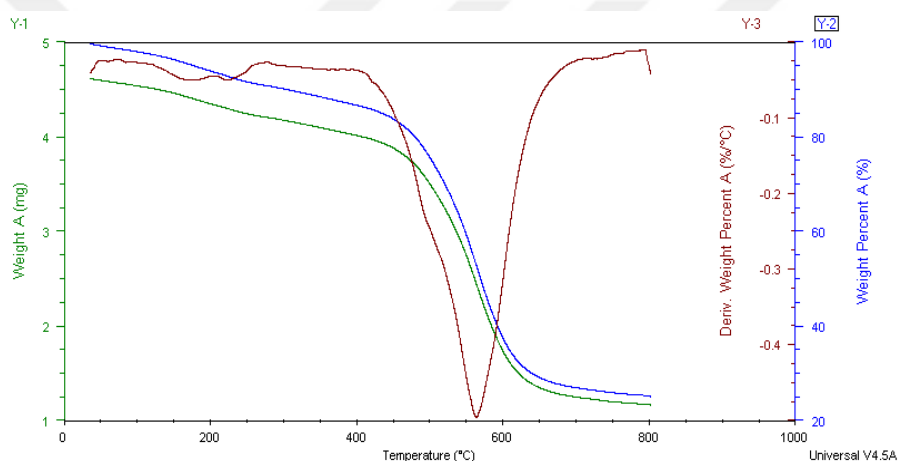
(a)
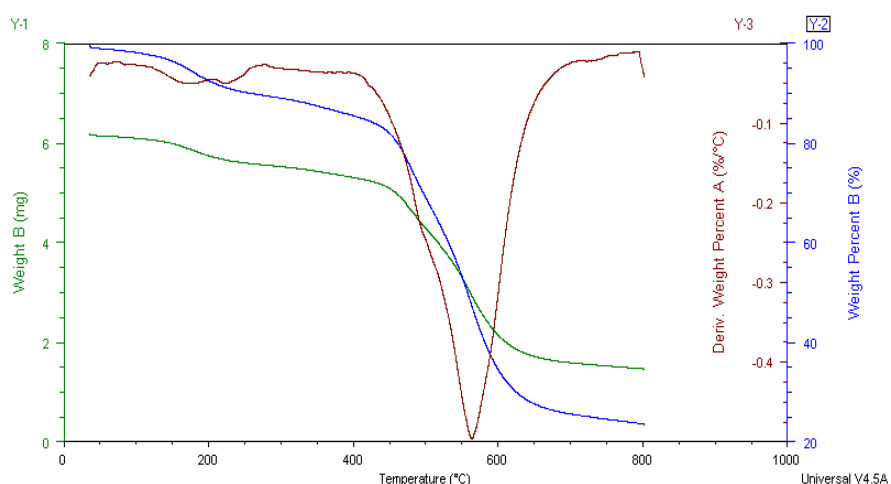
(b)

Figure 5.27 : Comparison of the TGA analysis results of PIS block copolymer samples for (a) unirradiated state (b) irradiated state.

Table 5.16 : The comparison of substance loss for the unirradiated and irradiated copolymers as a percentage and mg on a certain temperature range.

Temperature Range (ºC)	Substance Loss for PIS samples (%)	Substance Loss for PIS samples (mg)
Unirradiated State		
200	6.10	0.268
400	13.36	0.604
500	24.39	1.115
600	62.58	2.884
700	73.07	3.370
800	74.77	3.449
Irradiated State		
200	7.45	0.432
400	14.50	0.870
500	30.93	1.891
600	65.44	4.034
700	74.36	4.587
800	76.37	4.713

5.8.3 XRD results of the samples for unirradiated and irradiated PIS samples

The details about the diffraction peaks and changes of the diffraction peaks is not available for diffraction planes in BI flexible form of PIS (with the irradiation effect comparison on the PIS sample) at literature. X-ray diffraction peaks of unirradiated BI samples presented at 11.5 and 18.1 (2 theta degrees) corresponding to (330) and (050) diffraction planes, respectively (Figure 5.28). The irradiated BI sample presented XRD peaks at 11.5, 16.05, and 18.1 (2 theta degrees) corresponding to (330), (730), and (050) diffraction planes, respectively (Figure 5.28) in this study. The improvements in the intensity of the XRD peak of irradiated BI sample at 16.05 (2 theta degrees) indicated the enhancement of crystalline properties of irradiated BI at (730) diffraction plane. The similar XRD diffraction planes were determined in a different siloxane polymer (cyclotetrasiloxane) in the literature [29]. Besides, XRD measurements indicated the polyimide structure is recorded around ~ 16 (2 theta degrees) [90].
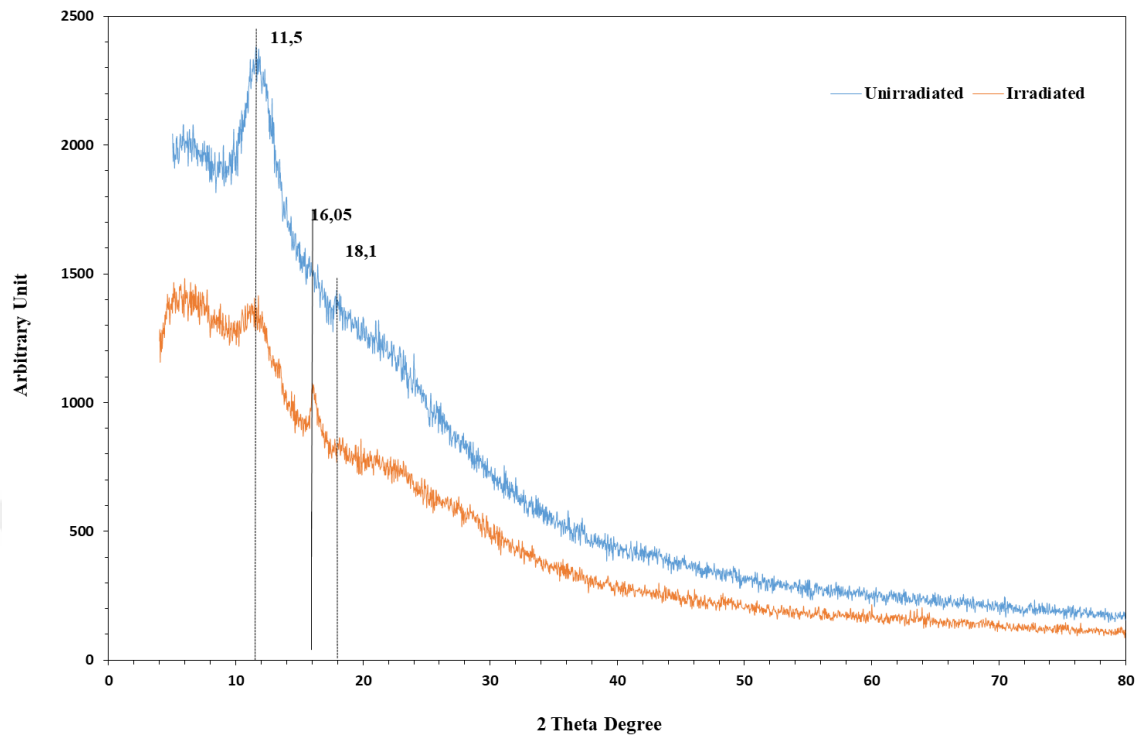
Figure 5.28 : Comparison of the XRD analysis results of PIS block copolymer samples for (a) unirradiated and (b) irradiated samples.

5.8.4 Surface morphology of the unirradiated and irradiated PIS block copolymer samples

There are no details about the changes in surface morphology of the PIS BI sample on the irradiation effect in the literature. There was no considerable change in the surface morphology of the unirradiated and irradiated (at 10 kGy) samples (Figures 5.29 a-b). SEM images of the samples are shown for the unirradiated and irradiated states of PIS block copolymer samples in Figure 5.29 a-b.

95
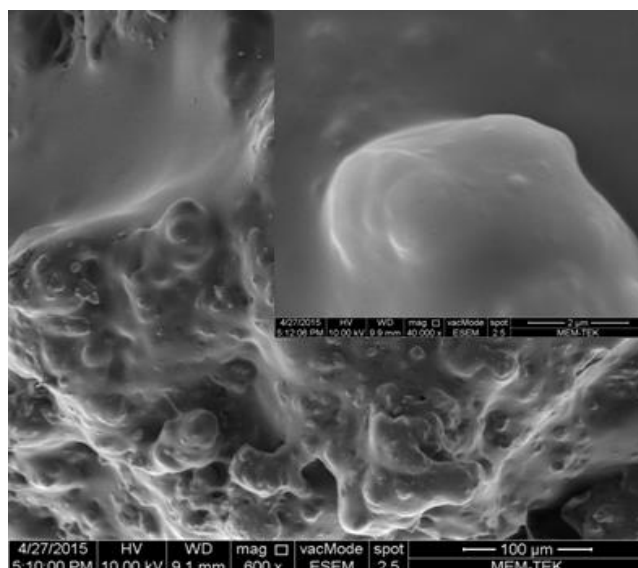
(a)
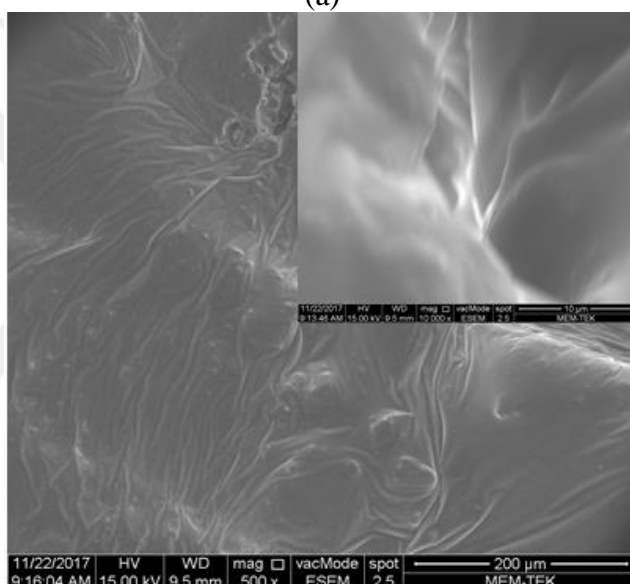
(b)

Figure 5.29 : SEM image of PIS block copolymer samples for (a) unirradiated and (b) irradiated states.

5.8.5 The changes in gamma transmittance of the irradiated PIS BI sample

The changes in gamma transmittance of the irradiated PIS BI were evaluated to examine the variations in penetration of gamma-rays at the irradiated sample. The gamma transmittance of the irradiated copolymer samples was performed at the same measurement conditions with the unirradiated samples by using the same experimental settlements and the same Cs-137 and Co-60 radioisotopes. The changes in relative intensity I/I_0 were showed for Cs-137 radioisotope (in Figure 5.30) and for Co-60 radioisotope (in Figure 5.31).
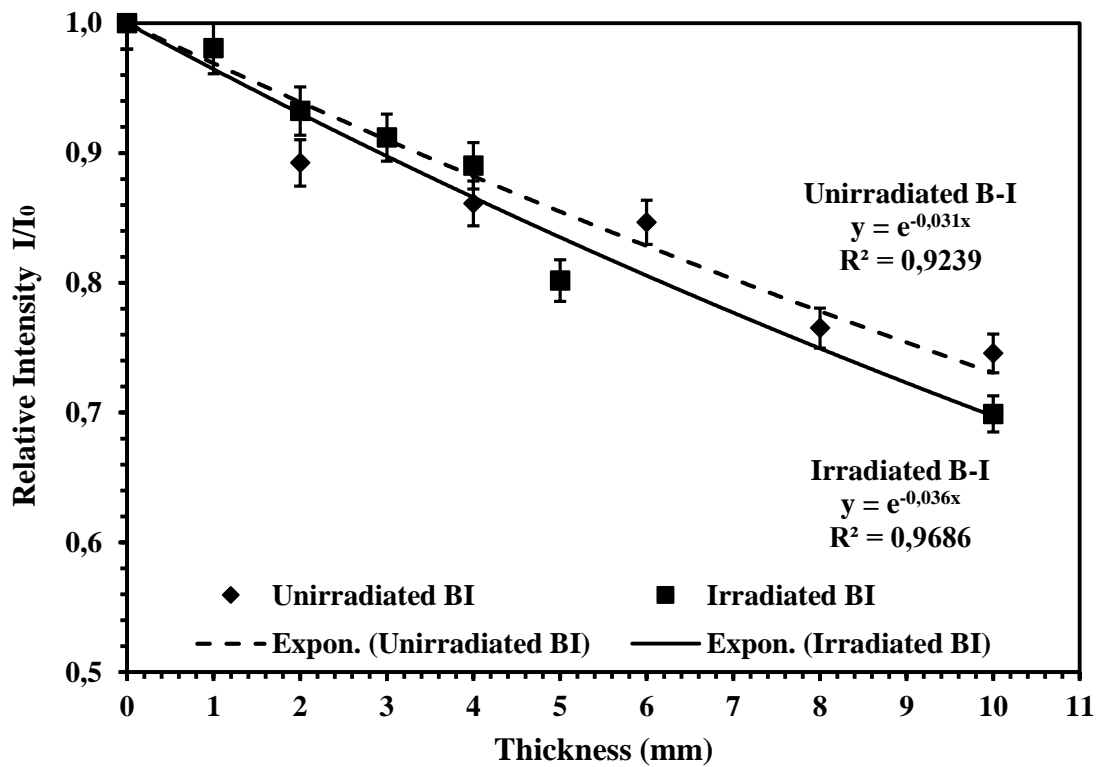
Figure 5.30 : Comparison of irradiation effect on unirradiated and irradiated PIS samples by using gamma transmission technique with Cs-137.
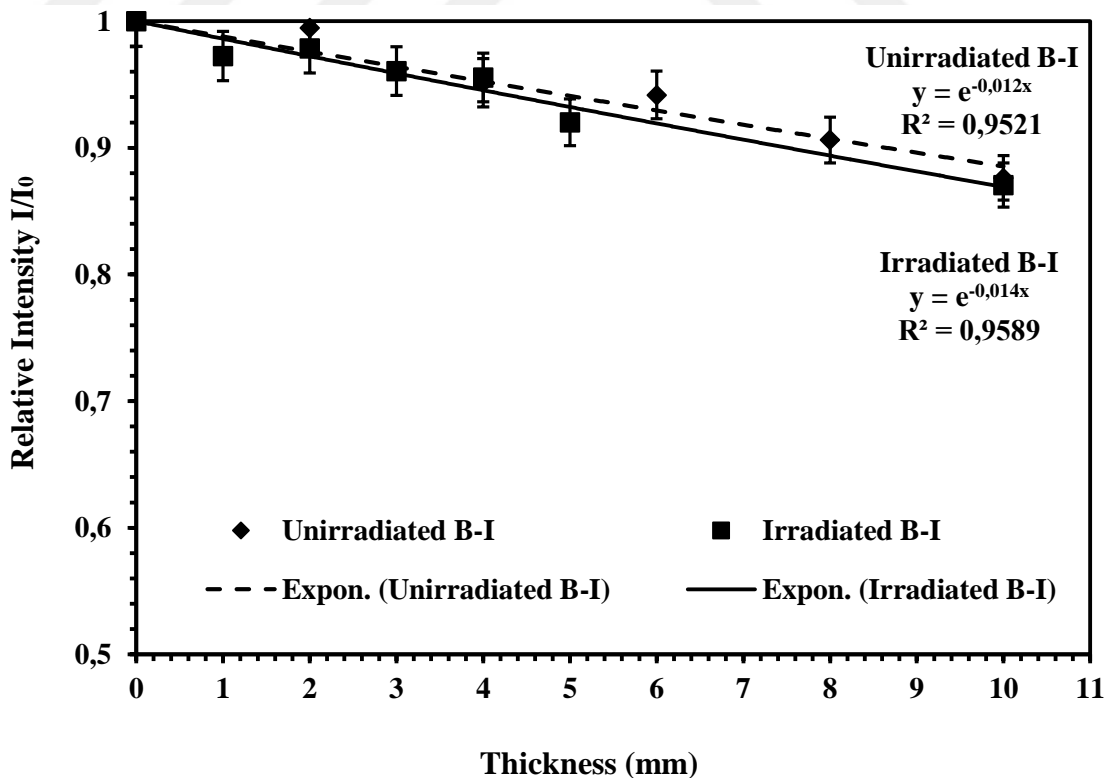
Figure 5.31 : Comparison of irradiation effect on irradiated and unirradiated PIS samples by using gamma transmission technique with Co-60.

The half-value layer (HVL) of PIS BI samples was determined for the unirradiated and irradiated states by using the linear attenuation coefficients in Table 5.17. The changes in HVL values of the unirradiated and the irradiated specimens were compared at two different gamma energy such as 0.662 MeV (emitted from Cs-137 radioisotope) and 1.25 MeV (emitted from Co-60 radioisotope) in Figure 5.32. HVL results indicated that there was a decrease in HVL of the irradiated samples and this change was distinguished more clearly by using Cs-137 radioisotope.

Table 5.17 : The comparison in the linear attenuation coefficients and HVL of the unirradiated and irradiated PIS BI block copolymers by using Cs-137and Co-60 radioisotopes.

Radioisotope	μ_l (cm^{-1})		HVL(cm)	
	Unirradiated BI	Irradiated BI	Unirradiated BI	Irradiated BI
Cs-137	0,031	0,036	22,360	19,254
Co-60	0,012	0,014	57,762	49,510
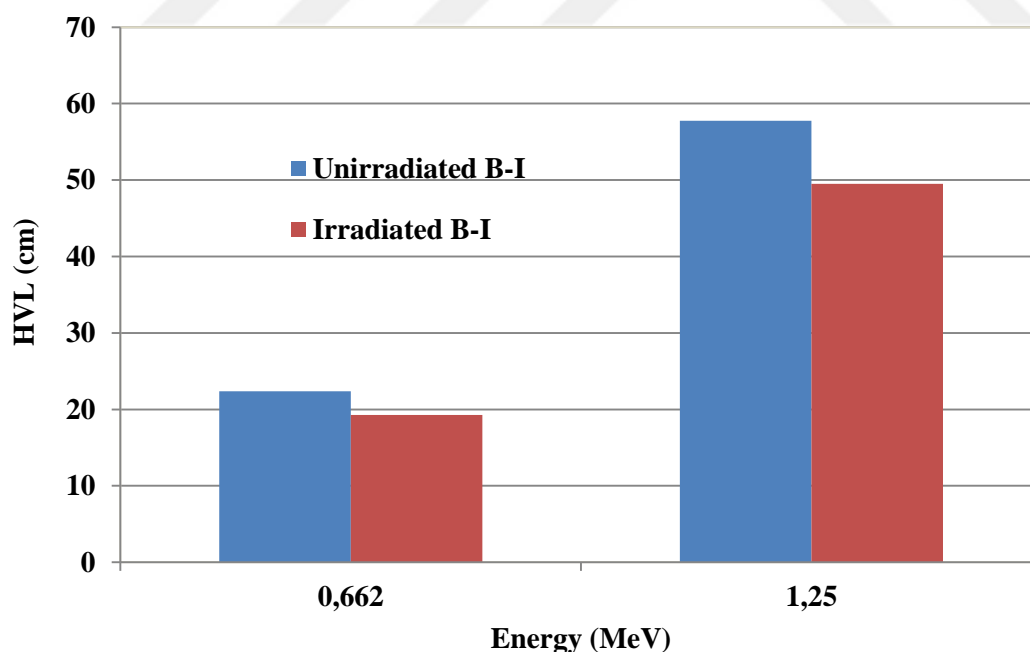
Figure 5.32 : HVL of the unirradiated and irradiated BI samples.

5.8.6 The changes in beta transmittance of the irradiated PIS BI sample

The changes in beta transmittance of the irradiated PIS BI were evaluated to examine the variations in beta penetration. The beta transmittance of the irradiated copolymer samples was performed at the same measurement conditions with the unirradiated samples by using the same experimental settlements and the same Sr-90 radioisotope. The comparison of relative intensity considering the beta transmission of the samples was performed for unirradiated and irradiated block copolymer samples to detect beta attenuation of the samples by using Sr-90 radioisotope(in Figure 5.33). The half-value layer (HVL) values of the samples were determined for Sr-90 radioisotope by using the linear attenuation coefficients in Table 5.18. The comparison of the beta transmission effect (for irradiated and unirradiated states) indicated that the transmission of beta particles (for Sr-90 radioisotope) decreased after the irradiation treatment of the PIS BI samples at 10 kGy.
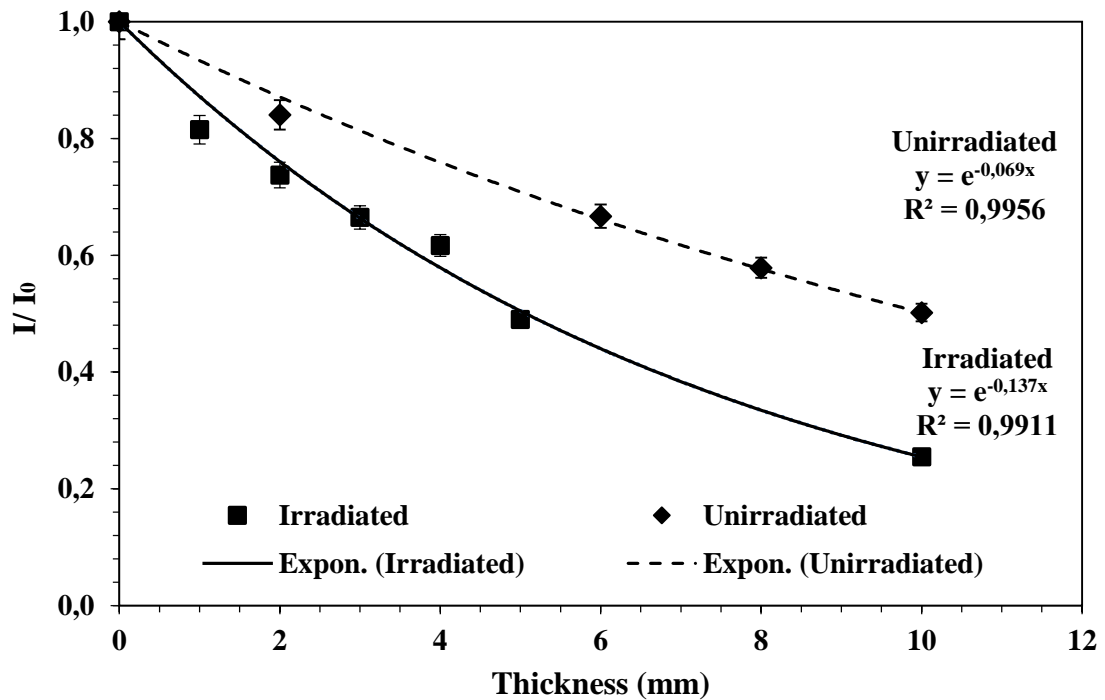
Figure 5.33 : Comparison of irradiation effect on unirradiated and irradiated PIS samples by using the beta transmission technique with Sr-90.

Table 5.18 : The comparison of HVL of the samples for unirradiated and irradiated states for Sr-90 radioisotope.

Radioisotope	μ_l (cm^{-1})		HVL(cm)	
	Unirradiated BI	Irradiated BI	Unirradiated BI	Irradiated BI
Sr-90	0,069	0,137	10,04	5,08

5.8.7 The neutron measurement results by using a ^{239}Pu-Be neutron source after irradiation of PIS BI sample

For the evaluation of the variations in neutron shielding by using ^{241}Pu-Be neutron source (NH3 Neutron Howitzer) was used to evaluate neutron attenuation of the irradiated PIS BI samples (in Figure 5.34) after the application of 10 kGy irradiation. The comparison of the half-value layer (HVL) and total macroscopic cross-section $\sum$(cm^{-1}) (for Pu-Be NH3) of the samples for unirradiated and irradiated states was shown in Table 5.19. The variations in neutron shielding of the PIS BI sample indicated that there was an improvement of the neutron shielding of the irradiated PIS BI sample at 10 kGy with the decrease of the HVL of the sample.
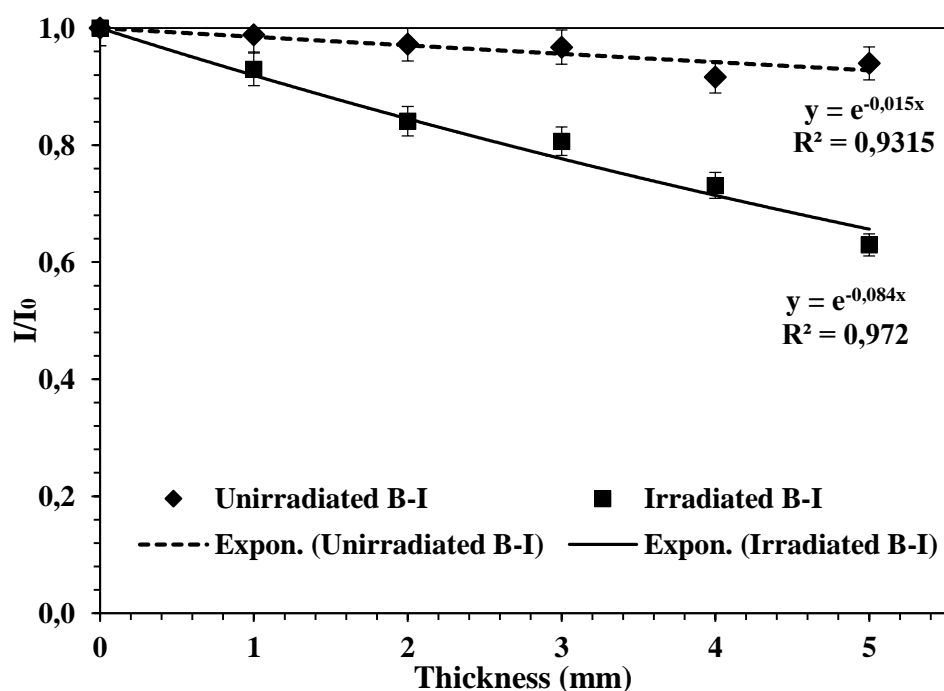
Figure 5.34 : The irradiation effect on unirradiated and irradiated PIS samples by using neutrons (Pu-Be).

Table 5.19 : The comparison of HVL and $\sum(cm^{-1})$ of the samples for unirradiated and irradiated states for neutrons.

Neutrons	Total macroscopic cross-section $\sum(cm^{-1})$ of BI		Half Value Layer (HVL) of BI in (cm)	
	Unirradiated	Irradiated	Unirradiated	Irradiated
Pu-Be	0,015	0,15	46,20	4,62

The cross-linkings are formed in the silicone rubber by irradiation application. The silicone rubber is crosslinked and strengthened by gamma radiation as a crosslinking degree of silicone rubber rises and network density increases by radiation exposure. The decrease of the HVL of the irradiated poly(imide siloxane) BI sample indicated that the radiation shielding was enhanced by crosslinking of the irradiated PIS BI sample at 10 kGy within this study [97].

6. DISCUSSIONS ON EXPERIMENTAL RESULTS

The various flexible polymers are available with the explaining of synthesis at different forms of the polysiloxanes or polyimides in literature [98-104]. But the details of the synthesis conditions to obtain the flexible sheet form and the pellet form of poly(imide siloxane) block copolymer and the comparison of the differences about characteristic properties of poly(imide siloxane) for the flexible sheet form and the pellet form are not available in the literature.

In the literature, block copolymers are produced by PDMS (polydimethylsiloxane) and TDPA (4,4'-terephthaloyldiphthalic anhydride). The patent (the patent number of US2007129492 A1) [98], which General Electric owns entitled as "Polysiloxane copolymers, thermoplastic composition, and articles formed therefrom", the polysiloxane copolymer structure consists of aryl ester units, aromatic carbonate units, resorcinol carbonate, polyester-polycarbonate containing aryl ester units, bisphenol carbonate units. The production conditions of the material produced within the scope of this patent are suitable for use in aircraft glass, plastic mirror, and aircraft leggings. This patent discloses the production conditions of the structure having flame retardant properties of the structure used around the window used in aircraft. This patent study describes polysiloxane copolymers, thermoplastic compositions containing them, production methods, and their use [98]. In this Ph.D. thesis it was poly(imide siloxane) block copolymer synthesis.

The patent (with the patent number of US2007129492 A1) explains that the polysiloxane copolymer can be produced as radiation-resistant thermoplastic. In this thesis study, polydimethylsiloxane monomer and aromatic anhydride compound were reacted to obtain high-temperature resistant polyimide compound (poly(imide siloxane)) [98]. Also, as mentioned in this patent application and Ph.D. study, the poly(imide siloxane) structure is produced in two different forms as flexible structure and pelletized form from poly(imide siloxane) powders; then the differences in radiation shielding performance of the produced structures have been evaluated comparatively [98]. In this patent, polysiloxane with aromatic ester, resorcinol, and

bisphenol-A copolymer was used to synthesize copolymers. Different monomers and different reactions were formed from our work. Thus, the poly(imide siloxane), which was presented in this thesis are different from the monomers of the polysiloxane copolymer provided in this patent and there is no similarity in terms of production method [99]. In this thesis, the polymer was synthesized to determine the difference of the characteristic properties between the flexible sheet form and the pellet form of poly(imide siloxane) by using poly(dimethylsiloxane), bis (3-aminopropyl) terminated-APPS, 4,4'-oxydianiline, benzophenone-3,3',4,4'-tetracarboxylic dianhydride, N-methyl-2-pyrrolidinone, and 1,2-dichlorobenzene. In this thesis, the produced material was obtained by reacting to the polydimethylsiloxane monomer with the aromatic anhydride compound and using the polyimide compound as poly(imide siloxane) by step polymerization technique (the condensation polymerization method).

In the patent with the patent number of US 2007129492 A1, the "interface polymerization technique" was used [98]. Alternatively, melting processes were carried out. Generally, in the molten polymerization process, polycarbonates are produced by reacting a dissolved dihydroxy reactant(s) and a diaryl carbonate esters such a diaryl carbonate ester with a transesterification catalyst and by a mixer and twin screw extruder with an even distribution (and like this) were prepared to form. The volatile monohydric phenol was removed by distillation from the molten reactants and the polymer isolated as a molten residue [98]. In this thesis, a more practical method was used to produce pellet structure and flexible structure: All the reactants can be mixed with step polymerization technique at 150-200ºC to produce pellet and flexible structure economically and practically. The polysiloxane copolymer mentioned in the patent work with the patent number of US 2007129492 A1 is one of the soft thermoplastic materials which deform rapidly. The poly(imide siloxane) material mentioned in this thesis and the patent application related to the thesis is higher and more resilient (elastomeric rubber) material against heat, radiation and strong solutions compared to other polyimide compounds. In this USA origin patent study, it is stated that the capacity of the polysiloxane copolymer structure to filter gamma radiation can be increased by using dyes. It is known that as the energy of gamma photons increases, the ability of gamma photons to penetrate the material increases. However, in this patent, it isn't specified how much of the gamma photons at which

energies of the polysiloxane copolymer whose gamma filtering ability is enhanced by using dyes, is capable of filtering. In this thesis study, a poly(imide siloxane) material, which is a structure different from the polysiloxane copolymer, was formed and dyes were not used to improve gamma filtering performance. In this thesis study and in the patent application related to the thesis, the gamma radiation transmission of the flexible and pellet form of the poly(imide siloxane) block copolymer structures are examined. For this purpose, the flexible poly(imide siloxane) structure is compared in detail with the structure created by pelletizing the poly(imide siloxane) block copolymer powders with respect to the gamma delivery technique. In this thesis and thesis-based patent application, two different gamma radioisotopes, Co-60, and Cs-137 radioisotopes are used to compare the gamma filtering performance of poly(imide siloxane) samples. Thus, the performance of poly (imide siloxane) samples was evaluated using the Cs-137 radioisotope to filter acceptable and suitable gamma photons at a moderate energy level. In addition, the performance of poly(imide siloxane) samples can be evaluated using the Co-60 radioisotope to filter acceptable gamma photons at medium to high energy levels. In this thesis study and patent application, poly (imide siloxane) was produced in two different forms as pellet and flexible. The radiation resistance of these samples was examined by the gamma transmission technique. Cs-137 (photon emission is known at 0.662 MeV energy) and Co-60 (photon emission known at ~1.25 MeV energy) radioisotopes are more suitable for gamma radiation shielding capacity. This is shown by increasing the linear attenuation coefficient, and these linear attenuation coefficient values can be compared in this way. As part of this patent (US 2007129492 A1 patent number), the pellet form of the polysiloxane copolymer is not produced, such a comparison with the flexible form of the polysiloxane copolymer cannot be made.

In the Ukrainian patent study entitled "Combined ionizing radiation detector" (with patent number UA 71 833 A G 01T 1/20), polysiloxane was used to provide optical linkage between the detector elements [99]. It is stated in this patent that polysiloxane can be used as a coupling element in ionizing radiation detectors. The structure stated in this doctoral dissertation and thesis-based patent application is a very different structure and is poly(imide siloxane). Therefore, this thesis study and patent application are different from the material specified in this patent. In the examined patent (UA 71 833 A G 01T 1/20 patent), polysiloxane, which is different from the

content of this thesis study, can be used as a connection to provide optical connection in optoelectronic elements in ionizing radiation detectors. Therefore, this patent does not mention the gamma radiation transmission of the polysiloxane. In this patent, the working mechanism of the semiconductor detector using NaI crystal is mentioned [99]. In this thesis study, poly(imide siloxane) block copolymer is different from produced polysiloxane. Gamma radiation transmission of flexible and pelleted poly(imide siloxane) block copolymer structures was examined. In this thesis and patent application, for this purpose, the gamma attenuation capacity of the flexible poly(imide siloxane) structure by gamma transmission technique, according to the structure formed by pelleting poly(imide siloxane) block copolymer powders, is compared in detail. In this thesis study and patent application, two different gamma radioisotopes were used as Co-60 and Cs-137 radioisotopes to compare the gamma filtering performance of poly(imide siloxane) samples; therefore, the performance of poly (imide siloxane) samples to filter acceptable gamma photons at a moderate energy level was evaluated using the Cs-137 radioisotope. In addition, the performance of poly(imide siloxane) samples to filter acceptable gamma photons at medium to high energy levels was evaluated using Co-60 radioisotope.

In the patent study with the patent number of GB1551483 as entitled "Polymer compositions and method of using same to produce thermostable insulating materials", which is a Great Britain origin patent, (as insulating tapes in electrical engineering, as the electrical and thermal insulating material in the manufacture and repair of electrical equipment, to protect gas and oil pipelines, to produce insulating and corrosion-resistant tapes), it is indicated that polysiloxane and organic rubber may be used [100]. In this patent, these polymer compositions molded on the substrate are exposed to ionizing radiation ranging from 5 to 50 megarads. In this patent, the gamma rays processes for the material are completely different, and changes in the transmission of gamma rays of the structure are examined. The effect of the absorbed dose on the polymer structure specified in this patent is directed to the thermal stability of the structure. Co-60 radioisotope (known to emit ~1.25 MeV energy photons and can be assumed to emit gamma photons with medium to high energy ranges) was used as the source of gamma radiation. However, the Cs-137 radioisotope (acceptable to emit gamma photons at 0.663 MeV energy and emit gamma photons in the medium energy range) has not been studied in the patent. Thus, in this patent study, the effect of Co-

60 radioisotope expressing the effect of gamma photons (for Co-60) on the polymer composition in the medium energy range is mentioned. In this patent study (patent number GB1551483), it is stated that when ionizing radiation for organic polymers such as polyolefins, olefins and dienes and the halogenated derivatives of these two species are absorbed in the structure as a cumulative dose, the structure may be partially or destroyed. In addition, these evaluations are made for polysiloxane rubbers and poliorosiloxane, which differ from the material described in this thesis and thesis-based patent application [100].

In the patent study (with the patent number of IT10747 as entitled "Procedure of polymeric composition with the thermo-resistant insulation ", which is an Italian origin patent), polymeric compositions and organic rubber-siloxane-based polymer compositions are used, which are different from the materials used in the thesis study and thesis-based patent application. In this patent, organic polymer, organopolysiloxane, low molecular weight silicon dioxide, variable-value metal oxides, siloxane rubber, organic polymer, low-weight organolysiloxane, silicon dioxide, variable-value metal oxide are used. They are completely different from the stated chemicals in the thesis and thesis-based patent application. Dimethylsiloxane polymers and vinyl polymers used as siloxane rubber are other chemical compounds used in this patent that differ from the materials specified in the thesis and patent application [101]. In this patent study with IT10747 patent, the material was allowed to absorb gamma-rays in the dose range of 6-35 Mrad using Co-60 radioisotope in order to improve its thermal insulation property and obtain more heat resistant structure [101]. In this thesis and in the patent application based on the thesis, the gamma rays applied to the material are completely different and the changes in the transmission of the gamma rays of the material were examined.

In the patent study (with the patent number of US6239039 B1 as entitled "Semiconductor wafers processing method and semiconductor wafers produced by the same "), which is a USA origin patent, the surface coating material was made from the siloxane in form of resin. Thus, the surface is coated with waterproof resin to obtain a waterproof coating. Furthermore, the behavior of the structure against ionizing radiation doesn't mention [102].

In the patent study US42050, which is the US patent "Radiation curable polyborsiloxane polymer composition and its use for producing heat-resistant

insulating materials", the polymer composition contains polyborsiloxane containing structural units having Si molar. In this patent, the Co-60 radioisotope has been used to absorb gamma rays at a dose of 6-35 Mrad to improve thermal insulation and obtain a more heat-resistant structure [103]. In this thesis, the procedures related to gamma rays applied to the material are completely different and changes in the permeability of gamma rays of the structure were examined.

In another USA origin patent study, (with the patent number of US4362674 as entitled "Process for making radiation cured silicone rubber articles"), radiation curing of a hydroxyl-terminated polysiloxane structure modified with silicone rubber was examined [104]. In this patent, the absorption of the gamma dose in the range of 1-50 megarads using the Co-60 radioisotope is addressed by the material structure. For this purpose, gamma rays are absorbed by the material using the gamma absorption technique. According to this patent, crosslinking can be formed in the structure by absorbing gamma-rays in the structure. There are differences between this patent and the studies mentioned in the thesis study and thesis-based patent application; In this patent numbered US4362674, the method used for radiation applications with gamma rays is quite different [97]. The absorption technique is used in this patent. On the other hand, the transmission method was used in the thesis study and thesis-based patent application. As can be seen, in all the studies defined and specified in the literature, very different monomers were used from our study, and material production was carried out with different reactions [19, 25, 27, 31-32, 81]. There is no similarity between the literature and thesis work.

Regarding this thesis, BTDA anhydride was added to the soft block polyamic acid in this thesis to compare the pellet form of the new thesis with a flexible form. In other words, BTDA anhydride was added to APPS. Thus, flexible poly(imide siloxane) copolymer structures suitable for pelleting were produced. When different temperatures were applied to the resulting solution samples, the structures were produced in a flexible poly(imide siloxane) block copolymer structure or suitable for pelletization.

In this thesis, a product with light and high mechanical performance properties has been developed with the produced material, and production details of poly(imide siloxane) have been determined for the radiation shielding. The poly(imide siloxane) production design for the radiation shield also provided a lightweight and flexible

material. Poly(imide siloxane) is developed in the form of flexible rubber physical form for use in existing systems in aerospace, solar energy technologies, cable industry, and medical applications. Samples with improved mechanical performance and radiation shielding capacity were produced.

6.1 Comparison of Characteristic Properties of Flexible Materials According to Literature

Different details of the PIS block copolymer structure produced under inhomogeneous conditions support the safer use of flexible material produced in known systems [15]. In existing systems, PIS block copolymers are manufactured in a flexible sheet form to increase radiation shield performance and create material production differences. Thus, PIS block copolymers have been developed as a more suitable and alternative product [82]. In previous studies, the radiation shielding capacity of PIS block copolymer samples with flexible rubber physical form has not been compared comparatively. Gamma radiation shielding capacity for use in gamma-ray fields has been evaluated with this thesis. In this thesis, poly(imide siloxane) block copolymers were produced in the flexible rubber form with high radiation attenuation capacity. Poly(imide siloxane), which has a flexible structure to examine the screening capacity of gamma rays, was produced in the form of synthetic rubber. Radiation shielding capacity was examined and results were compared.

In applications that require protection against ionizing radiation, an alternative to flexible surfaces, elastomeric rubber material with high mechanical performance has been developed compared to existing systems on light, flexible surfaces of thin-film solar cells (containing II-VI semiconductors) [15 94-96]. Thus, the material has been produced in a way to make differences in usability as an alternative, flexible, and lightweight structure in both aviation technologies and medical applications [94-96].

In this thesis, considering the dynamic mechanical performance of the flexible BI block copolymer, BI PIS block copolymer samples appear to have the appropriate compressive strength (compression test, elastic modulus (strain ~5 kPa)). Therefore, it is understood that these materials are extremely suitable for use in biomedical and aerospace applications.

The compression testing results of the several biomedical polymers (with the in-vivo elasticity) presented soft polymeric properties between 2–5 kPa [94]. The soft

polymeric biomedical materials are suitable to use as the soft tissue (for example at blood vessels) [95]. In this thesis, BI PIS block copolymer has shown the soft tissue properties with low elasticity (~5 kPa).

Lightweight flexible polymer substrates are used in solar panels, in electronic components, and in the aviation industry. For that reason, those materials are subject to unexpected collisions in the service area (as the International Space Station (ISS) manages operations in low Earth orbit (LEO and the LEO medium are affected by the collision of micrometeoroids) [96]. In addition, orbital deposits cause collision problems in LEO. Impacts can be caused by an orbital speed of about 7 km/sec to 40 km/sec. The collision damage range can range from deterioration of surface properties to damage that penetrates the material [96]. It is preferable to use radiation-resistant light flexible polymers in satellites since several objects (such as meteoroids and celestial bodies) can hit the surface of light polymers with high compression performance used in satellites and the collision intensity can be more lightly overcome due to the flexibility of the material.

There is some information that takes into account the synthesis parameters of the elastomeric polymer about DMA analysis results for another type of polymer in the literature [94-96]. Dynamic Mechanical Analysis (DMA) of poly(imide siloxane) block copolymer was performed to examine creep recovery in many applications including biomedical applications, organic electronics, and photonics, nanostructures, micro and nanofabrication, biological molecules (DNA, proteins, carbohydrates). This research can give an advance on the researches for potential industrial application areas such as biodegradables, biorefining, pharmaceuticals, macromolecular substances utilizing the creep-recovery test results of this novel polymer.

The viscoelastic and time-dependent behavior of the BI PIS block copolymer was investigated in this study to evaluate its soft polymeric properties by compression testing at controlled stress rates by DMA. Because the compression test results of various biomedical polymers (with in-vivo elasticity) showed soft polymeric properties between 2-5 kPa [94-95]. BI PIS block copolymer material showed soft tissue properties such as blood vessels with extremely low elasticity (~5 kPa) in this study.

The suitability of the BI sample for use in biomedical and industrial applications, based on the results of the analysis of the uniaxial hydraulic press test (10, 20 and 30 tons) between parallel plates, and then with the digital radiographic image (for uncompressed and compressed states) can be summarized as follows:

1. As an alternative flexible and lightweight structure, due to its high mechanical resistance, the BI sample is a material that can be used in aerospace and solar technologies with respect to the literature [25, 81, 94, 96]. The thermal resistance for the pelletized PIS structure is higher than that of the likes.

2. PIS structure which is produced as the flexible plate has a very flexible feature with respect to pressure tests at 10, 20, and 30-ton presses.

3. Esnek ve hafif malzemelerin kullanılması gereken alanlarda, radyasyona karşı koruyucu malzeme olarak kullanım detayları belirlenmiştir. Uzay, havacılık ve uydu teknolojilerinde yer alan elektronik cihazlarda, uzaydan gelen kozmik ışının yarattığı yüksek radyasyonun neden olduğu mekanik bozulmaya karşı (basınç testlerine göre) koruyucu malzeme olarak kullanılabilecek bir malzemedir [94-96].

4. This material has no chemical interaction structure. According to the literature, when used as a substrate in aviation, solar technologies, cable industry, and medical applications, there is no possibility of physical and chemical interaction with the layer (or thin-film, etc.) they carry.

5. It is suitable for use as a flexible substrate with an adhesive property.

6. The structure of this material has properties of resistant, insoluble, non-dispersible.

7. When they are used as a substrate in applications, such as medical applications, solar cells, and so on, they are not oxidized.

8. Such superior properties enable the material to be used in aerospace and solar technologies, as well as in biomedical devices, in soft electronics and medical technologies such as sub skin micro-electronic devices (sub-device). Sensor and electronic systems to be used in the automotive and electronics sectors can also be used. It can be used in biomimetic sensors and electronic systems that will work together with biological and medical materials with respect to the literature [2-7, 94-96, 96].

9. Biocompatible property of the material is an extremely high material because of its hydrophobic nature, against chemical interaction and oxidation. Therefore, they can be used very easily with any soft microelectronic devices which are in contact with the body without causing any adverse reactions in the body [2-7, 96].

10. Because of their extremely lightweight property, they can be used in all fields from aerospace technologies to medical applications together with all kinds of microelectronic devices with respect to the literature [94-96].

The solutions and benefits of our invention; To develop radiation field applications by producing light and flexible poly(imide siloxane) block copolymers with heat resistance and high mechanical performance properties. All this can be summarized as developing material production and applications for industrial production.

The benefits obtained from the flexible material produced with this thesis study are aimed to produce flexible sheets and pellet forms for different applications and to produce effective solutions for the needs of different industry areas. For this purpose, production parameters have been determined in order to obtain suitable gamma radiation shielding with a high gamma attenuation coefficient with light and flexible material applications.

The uniaxial hydraulic press was used to examine the elastic properties of block copolymer samples. After the uniaxial press test, up to 950 kg press test was done and there was no significant difference between unpressed samples. For this reason, poly(imide siloxane) block copolymer BI samples were compressed using Single Axis Hydraulic Press, using 10, 20, and 30 tons presses respectively. The elastic recovery of the sample was determined by this mechanical test. PIS samples have the property of silicone rubber and this structure is highly flexible. After a few minutes, the samples returned to their original flexible form and the structure was given elastic recovery ability. Subsequently, the radiographic examination of the compressed poly(imide siloxane) copolymer structure was performed.

Digital X-ray systems provide fast industrial operations using advanced technology and are very sensitive to detect defects in polymer materials as digital X-ray systems provide a permanent visual recording of the distortion pattern [73]. In this thesis, the radiographic images in the pressed copolymer samples were compared to the unpressed ones in light of quality control. Uniaxial hydraulic press in the values of 10, 20 and, 30 tons were applied to press the copolymer BI samples by radiographic

examination which is one of the most important non-destructive test methods. The homogeneity of the produced structure was analyzed by using the radiography technique in a more sensitive and volume-depth, comprehensive and non-invasive manner without damaging the internal structure instead of applying a mechanical test to the internal structure. To obtain radiographs, the breadth between the X-ray tube and the polymer sample was set to 60 cm in the digital radiography system.

The degree of discontinuity in variations seen on radiographic images shows the difference in density between the pressed and unpressed samples [73]. There was no significant change in the homogeneity of the pressed (hydraulically) samples in radiographic images compared to the unpressed sample at three different pressing values (10, 20, and 30 tons).

The irradiation effect was examined using Co-60 radioisotopes at 10 kGy to examine variations in the structural properties of the PIS block copolymer. The effect of gamma conduction properties at different thicknesses in block copolymer samples was measured using gamma conduction method Cs-137 (0.662 MeV) and Co-60 (~1.25 MeV) radioisotopes.

Beta attenuation properties were examined by using Sr-90 radioisotope. The rise of beta attenuation was determined after the gamma irradiation process at 10 kGy. Compatibility of these materials for medical, solar cell applications, flexible organic microelectronic devices, and aerospace technology applications was demonstrated by these results.

Irradiation of the samples with gamma radiation increased cross-linking in the network density of the sample. The decrease in the HVL of the irradiated poly (imide siloxane) BI sample showed that the radiation shielding feature increased in this study with the formation of cross-links with 10 kGy in the structure.

Gamma, beta, and neutron weakening of samples were measured with neutrons, Sr-90, gamma (Cs-137, Co-60) radioisotopes. Changes in the transmission of gamma, beta, and neutrons according to different energy peaks made it possible to investigate the effect on irradiated samples in different thicknesses.

Two different PIS specimens were synthesized to examine neutron shielding capacity and to investigate similarity and compatibility with the human body due to high hydrogen and carbon content at PIS. For the evaluation of neutron shielding [241]Pu-Be

neutron source (NH3 Howitzer) was used to evaluate neutron attenuation of the PIS samples.

The relative intensity (I/I_0) of the block copolymer samples at five different thicknesses was determined using radioisotopes (Cs-137 and Co-60). The relative intensity changes of the block copolymer samples were assigned for Cs-137 and Co-60 radioisotope by increasing thickness. The ionizing radiation attenuation coefficients were determined for the flexible sheet form.

The gamma attenuation coefficient was investigated for gamma photons at ~1.25 MeV using Co-60 radioisotopes and ~0.662 MeV using Cs-137 radioisotope. The increase in the thickness of the flexible form in the poly(imide siloxane) block copolymer sample caused a slight increase for the linear attenuation coefficient about gamma rays due to the removal of gaps and cracks in the structure.

6.2 Comparison of Characteristic Properties of Produced Pelleted Materials Concerning The Literature

Pelletized poly(imide siloxane) production details for radiation shielding have not been established in previous studies. For use in industrial applications, details of ionizing radiation attenuation are not available in the case of material pelletizing. In this study, it is also provided to develop a light product derived from poly(imide siloxane) by pelletizing for radiation shielding.

In this thesis, poly(imide siloxane) block copolymer samples produced with improved radiation protection capacity and mechanical performance have been also turned into pellets for use in existing systems such as aviation, solar technologies, cable industry, and medical applications.

Poly(imide siloxane) block copolymer samples produced with improved radiation shielding capacity and high mechanical performance properties have been turned into pellets in this thesis for use in existing systems in aviation, solar energy technologies, cable industry, and medical applications.

In order to increase the radiation shield performance in existing systems, the product was developed by pelletizing in this thesis and this new technique created production differences. The radiation shielding capacity of the poly(imide siloxane) copolymer produced in pellet forms has not been compared before. Pelletizing of poly(imide siloxane) block copolymer sample in granule form provided high radiation attenuation

capacity. Poly(imide siloxane) powders were produced by pelletizing to analyze the shielding capability of gamma rays. Thus, the radiation shielding capacity was examined and the results were compared.

PIS block copolymer samples produced in pelletized and pellet form for different applications will be able to produce effective solutions for those who need it in different areas of the industry. For this purpose, production parameters have been determined in order to obtain suitable gamma radiation shielding with a high gamma attenuation coefficient in areas where light material use is required.

Uniaxial pressing is one of the most widely used forming technologies in various materials [15, 28, 94-96]. According to European Union standards, no details are given in the uniaxial pressing of the poly(imide siloxane) block copolymers for use as a substrate or carrier in irradiation effect, to use as a radiation shield, where pelletizing and light material applications are required (eg solar cell applications).

Since uniaxial pressure test results show the reusability of the poly(imide siloxane) rubber structure (Si-O-Si polymeric structure), companies are trying to develop standards for uniaxial compression testing for polyimides. In addition, companies are trying to produce uniaxial pressure testing standards for poly(imide siloxane) based on good weather resistance of polyimides, high-temperature antioxidative property resistance, and corrosion resistance in rainy weather conditions.

The relative intensity (I/I_0) of the block copolymer samples (considered at five different thicknesses) was determined using Cs-137 and Co-60 radioisotopes. Relative intensity changes in the block copolymer samples with increasing thickness were determined for Cs-137 radioisotope and Co-60 radioisotope. The ionizing radiation attenuation coefficients were determined for the pelleted form.

The samples were pelletized by placing them in a stainless steel mold, and the pellets were formed at the desired scale to suit the collimator hole used in the radiation system used in the gamma transmission technique. The linear attenuation coefficient for the samples was determined by using Cs-137 and Co-60 radioisotopes.

The gamma attenuation coefficient for the BII sample in the pelleted form is higher than the BI sample in flexible form. For the BII sample, the linear attenuation coefficient increased because it was exposed to high temperatures during production. The radiation test results of block copolymer samples have shown that the pelleted PIS

block copolymer sample is suitable for use in a variety of industrial fields, such as the solar technology, aerospace, and aerospace industries.

Poly(imide siloxane) block copolymers produced in flexible sheets and pellet form have industrial applicability. The radiographic images in the pressed copolymer samples were compared to the unpressed ones in light of quality control. Industrial application of BII sample can be summarized as follows:

1. They can be produced suitable for use in electronic circuits and satellites in aerospace with respect to the literature [93-96]. It can be used as a superior material in aerospace and electronic technologies. It can be used as anti-reflective on low altitude surface areas, high altitude platforms, and low orbital satellites with heat resistance.

2. According to literature due to their resistance to radiation, they can be produced suitable for use in high-voltage electronic circuits of high-altitude aircraft and low-orbit satellites (International Space Station Orbit) against high destruction caused by high-radiation created from space [96].

3. In space technologies, especially when used at high altitudes in electronic devices, because of their high performance against aggressive environmental factors and high resistance to such effects, in photovoltaic applications, solar panels and all kinds of electronic devices (soft-micro), these materials can be used definitely very comfortable compared to the literature [93-96].

4. In space technologies, in new-generation photovoltaic applications, all electronic circuits from cameras to polyimide structure allow the use of literature in accordance with many applications such as telecommunication fields with the extra features of the new design [25, 81, 93-96].

5. To ensure that cancer drugs used in cancer treatments in the body exposed to radiation (especially radiation therapy) are more effective, these cancer drugs can be transported with a non-polar, hydrophobic, organic structure, PIS block copolymer material with high radiation and heat resistance until it reaches cancerous tissues in the body [15, 19, 28].

6. It can be used in resistor applications with its high dielectric coefficients, high heat resistance, in any electronic devices used in computers with respect to the literature [25, 81].

7. It is possible to use it in industrial devices used in cable insulation and radiation field in terms of being resistant to extreme temperatures, vibration, and other harsh environments [25, 81].

8. It is suitable for use as a radiation shielding material in aerospace applications (in satellites and in DSCOVR- Deep Space Climate Observatory). PIS block copolymer can be used for the protection from the effects of the space environment as heat insulating tapes and elements with respect to the literature [36, 70, 74, 82, 94-96].

In the industry, there are no competing materials with the same properties of the PIS block copolymer in pellet form. At the same time, the patent application of this new material produced in original forms was supported by Istanbul Technical University, since no patents were produced as radiation shielding products produced by these production methods and characterized by their radiation properties. The patent application of this produced new material was made to the Turkish Patent Institute (TÜRKPATENT) by the support of the rectorate of Istanbul Technical University with the patent application number of 2019/07219.

7. CONCLUSION

The results of FTIR analysis for poly(imide siloxane) block copolymers showed the structure of soft and hard flexible substrates. In these copolymer samples, APPS terminated the connections via BTDA to form anhydride. In FTIR results, diamine peaks indicate that a polymer chain ring is complete and closed. The chemical structure in block copolymers generally consists of siloxane Si-O and carbon chain-type structure.

Poly(imide siloxane) test results revealed the importance of creep recovery in various application areas including biomedical applications, organic electronics, and photonics, nanostructures, micro and nanofabrication, biological applications (DNA molecules, proteins, carbohydrates). This research also provided an advance in research for potential industrial applications such as biodegradable, biological refining, pharmaceuticals, macromolecular substances that use creep recovery test results of this new polymer.

These block copolymer samples were derived considering three different parameters in synthesis like concentration, time, and temperature. BI and BII samples had suitable solubility resistance against five different organic solvents and BI and BII samples did not have a chemical interaction with the solvents.

Changes in the mechanical performance of flexible PIS copolymer produced following compressive strength tests were investigated. For this purpose, 10, 20, and 30-ton pressings were applied to the flexible poly(imide siloxane) copolymer samples. As a result, after applied three different pressings to the flexible polymer structure, differences in the mechanical degradation of PIS copolymers were compared with the X-ray radiography technique, and no significant difference was found after the mechanical test. Both characterization methods yielded evidence-oriented results of the high mechanical strength and flexibility of the material.

Comparison of gamma attenuation behaviors of the flexible sheet (BI) and the pelletized powder (BII) samples have explained the variations of gamma absorbance

performance in BI and BII samples. The variations of gamma attenuation coefficients were compared for the photons with 0.662 MeV emitted from Cs-137 and the photons with ~1.25 MeV emitted from Co-60. The relative intensity changes of the block copolymer samples were determined with the increase in thicknesses for the Cs-137 and Co-60 radioisotopes, and the ionizing radiation attenuation coefficients were determined for both the flexible sheet and pellet forms. Increasing the linear attenuation coefficient of the BI sample demonstrated that flexible sheet form of polymer sample presented a more suitable performance for gamma shielding depending decrease of the voids between the grains at the flexible sheet of PIS block copolymers. The linear attenuation coefficient of PIS with flexible form (BI) presented a more effective radiation shielding capacity than the linear attenuation coefficient of PIS block copolymer with the pelletized grainy form (BII) against to the electromagnetic waves (including gamma rays) in this study. In Cs-137 radioisotope, improvement for the gamma shielding performance for the flexible sheet form of PIS (BI) sample was more apparent than the pelletized form depending on the decreasing of the voids between the grains. The difference of the gamma shielding in the flexible sheet of PIS block copolymer sample against gamma radiation (for Cs-137 radioisotope) was more apparent than the pelleted sample. Because the energy (~1.25 MeV) of photons emitted from Co-60 radioisotope was higher than the energy (0.662 MeV) of photons emitted from Cs-137 radioisotope.

The results of the BI sample indicated that this sample is suitable for various applications requiring long-term use in flexible applications in the microelectronics industry since they are superior, resistant materials at aggressive ambient.

The results of this study indicate that PIS block copolymer (BI) has critical radiation shielding features. This study points out the importance of flexible sheet form of PIS in biocompatibility usage and against to biodegradability at the biomaterial production.

The irradiation effect of gamma radiation supported cross-linking in the BI sample. Reducing the HVL of the irradiated poly(imide siloxane) BI sample aims to increase the radiation shield properties of BI at 10 kGy in this study.

PIS samples in two different forms, pelletized and flexible structures, were synthesized to form a suitable neutron protector and provide similarity and compatibility with the human body based on the high hydrogen and carbon content in the material. The use

of the radiation transmission technique in BI flexible and BII pelletized samples has helped analyze the variances in beta radiation and total neutron macroscopic section attenuation to study human-polymer interaction in medical applications. As a further study, the grains of the BII sample were pelleted to obtain more effective radiation shielding for the PIS block copolymer sample. The radiation transmission technique was suitable for studying density changes between BI and BII block copolymers. Changes in the depth of radiation penetration into the PIS block copolymer showed the critical importance of temperature curing application at the synthesis stage of the BII sample. The application of the radiation transmission technique to the pelleted BII sample posses a key role to express the relationships between changes in the penetration deepness of the ionizing radiation (for negative beta particles and neutrons) and the necessary thickness of the samples to attenuate the incident ionizing radiation (about 50% decrease for HVL value).

The variations in neutron attenuation of BI and BII block copolymer samples were assigned to figure out the neutron absorption capability by using neutron howitzer as a neutron generator containing ^{239}Pu-Be neutron source in this work. The total neutron macroscopic cross-section and HVL value for neutrons were detected to be 0.015 cm^{-1} and 46.27 cm, respectively for the BI sample. Also, the total macroscopic cross-section and HVL value for neutrons were assigned to be 0.047 cm^{-1} and 14.74 cm, respectively for the BII sample. HVL for the BII block copolymer sample was lower than the HVL for the BI block copolymer sample. The reduction in HVL value for the BII sample was relevant to the increase in the neutron scattering from granules in the pelletized BII sample.

The linear attenuation coefficients for BI and BII block copolymer samples were assigned to understand the beta absorption capability of PIS for Sr-90 radioisotope in this work. The increase in the scattering negative beta particles from the grains of the pelletized BII block copolymer sample demonstrated a more adequate beta attenuation coefficient than BI flexible form. The linear attenuation coefficient and HVL value of negative beta particles were detected to be 0.069 cm^{-1} and 10.04 cm, respectively for the BI block copolymer sample. Also, the total macroscopic cross-section and HVL value for neutrons were found to be 0.073 cm^{-1} and 9.5 cm, respectively for the BII block copolymer.

BII block copolymer showed a more appropriate shielding feature and more functional radiation attenuation for the utilization in medical engineering applications, aerospace, and solar energy technologies. The pelletized BII sample showed more influential radiation shielding performance against beta and neutrons. The alterations of BII polymer by the pelletization of BII grains advanced radiation shielding features in the samples.

To summarize, in applications requiring shielding against ionizing radiation, as an alternative to flexible substrates, a new polymer elastomeric rubber material with high mechanical performance has been developed compared to existing systems in substrates of thin-film solar cells (containing II-VI semiconductors). These results indicate that this novel and innovative samples can be used as an alternative flexible and lightweight structure in both aerospace technologies and medical applications.

This novel and innovative samples were developed as flexible, high thermal resistance, and high mechanical performance, nonpolar, hydrophobic, high dielectric coefficient materials for radiation field applications of light and flexible materials.

The benefits from this study show that the material can be produced in two different forms pelletized for different applications or in flexible sheets to create effective solutions in different sectors. For this purpose, production parameters have been determined to obtain gamma radiation shielding with a high gamma attenuation coefficient in light and flexible material applications.

As a result, poly(imide siloxane) block copolymer samples developed with new and innovative techniques in this doctoral thesis are in high standard materials. These materials are very suitable for use in long-term durability and long-term use in such areas as medical, aerospace, solar cell technology applications and electronics industry application (especially in flexible organic microelectronic devices).

REFERENCES

[1] **Onaran, K.** (2000). *Material Science*. (8th ed., pp.328-341). Science Technique Publication.

[2] **Baysal, B.** (1994). *Polymer Chemistry*. (2nd ed., pp.1-12) Middle East Technical University, Science and Literature Faculty Publication. pp.1-12.

[3] **Takekoshi, T. & Overberger, C.G.** (1990). New polymer materials, advances in polymer science. Vol. 94, pp.1-25. Springer-Verlag; Berlin.

[4] **Volkesen, W.** (1994). *High performance polymers*. Vol. 117. Berlin: Springer-Verlag.

[5] **Dogan, T., Baydogan, N. and Koken, N.** (2015). Production of poly(imide siloxane) block copolymers. *Energy systems and management* (1st ed., Vol. 1, pp.207-216). New York: Springer International Publishing.

[6] **Friedrich, K. & Dominik, R.** (2004). Technological aspects of flexible CIGS solarcellsandmodules, *Solar Energy*, *77* (6), 685-695.

[7] **Ghosh, A., Banerjee. S., Komber, H., et al.** (2009). Synthesis and characterization of fluorinated poly(imide siloxane) block copolymers, *European Polymer Journal*, *45*, 1561-1569.

[8] **Stenzenberger, H.** (1990). Chemistry and Properties of Addition Polyimides. In Wilson D, Stenzenberger HD, et al.,edts. *Polyimides*. Chapman and Hall. pp.79-128.

[9] **Bowens, Andrea.** (1999). *Synthesis and characterization of poly(siloxane imide) block copolymers and end-functional polyimides for interphase applications.* (Doctoral dissertation). Retrieved from https://vtechworks.lib.vt.edu/bitstream/handle/10919/29985/etd.PDF.

[10] **Besergil, B.** (2008). *Polymer Chemistry*. (2nd ed., pp.1-12) Gazi Bookstore. ISBN 9789758640355.

[11] **Yang, C.-H. et al.** (2014). *Mesoscopic phenomena in multifunctional materials: synthesis, characterization, modeling and applications*. Springer Series in Material Science.

[12] **Yeager, J.D. et al.** (2008). *Shock phenomena in granular and porous materials*. In Tracy J. Vogler, D. Anthony Fredenburg (Eds.). Springer Series.

[13] **Meyer, J.U.** (2011). Handbook of biomimetics and bioinspiration: Bioinspired Materials. Edts: Jabbari Esmaiel, Lee Luke P, Ghaemmaghami Amir. World Scientific Series in Nanoscience and Nanotechnology. Vol.9.

[14] **Mittal, K.L.** (1984) *Polyimides*. Synthesis, characterization and applications. Vol. 1.Plenum Press. p. 22-29.

[15] **Pei,X., Chen, G. and Fang, X.** (2013). Synthesis and properties of poly(imide siloxane) block copolymers with different block lengths. *J Appl Poly Sci*, *3718.* p. 3727-3727.

[16] **Ghosh, A. & Banerjee, S.** (2008). *Polym For Adv Tech*, *109*, 1486-1486.

[17] **Ghosh, A. & Banerjee, S.** (2008). *J Appl Polym Sci, 109,* 2329-2329.

[18] **Fraser, D.M.** (1997). *Biosensors in the Body: Continuous _In Vivo Monitoring.*

1st ed.

[19] **Dogan, T. & Baydogan, N.** (2019). Comparison of beta and neutron attenuations of poly(imide siloxane) block copolymers for medical applications. International *Journal of Polymeric Materials and PolymericBiomaterials*. https://doi.org/10.1080/00914037.2019.1616204.

[20] **Croft, S.** (2006). Observations on the experimental determination of mass attenuation coefficients. *Ann Nucl Energy*, *33*, 466-471.

[21] **Buyuk, B. & Tugrul, A.B.** (2014). An investigation on gamma attenuation behaviour of titanium diboride reinforced boron carbideesilicon carbide composites. *Radiat Phys Chem, 97*, 354-359.

[22] **Hill, D.** (1998). *Design engineering of biomaterials for medical devices.* NewYork: Wiley. John Wiley & Sons.

[23] **Gonsalves, K.E., Halberstadt, C.R., Laurencin, C.T., et al.** (2007). Biomedical Nanostructures. *Wiley Publication.* ISBN: 978-0-471-92552.

[24] **Croft, S.** (2006). Observations on the experimental determination of mass attenuation coefficients. *Ann Nucl Energy*, *33*, 466-471.

[25] **Dogan,T., Baydogan, N. and Koken, N.** (2015). High performance randomly segmented poly(urethane siloxane) and poly(imide siloxane) copolymers. *Procedia - Social and Behavioral Sciences, 195*, 2221–2227.

[26] **Dogan, T., Baydogan, N. and Koken, N.** (2016). Characterization of high performance randomly segmented poly(urethane siloxane) and poly(imide siloxane) block copolymers. *AIP Conference Proceedings, 1722*,1-4.

[27] **Dogan, T., Baydogan, N. and Koken, N.** (2016). Synthesis of randomly segmented poly(urethane siloxane) and poly(imide siloxane) block copolymers. *18th JCF-Frühjahrssymposium*. Kiel, Germany.

[28] **Wohl, C.J., Atkins, B.M., Belcher, M.A., et al.** (2012). High Performance Polymers, *24*, 40-40.

[29] **Takenami, K., Uemura, S. and Funahasni, M.**(2016). In situ polymerization liquid- crystalline thin films of electron-transporting perylene tetracarboxylic bisimide bearing cyclotetrasiloxane rings. *RSC Adv, 6*, 5474-5474.

[30] **Zhang, X., Ma, G., Nie, J., et al.** (2018). Restorative dental resin functionalized with methacryloxy propyl trimethoxy silane to induce reversible in situ generation of enamel-like hydroxyapatite. Biomaterials. *J Mater Sci*, *53*, 16183–16197.

[31] **Coran, A.Y., Patel, R.P., Holden, G.,et al.** (1996). *Thermoplastic elastomers.* Chapter 7. Hanser Publishers.

[32] **Liaw, W.C., Chang-Chien, J. and Kang, H.A.** (2008). Straightforward synthesis and characterization of a new poly(imide siloxane)-based thermoplastic elastomer. *Polymer Journal, The Society of Polym Sci.*

[33] **Farokhzad, C., Sangyong, J., Khademhosseini, A., et al.** (204). Nanoparticle-aptamer bioconjugates: a new approach for targeting prostate cancer cells. *Cancer Res*, 64, 7668–7672.doi:10.1158/0008-5472.CAN-04-2550.

[34] **Gu, Y., Angelaki, D. E. and Deangelis, G. C.** (2008). Neural correlates of multisensory cue integration in macaque MSTd. *Nat Neurosci*, *11*, 1201–1210.

[35] **Dresher, W. H.** (2013). Copper Applications in Innovative Technology Area. Copper Devices.

[36] **Sheets, N. C. & Wang, A. Z.** (2011). *Radioisotopes applications in bio-medical science*, ed. by nirmal singh (InTech, Rijeka, Croatia) p.47. doi: 10.5772/1937.

[37] **Fischell, R. E. and Fischell, T. A.** (1989). Intra-arterial stent with the capability to inhibit intimal hyperplasia, *US Patent, No.5059166A*.

[38] **Kim, W., Spear, E.D. and Ng, D.T.** (2005). Yos9p detects and targets misfolded glycoproteins for ER-associated degradation. *Mol Cell*, *19*(6), 753-64. doi: 10.1016/j.molcel.2005.08.010.

[39] **Ermis, E. E. & Celiktas, C.** (2012). Determination of beta attenuation coefficients by means of timing method. *Ann Nucl Energy*, *41*, 115–118.

[40] **Sarray, E. H. A. and Jabbar, A. S.** (2018). Investigate the ability of the eggshell to attenuate the gamma and beta rays as compared with composite $FeSO_4.7H_2O$. *Nuclear Science*, *3*(1), 16-22.

[41] **Evcin, O., Evcin, A., Bezir, N.C., et al.** (2017). Production of barite and boroncarbide doped radiation shielding polymer composite panels. *Acta Phys Pol A*, *132*, 3-II. doi:10.12693/APhysPolA.132.1145.

[42] **Irim, I.G., Wis, A.A., Keskin, M. A., et al.** (2018). Physical, mechanical and neutron shielding properties of h-BN/Gd_2O_3/ HDPE ternary nanocomposites. *Radiat Phys Chem*, *144*, 434–443.

[43] **Ozdemir, T. & Yılmaz, S. N.** (2018). Mixed radiation shielding via 3-layered polydimethylsiloxane rubber composite containing hexagonal boron nitride,boron (III) oxide, bismuth (III) oxide for each layer. *Radiat Phys Chem*, *152*, 17-22. doi:10.1016/j.radphyschem.2018.07.007.

[44] **Sayyed, M.I.** (2016). Investigation of shielding parameters for smart polymers. *Chinese J Phys, 54*, 408-415. doi:10.1016/j.cjph.2016.05.002.

[45] **Ozdemir, T., Gungor, A. and Reyhancan, I.A.** (2017). Flexible neutron shielding composite material of EPDM (Ethylene Propylene Diene monomer) rubber with borontrioxide: Mechanical, thermal investigations and neutron shielding tests. *Radiat Phys Chem, 131*,7-12.

[46] **Samir, A. M. & Fadel, O.** (1994). Neutron attenuation characteristics of polyethylene, polyvinyl chloride, and heavy aggregate concrete and mortars, *Health Phys, 66*, 3, 327-38.

[47] **Url-1** < *https://www.thoughtco.com/definition-of-radiation-and-examples-605579*> Retrieved: 29 Nov.2019.

[48] **Url-2** < *https://www.world-nuclear.org/nuclear-basics/what-is-radiation.aspx* > Retrieved: 12 Dec. 2019.

[49] "The Electromagnetic Spectrum". *Centers for Disease Control and Prevention. 7 December 2015,* Retrieved: 29 August 2018.

[50] **Mettler, F.A. Jr. & Upton, A.C.** (2008). *Medical effects of ıonizing radiation.* 3rd ed. Philadelphia, Pa: Saunders Elsevie*r*, page 552.

[51] **Url-3** < *https://www.remm.nlm.gov/dictionary.htm*> Retrieved: 12 Dec. 2019.

[52] **Knoll, G. F.** (2010). *Radiation detection and measurement*. John Wiley & Sons.

[53] **Görür, Ş.** (2006). *Çevresel radyoaktivite ile bu çevrede yaşayanlara ait diş örneklerindeki radyoaktivite arasındaki ilişkinin araştırılması* (Yüksek Lisans Tezi, Çukurova Üniversitesi).

[54] **Bilge, A. N. & Tuğrul, B.** (1990). *Endüstriyel radyografinin esasları*. İTÜ.

[55] **L'Annunziata, M.F.** (2007). *Radioactivity: introduction and history*. Elsevier BV. Amsterdam, Netherlands. ISBN 978-0-444-52715-8.

[56] **Rothkamm, K. & Löbrich, M.** (2003). Evidence for a lack of DNA double-strand break repair in human cells exposed to very low X-ray doses. *Proceedings of the National Academy of Sciences of the United States of America. 100* (9): 5057–62. doi:10.1073/pnas.0830918100.

[57] **Rutherford, E.** (1903). The magnetic and electric deviation of the easily absorbed rays from radium. *Philosophical Magazine*, Series 6, vol. 5, no. 26, pp. 177– 187.

[58] **Villard, P.** (1900). Sur la réflexion et la réfraction des rayons cathodiques et des cathodiques et des rayons déviables du radium. *Comptes rendus*, *130*, 1010–1012.

[59] **Url-4** < https://images.app.goo.gl/GskbbxfiPsBUyoz3A>, Retrieved: 2 Dec. 2019.

[60] **Url-5 <** https://images.app.goo.gl/Bi3aAWSinjehK1HR9>,Retrieved:1 Oct. 2019.

[61] **Url-6 <** https://images.app.goo.gl/komkrUfp44kApjdG7>,Retrieved:9 Oct. 2019.

[62] **L'Annunziata, M. F. (Ed.).** (2012). *Handbook of radioactivity analysis*. Academic Press.

[63] **Url-7 <** https://images.app.goo.gl/MHosksrL1HW3R141A>,Retrieved:5 Oct.019.

[64] **Zuo, J.M. & Spence, J.C.H.** (1992). Electron Microdiffraction. *Springer Publ.* doi: 10.1007/978-1-4899-2353-0.

[65] **Url-8** < hm.ankara.edu.tr/tac/YAZOKULU/yazokulu4/dersnotlari /Latife_sahin.doc > date of access: 10.06.2016.

[66] **Url-9 <** *https://www.sciencedirect.com/topics/earth-and-planetary-sciences/elastic- scattering>,* Retrieved: 27 Nov. 2019.

[67] **Url-10 <** https://www.iaea.org/>, Retrieved 17 Dec. 2019.

[68] **Url-10 <** https://images.app.goo.gl/S4KsCsgUXuUjYTL7A>,Retr. 14 Dec. 2019.

[69] **Url-11** < *https://www.world-nuclear.org/information-library/nuclear-fuel-cycle/fuel- recycling/plutonium.aspx>*, Retrieved 15 Dec. 2019.

[70] **Adlienė, D.** (2017). Applications of ionizing radiation in materials processing. ed. by Y. Sun, A. G. Chmielewski. *Institute of Nuclear Chemistry and Technology*, Warszawa, p.7.

[71] **Baydogan, N., Ozdemir, O. and Cimenoglu, H.** (2013). The improvement in the electrical properties of nanospherical ZnO:Al thin film exposed to irradiation using a Co-60 radioisotope. *Radiat Phys Chem*, *89*, 20-27.

[72] **Croft, S.** (2006). Observations on the experimental determination of mass attenuation coefficients. *Ann Nucl Energy*, *33*, 466-471.

[73] **Tugrul, A.B., Baydogan. N. and Altinsoy, N.** (2008). Radiographic investigations on utomotive parts, *3rd international non-destructive testing symposium and exhibition.*

[74] **Ozdemir, T., Akbay, I.K., Uzun, H., et al.** (2016). Neutron shielding of EPDM rubber with boric acid: mechanical, thermal properties and neutron absorption tests. *Prog Nucl Energ, 89*, 102-109.

[75] **Wiesendanger, R.** (1994). *Scanning Probe Microscopy and Spectroscopy.* Cambridge: Cambridge University Press.

[76] **Piner, R. D., Zhu, J., Xu, F., Hong, S. and Mirkin, C.A.** (1999). *Science* 283.

[77] **Xia,Y. & Whitesides, G.M.** (1997). *Langmuir, 13***,** 2059.

[78] **Magono, S.N. & Whangbo, M.H.** (1996). *Surface Analysis with STM and AFM. Weinheim.* Germany VCH Publishers. ISBN-10: 3527293132.

[79] **Magonov, S.N. & Reneker, D.** (1997). Characterization of Polymer Surfaces with Atomic Force Microscopy. *Ann. Revs. Mat. Sci.*, 27, 175-222.

[80] **Jing-jiang,Y. & Sergei, N. M.** *Application of Atomic Force Microscopy (AFM) in Polymer Materials*. http://www.agilent.com/find/afm.

[81] **Boukharouba, T., Elboujdaini, M. and Pluvinage, G.** (2009). Damage and Fracture Mechanics. *Failure Analysis of Engineering Materials and Structures.* Springer Netherlands.

[82] **Manjunatha, H.C.** (2017). A study of gamma attenuation parameters in poly methyl methacrylate and Kapton. *Radiation Physics and Chemistry*, *137*, 254-259.

[83] **Min W., Ling X., Maolin Z., et.al.** (2008). Gamma-ray radiation-induced synthesis and Fe(III) ion adsorptionof carboxymethylated chitosan hydrogels, *Carbohydrate Polymers*, *74*, 498–503.

[84] **Wenfei L., Zhanhai Y., Yue Y., et.al.** (2012). Synthesis and characterization of linear low density polyethylene grafted glycerol monolauric acid monoitaconic acid diester. *Polymer-Plastics Technology and Engineering*, *51*, 620–625.

[85] **Alejandro R.-B. & Emilio B.** (2019). Effect of gamma radiation on pyromellitic acid (PMA) and UO solutions. *Radiation Physics and Chemistry*, *165*, 108-3782.

[86] **Mohammadian-Kohol, M., Asgari, M., Shakur, H. R. (**2018). Effect of gamma irradiation on the structural, mechanical and opticalproperties of polytetrafluoroethylene sheet. *Radiation Physics and Chemistry*, *145*, 11–1812.

[87] **Soledad Lencina M.M., Chiara R., Christian D., et.al.** (2019) Rheological analysis of thermo-responsive alginate/PNIPAAm graftcopolymers synthesized by gamma radiation. *Radiation Physics and Chemistry*, *156,* 38–4339.

[88] **Akınay,E. & Tincer,T.** Radiation Grafting of Vinyl Monomers onto poly(tetrafluoroethylene) powder produced by gamma irradiation and properties of grafted poly(tetrafluoroethylene) filled low density polyethylene. *Journal of Applied Polymer Science*, *79* (5), 816-826.

[89] **Poddubny S., Averyanov, V., Lidia A. A.** (1980). Radiation curable polyborsiloxane polymer composition and method of using same to produce thermostable insulating materials. *United States Patent*, USA Patent No.4,205,026.

[90] **Meng-ge, H., Yan Z., Xin-ling, Z., et.al.** (2019) Preparation and Thermal Evaluation of Novel Polyimide Protective Coatings for Quartz Capillary Chromatographic Columns Operated over 320°C for High- Temperature Gas Chromatography Analysis. *Polymers*, *11*, 946.

[91] **Musavir, B. & Parvathy R.** (2018).A review on electroactive polymers development for aerospace applications. *Journal of Intelligent Material Systems and Structures*. doi: 10.1177/1045389X18798951.

[92] High-Dose Measurements in Industrial Radiation Processing, Technical Reports Series No. 205, Report of an Advisory Group Meeting on Standardization and High-Dose Intercomparison for Industrial

Processing Organized by The International Atomic Energy Agency and Held in Vienna, 25-29 September 1978, IAEA, Viana, ISBN 92-0-015081- 0, 1981.

[93] **Url-12 <** http://www.isas.jaxa.jp/>, Retrieved Jul. 2019.

[94] **Kathryn, W., Walter, B., Yan ,T., et al.** (2012). Compressive elasticity of three dimensional nanofiber matrix directs mesenchymal stem cell differentiation to vascular cells with endothelial or smooth muscle cell markers. *Acta Biomater* , *8*(4),1440–1449.

[95] **Tanzi, M. C. & Farè, S. (**2017). *Characterization of Polymeric Biomaterials*, Woodhead Publishing, Elsevier.

[96] **Drubka, R. E., Blackman, J. B., Glover, G. W., et.al.** (1993). *Advanced Survivable Radiator Development Program*. WL-TR-9 3-20, Huntington.

[97] **John G. DuPont & Paul A. G.** (1982). Process for making radiation cured silicone rubber articles. *United States of America Patent,* US Patent No. 4,362,674,Date: Dec 7, 1982.

[98] **Colbort, R.E., Gary, C.D., Jianbo, D., et.al.** (2007). Polysiloxane copolymers, thermoplastic composition, and articles formed therefrom. *United States of America Patent*, USA Patent No. US2007129492 A1, Date: June 7, 2007.

[99] **Andryushchenko, L. A., Andrey, A. A., Vidaj, Y. T., et al.** (2004). Combined ionizing radiation detector. *Ukraine Patent*, UA Patent No. UA 71 833 A G 01T 1/20, Date: Dec 15, 2004.

[100] **Isaak, Y.P., Sergei, V.A., Lidia, A.A., et al.** (1979). Polymer compositions and method of using same to produce thermostable insulating materials. *United Kingdom Patent*, UK Patent No. 1551483, Date: Aug 30, 1979.

[101] **Isaak, Y.P., Sergei, V.A., Lidia, A.A., et al.** (1977). Procedure of polymeric composition with the thermo-resistant insulation. *Italy Patent*, IT Patent No. IT10747, Date: Jan 10, 1977.

[102] **Takashi, N., Seiichi, M., Masahiko.** (1998). Semiconductor wafers processing method and semiconductor wafers produced by the same. *USA Patent*, USA Patent No. US6239 039 B1.

[103] **Isaak, Y.P., Sergei, V.A., Lidia, A.A., et al.** (1980). Radiation curable polyborsiloxane polymer composition and method of using same to produce thermostable insulating materials, *United States of America Patent, USA Patent No. US 4,205,026 A1, Date: May 27, 1980.*

APPENDICES

APPENDIX A.1: Production of randomly segmented RI poly(imide siloxane) copolymers
APPENDIX A.2: Curing of randomly segmented RI poly(imide siloxane) copolymers
APPENDIX A.3: Collecting water to obtain randomly segmented RI poly(imide siloxane) copolymers with viscous property
APPENDIX A.4: The formulation of randomly segmented PIS RI copolymer samples
APPENDIX A.5: FTIR analysis of randomly segmented PIS RI copolymer
APPENDIX A.6: FTIR analysis of randomly segmented PIS RI copolymer
APPENDIX A.7: TGA of randomly segmented PIS RI copolymer
APPENDIX A.8: Substance loss of the randomly segmented PIS RI copolymers as a percentage on a certain
temperature range
APPENDIX A.9: Solubility in the randomly segmented PIS RI copolymers
APPENDIX A.10: DSC of the randomly segmented PIS RI
APPENDIX A.11: SEM image and (b) general surface appearance of randomly segmented PIS RI
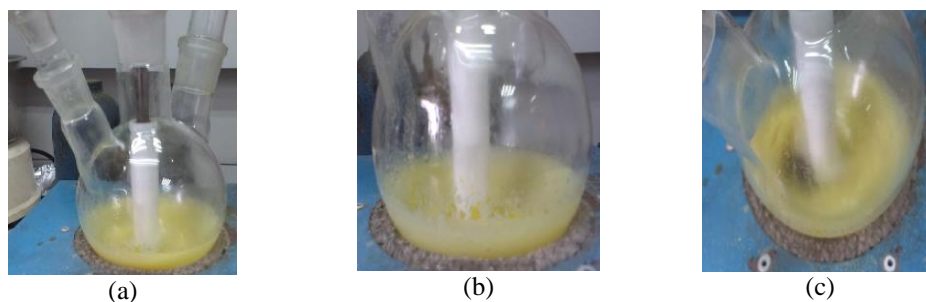
APPENDIX A.1

(a)   (b)   (c)

Figure A.1(a-c): Production of randomly segmented RI poly(imide siloxane) copolymers with the viscous property at ten steps*: (a) Synthesis at a three-necked flask in a nitrogen atmosphere, (b) The stirred mixture at room temperature, (c) the solution after mixing.

*Production steps of RI:

1. BTDA (3.26 g), NMP (15 mL), and ODCB (10 mL) were put into a three-necked flask in a nitrogen atmosphere.

2. Nitrogen gas was applied to the neck of the flask glass by a hose from the tube.

3. After BTDA dianhydride was dissolved completely. ODCB was inserted into a different beaker. When it was stirred together,

4. APPS (53 gr) was put into the mixture.

5. ODA (1.24 gr) was added and all adding were mixed.

6. The last mixture was mixed with the first mixture in the three-necked flask tube.

7. Then, the last mixture was stirred for 12 hours at room temperature until a viscous solution was obtained.

8. The total solution was converted into light yellow color. The flask tube was charged with nitrogen gas.

9. The general appearance of the structure during evaporation and discoloration starting with a temperature of 185°C.

10. Then, the temperature of the reaction was increased until $185°$C.

11. It was stirred for 8 hours at this temperature.

APPENDIX A.2

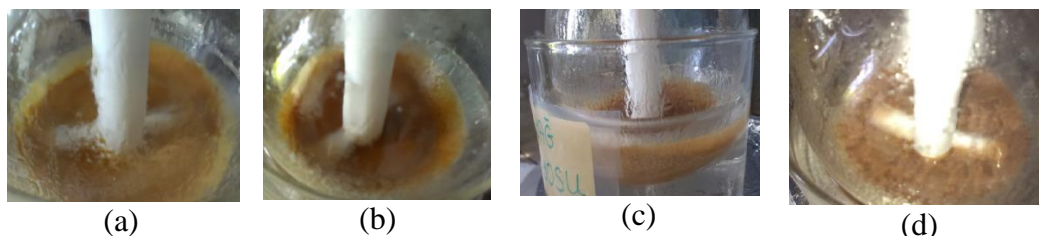(a)   (b)   (c)   (d)

Figure A.2 (a-d): Curing of randomly segmented RI poly(imide siloxane) copolymers to obtain viscous property** (a) General appearance of the solution. (b) Discoloration starting with a temperature of $185^{o}C$. (c) The starting of the evaporation. (d) The dehydration process of the solution during mixing.

** As the result of the mixture becomes viscous, a mechanical stirrer IKA WERK RW – 20 was put into the flask tube.

12. After 8- hour period was over, the mixture was cooled until room temperature.

13. It was diluted in NMP and washed with excess ethanol by stirring to get a precipitate.

14. Later, the mixture was mixed with ethanol.

15. Then, it was washed to remove the tackiness of the structure to give a relatively more solid-soft structure.

16. The resulting structure was dried off in a vacuum environment for 12 hours at $120^{o}C$ to obtain RI randomly segmented copolymer.

APPENDIX A.3

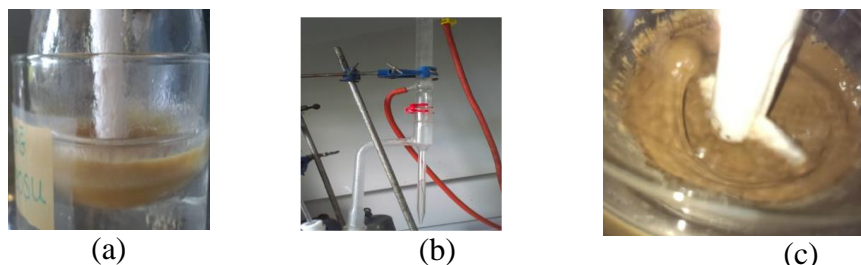<center>(a)   (b)   (c)</center>

Figure A.3 (a-c): Collected water to obtain randomly segmented RI poly(imide siloxane) copolymers with viscous property[3*] (a) Increase of evaporation during the heating process in the oil bath. (b) 12 mL of water was collected by evaporation from the dean-stark. (c) The mixture after 8 hours.

[3*]At the beginning of the synthesis of all samples, APPS was put into a solution of dianhydride for capping APPS effectively, and then non–siloxane diamines ODA was put to free dianhydride. APPS was capped by anhydride. Randomly segmented block copolymers were produced in a co-solvent system consisting of NMP and ODCB by distributing of APPS randomly in the RI copolymer chain. The molecular weight of polysiloxane diamines determined polysiloxane soft block lengths. Polyimide hard block length was accepted as a function of composition. Therefore, it was called randomly segmented poly(imide siloxane) copolymers.
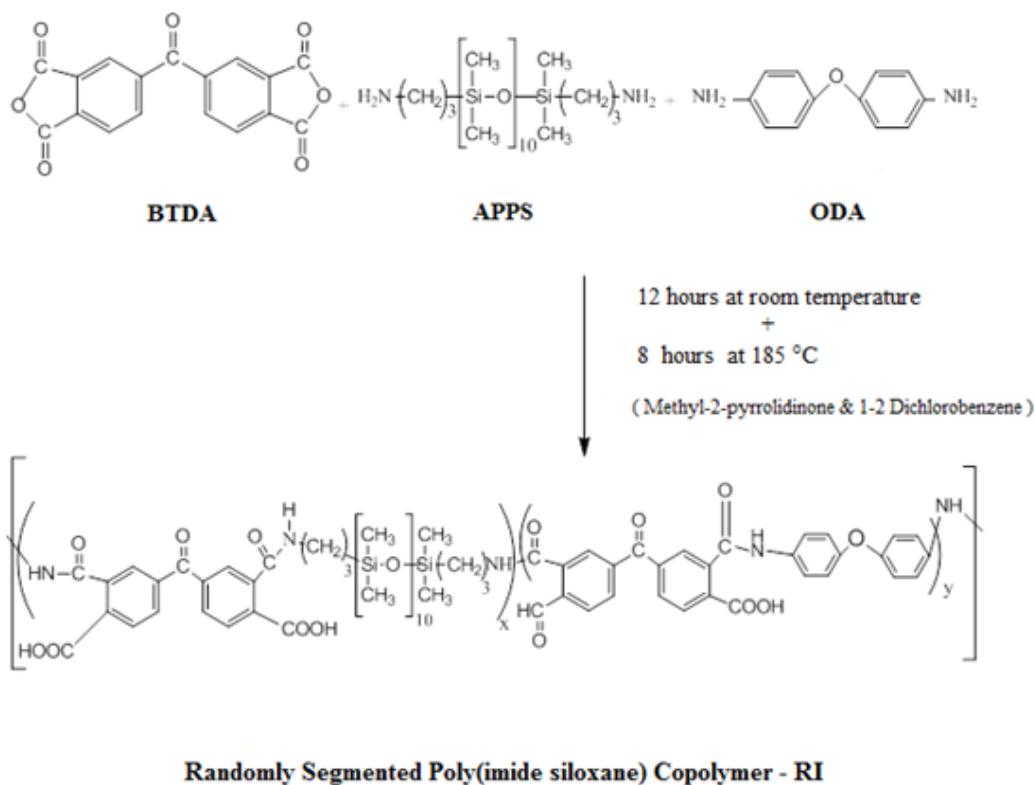
APPENDIX A.4

Randomly Segmented Poly(imide siloxane) Copolymer - RI

Figure A.4: Formulation of randomly segmented PIS copolymers. [4*]

[4*]The formulation of RI copolymer samples is produced to compare randomly segmented poly(imide siloxane) copolymers. The first two blocks of the structure are produced. Then, these two blocks are mixed to get the last form of PIS block copolymer samples for 12 hours at room temperature under nitrogen atmosphere. The formulation of this sample was derived and it was detected to exhibit good rubber property. A new chemical formula is obtained by the characterization process and using the ChemBio program.
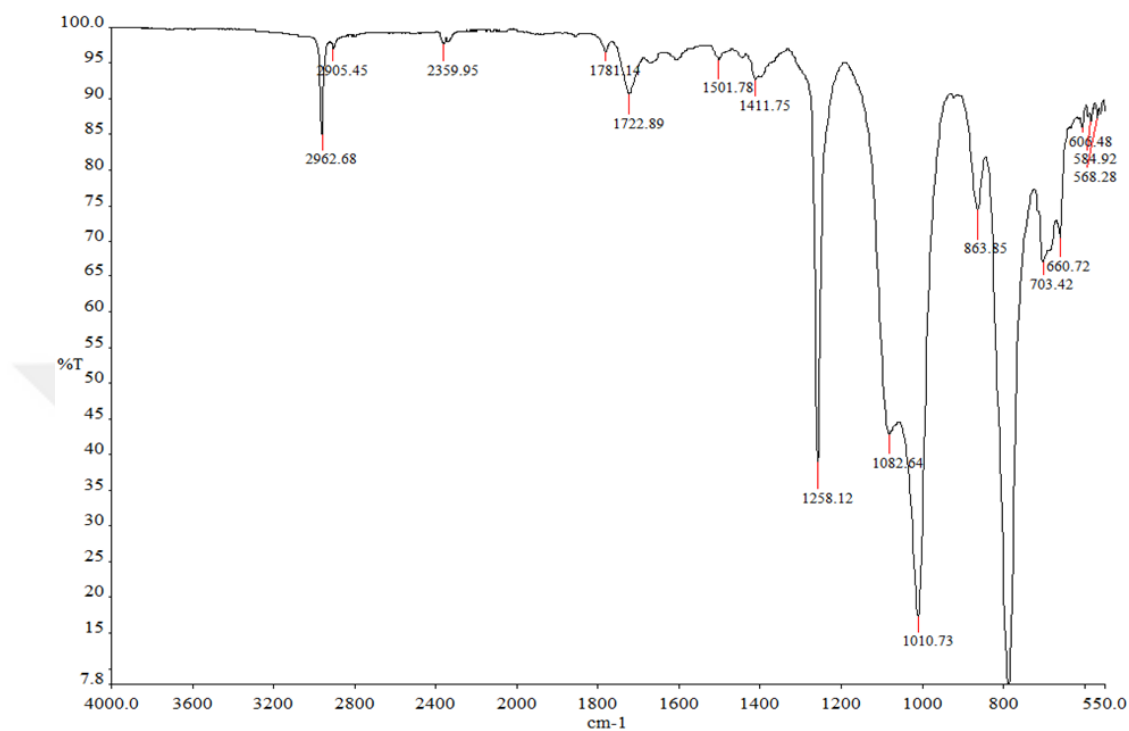
Figure A.5 : FTIR analysis of randomly segmented PIS RI copolymer with viscous property.[5]*

[5]* FTIR analyses indicated that the structures of the PIS block copolymers and randomly segmented PIS RI copolymers have exhibited similar structural characterization.

APPENDIX A.6

Table A.6 : FTIR analysis of randomly segmented PIS RI copolymer.

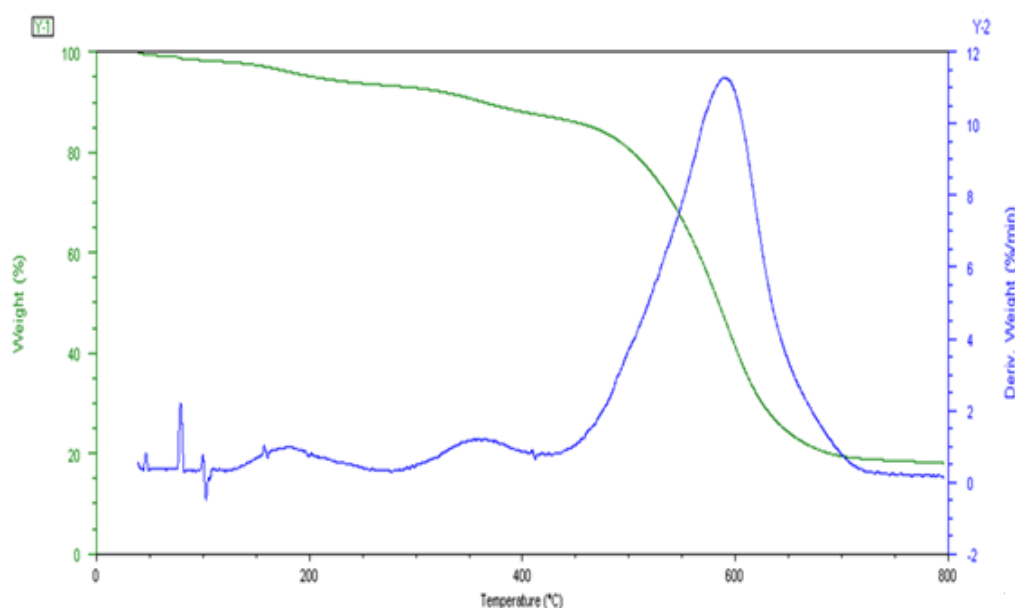| Bound		Peak (cm⁻¹)
aliphatic C - H	stretching	2962
asym C = O	stretching	1781
sym C = O	stretching	1722
asym Si- O-Si	stretching	1082
sym Si-O-Si	stretching	1010
Si-C	stretching	790

APPENDIX A.7

Figure A.7 : TGA of randomly segmented RI PIS copolymer. [7*]

[7*] Initial mass was 5.762 mg for the randomly segmented copolymer, RI sample. 4.81% and 0.277 mg weight loss of the randomly segmented copolymer structure was observed at 200°C. The weight loss was 11.91% and 0.686 mg at 400°C, 19.28% and 1.110 mg. Besides, loss of substance occurred by 58.69% and 3.381 mg at 600°C; 80.54% and 4.641 mg at 700°C; 81.98% and 4.723 mg at 800°C. The decomposition of the copolymers-RI structure started dominantly at 600°C.

APPENDIX A.8

Table A.8: Substance loss of the randomly segmented PIS RI copolymers as a percentage on a certain temperature range. [8]*

Temperature Range (^{o}C)	RI	
	Subst. Loss (%)	Subst. Loss (mg)
200	4.81	0.278
400	11.91	0.686
500	19.28	1.110
600	58.69	3.381
700	80.54	4.641
800	81.98	4.723

[8]*The substance loss as percentage and milligram.

APPENDIX A.9

Table A.9 : Solubility in the randomly segmented PIS RI copolymers.[9]*

Polymer	*Solvents*				
	NMP	ODCB	DMSO	Chloroform	R134a
RI	-	-	-	-	-

(-) nonsoluble on heating

[9]* Randomly segmented PIS RI copolymer wasn't dissolved in any solvents neither at room temperature and at room temperature by stirring nor on heating in any solvents.
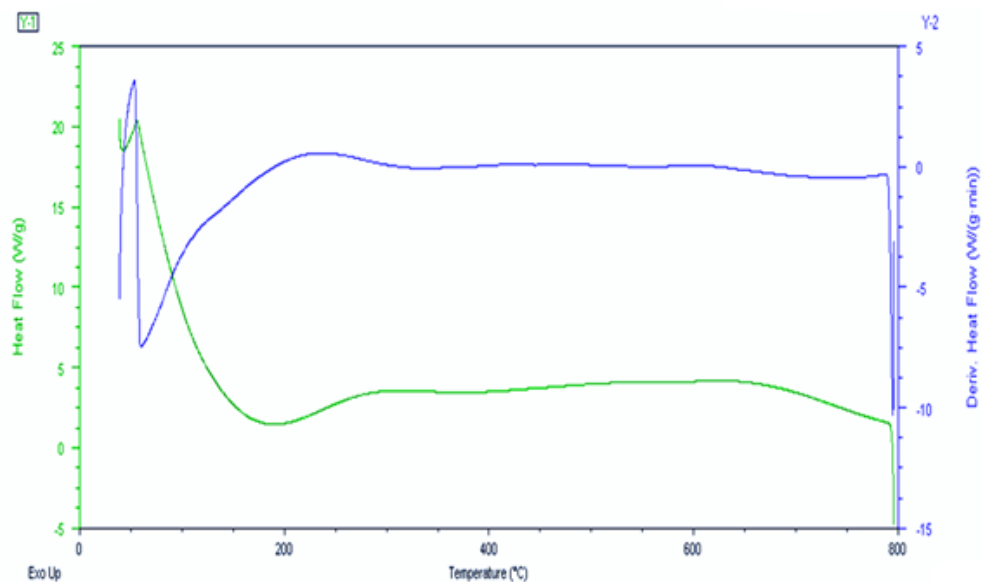
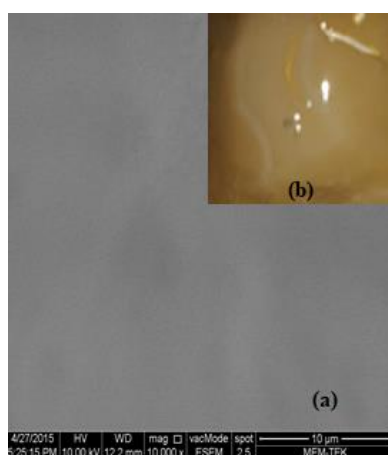**Figure A.10:** DSC of the randomly segmented RI PIS.

Figure A.11: (a) SEM image and (b) general surface appearance of randomly segmented PIS RI as a picture. [11*]

[11*] The decrease in hard segment content resulted in a homogeneous surface morphology in randomly segmented poly(imide siloxane) copolymer RI (in Figure A-11).

CURRICULUM VITAE

Name and Surname : Türkan Doğan

E-mail   **:** dgan.turkan@gmail.com

EDUCATION :

- **High School**   **:** Pertevniyal High School, Istanbul.

- **Bachelor Science**   **:** Marmara University, Atatürk Education Faculty,
  Physics (English)

- **Master of Science**   **:** Yıldız Technical University, Institute of Science,
  Physics

EXPERIENCE AND GRANTS:

- I have been working as a teacher in high schools affiliated to the Turkish Ministry of National Education.
- **Travel Grant from German Chemical Society (GDCh) for Conference Presentation :** The JungChemikerForum (Young Chemists Committee; JCF) of the Gesellschaft Deutscher Chemiker (German Chemical Society; GDCh) 18th JCF-Frühjahrssymposium, March 16-19, 2016, University of Kiel, Hamburg, Germany.
- **Travel Grant from German Chemical Society (GDCh) for Conference Presentation :** The JungChemikerForum (Young Chemists Committee; JCF) of the Gesellschaft Deutscher Chemiker (German Chemical Society; GDCh) 19th JCF-Frühjahrssymposium, March 29-April 1, 2017, Johannes Gutenberg University, Mainz, Germany.
- **Travel, Accommodation, and Registration Fee Grant from TUBITAK for Conference Oral Presentation in DSL-2019 :** TUBITAK - The Scientific and Technological Research Council of Turkey, 2019.

PUBLICATIONS, PRESENTATIONS, AND PATENT DERIVED FROM PHD:

Patents

The patent application with 2019/07219 patent number was made by ITU to Turkish Patent (TÜRKPATENT) with the invention title of "A Material for Use in Radiation Shielding and Production Method of the Material".

Papers Published in SCI index

1. **Dogan, T**., Baydogan, N., 2019. Comparison of Beta and Neutron Attenuations of Poly(imide siloxane) Block Copolymers for Medical Applications. *International Journal of Polymeric Materials and Polymeric Biomaterials, Taylor & Francis*, DOI: 10.1080/00914037.2019.1616204.
2. **Dogan, T**., Baydogan, N., 2019. Gamma Attenuation Behaviour of Poly(imide siloxane) Block Copolymer(pending).
3. **Dogan, T**., Baydogan, N.,2019. The Absorbed Dose Effect on Radiation Shielding Properties of Poly(imide siloxane) Block Copolymers (pending).

International Book Chapter:

1. **T.Dogan**, N.Baydogan, N. Koken, "Characterization of High Performance Randomly Segmented Poly(urethane siloxane) and Poly(imide siloxane) Block Copolymers", Edit: 9th International Physics Conference of the Balkan Physical Union (BPU-9) AIP Conf. Proc. 1722, 1, ISBN: 9780735413696, https://doi.org/10.1063/1.4944119 (2016).
2. **T.Dogan**, N.Baydogan, N. Koken, "Production of Poly(imide siloxane) Block Copolymers", Energy Systems and Management (1st ed.). Chapter: 20, DOI: 10.1007/978-3-319-16024-5_20 (pp. 13-18). Springer International Publishing (2014).

Papers Published in Peer Reviewed International Journals

- **T. Dogan**, N. Koken, Nilgun Baydogan, "Production of Poly(Imide Siloxane) Block Copolymers for Non-Smooth Surfaces", DSL 2019, 15th International Conference on Diffusion in Solids and Liquids, 24-28 June 2019, Athens Greece.
- **T.Dogan**, N.Baydogan, N. Koken, (2015), "High Performance Randomly Segmented Poly(urethane siloxane) and Poly(imide siloxane) Copolymers", Procedia - Social and Behavioral Sciences,DOI:10.1016/j.sbspro.2015.06.305.

Papers Published in International Conference Proceedings

1. **T.Dogan**, N.Baydogan, N. Koken, "High Performance Randomly Segmented Poly(Urethane Siloxane) and Poly(Imide Siloxane) Copolymers", WOCTINE 2015, World Conference on Technology, Innovation and Entrepreneurship for Technology and Innovation-Based Sustainable Development, 28-30 May 2015, Istanbul (Turkey).

2. **T.Dogan**, N. Baydogan, N. Koken, "Production of Poly(Imide Siloxane) Block Copolymers", ICEM 2014, International Conference on Energy and Management, 5-7 June 2014, Istanbul (Turkey).

Papers Published in International Conference Abstract Books

1. **T.Dogan**, N.Baydogan, N.Koken, "Synthesis of High Temperature Resistant, Flexible Poly(Imide Siloxane) Block Copolymers", Polymer & nanocomposites symposium, multi-scale self-healing nanocomposite shielding material, February 21-22, 2018, Istanbul, Turkey.
2. **T.Dogan**, N.Baydogan, N. Koken, "Synthesis of High Temperature Resistant Block Copolymers", The JungChemikerForum (Young Chemists Committee; JCF) of the Gesellschaft Deutscher Chemiker (German Chemical Society; GDCh) 19th JCF-Frühjahrssymposium, March 29-April 1, 2017, Johannes Gutenberg University, Mainz, Germany.
3. **T.Dogan**, N.Baydogan, N. Koken, "Synthesis of Randomly Segmented Poly(a-mide siloxane) and Poly(imide siloxane) Block Copolymers", The Jung Chemiker Forum (Young Chemists Committee; JCF) of the Gesellschaft Deutscher Chemiker (German Chemical Society; GDCh) 18th JCF- Frühjahrssymposium March 16-19, 2016, University of Kiel, Hamburg, Germany.
4. **T.Dogan**, N.Baydogan, N. Koken, "Characterization of High Performance Randomly Segmented Poly(Urethane siloxane) and Poly(Imide siloxane) Block Copolymers", Volume 1722, 9th International Physics Conference of The Balkan Physical Union (BPU-9), 24–27 August 2015, Istanbul, Turkey.
5. **T.Dogan**, N.Baydogan, N. Koken, "Production of Poly(Imide Siloxane) Block Copolymers", ICEM 2014, International Conference on Energy and Management, 5-7 June 2014, Istanbul(Turkey).

National Conference Papers Papers Published in National Conference Proceedings

- **T.Doğan**, N.Baydoğan, N.Köken, H. Çimenoğlu, "Mechanical Properties of Poly(Imide Siloxane) Block Copolymers", HITEK 2014, 3rd (Third) Advanced Technologies at National Aeronautic Conference, 18-19 June 2014, Air Force Academy, İstanbul (Turkey)

International Seminars / Workshop (with Oral/Poster Presentation)

- **T.Dogan**, N.Baydogan, N. Kizilcan, "Poly(Imide Siloxane) Block Copolymers With Different Block Lenghts and Their Structural Properties", HETECH 2014,The 23rd European Workshop on Heterostructure Technology,12-15 October 2014, Justus Liebig University Giessen (co-organized by Philipp University of Marburg), Frankfurt, Germany.

National Seminars / Workshop (with Oral/Poster Presentation)

- **T.Doğan**, N.Baydoğan, " Synthesis of Flexible Polymers For Using In Solar Cells", September 13th,2018, Istanbul Technical University, Energy Institute, Nejat Aybers Hall, Workshop on Doctorate Thesis.

Projects

- Istanbul Technical University Scientific Research Projects Foundation (ITU BAP)with the project no. of 37805. Investıgatıon of Changes in Structural Characteristics of Flexible Substrates Exposed to Ionizing Radiation Advisor: Prof. Dr. Nilgün BAYDOĞAN (2013- 2020).